

***Bacillus* sp. strains and their inducible *in vitro* antagonism: A biochemical and molecular study**

Laura Sierra-Zapata

**Thesis submitted in partial satisfaction
of the requirements for the degree of:
Doctor of Philosophy in Engineering – Bioprocesses**

Research line:

Bioprocesses - Research Group CIBIOP
PhD in Engineering from the School
of Engineering of Universidad EAFIT

Advisor:

Valeska Villegas-Escobar, PhD

Co-advisor:

Magally Romero-Tabarez, Dr. Rer. Nat.

**UNIVERSIDAD EAFIT
Medellín, Colombia
May 2018**

ABSTRACT

Discovering novel antibiotic substances from natural sources and revitalizing the pipeline for screenings of naturally sourced substances that could render new bioactive compounds, is a priority nowadays in the face of a world crisis of antimicrobial resistance. This research was focused on disclosing an observed antagonism system composed of *Bacillus* sp. strains producing inducible antimicrobial activity against the plant pathogen *Ralstonia solanacearum*, a widespread bacterium that causes bacterial wilt disease to a great variety of plant species, including many agriculturally important ones as are bananas. The inducible phenomenon was discovered during the screening of 1493 aerobic endospore forming bacteria against plant pathogens. It was observed that in the presence of the chemical compound Triphenyl Tetrazolium Chloride (TTC), which belongs to the group of synthetic compounds known as tetrazolium salts used to monitor cell respiration, *Bacillus* sp. strains produced inhibition zones against the bacterial plant pathogen and other pathogenic bacterial species, while in the absence of the compound they did not have any bioactivity. During biochemical characterization, it was evidenced that although the phenomenon was observable across several species of the order Bacillales, strains belonging to *B. cereus*, *B. pumilus* and *B. subtilis* were outstanding in their inducible antagonism potential, among other species tested. Besides, relevant traits revealed that other tetrazolium salts did not induce antagonistic activity and that the addition of antioxidant compounds did not reduce the inducible antagonistic activity. Also, *R. solanacearum* sensitivity to antibiotics was not increased by the addition of TTC and the inducible activity was independent of the presence of the pathogenic strain. In order to determine genes and pathways that were activated under TTC conditions, transcriptomic and metabolomics analysis were performed. Transcriptomic results revealed that specific pathways of the nitrogen metabolism, such as pyrimidines, purines and histidine biosynthetic routes, were 2 to 5 fold up-regulated in *B. subtilis* NCIB-3610 cells growing under TTC presence. On the other hand, metabolomic analysis showed that 28 specific compounds were either unique or 3 to 5 fold more abundant in active extracts obtained from inducible conditions, compared to non-induced controls. Data mining on public chemical databases, using intrinsic properties of the selected compounds, suggests that they mostly belong to chemical families of carbamates, imidazoles, pyrrolidines, pyrimidines, dipeptides and oligopeptides, all of which are part of the nitrogen metabolism. Results suggest that *Bacillus* cells reduction of TTC into triphenyl formazan (TPF) and its further accumulation inside the cells, induces the production of nitrogen-derived compounds, either by activation of nitrogen metabolism biosynthetic pathways or by a biotransformation of TPF into derivatives. Once produced, the compounds are secreted into the medium and act as antimicrobials against other bacteria.

CONTENTS

1.	Introduction	13
1.1	History of traditional antibiotics discovery and their diverse uses	14
1.2	Discovery of novel bioactive compounds.....	17
1.2.1	New cultivation techniques.....	19
1.2.2	Discovery and activation of biosynthetic gene clusters (BGCs).....	21
1.2.3	Exploring the total chemical space through metabolomics	23
1.3	Conclusion	26
2.	Background	27
2.1	Introduction.....	27
2.1.1	Importance of the target pathogen: <i>R. solanacearum</i> and Moko disease	28
2.1.2	Tetrazolium salts	29
2.1.3	Triphenil tetrazolium chloride (TTC).....	31
2.1.4	Traditional use of TTC in microbiology	32
2.1.5	Use of TTC in antagonism screenings against <i>R. solanacearum</i>	34
2.2	Methods	34
2.2.1	Microorganisms.....	34
2.2.2	Activity Trials	35
2.3	Results	36
2.3.1	Screening of AEFB strains collection against <i>Musa</i> sp. pathogens	36
2.4	Conclusions.....	38
3.	Characterization of the Inducible Antagonism System	39
3.1	Introduction.....	39
3.2	Methods	41
3.2.1	Strains screened for inducible antagonism potential.....	41
3.2.2	<i>R. solanacearum</i> and other target strains	41
3.2.3	Culture media	44
3.2.4	<i>In vitro</i> antagonism tests	44
3.2.4.1	Antagonistic activity by agar plug diffusion method	44
3.2.4.2	Antagonistic activity by agar well diffusion method	45
3.2.4.3	Antagonistic activity in liquid co-cultures.....	45
3.2.4.4	Antagonistic activity in liquid monocultures	45
3.2.5	Antibiotics sensitivity tests	46
3.2.6	Other tetrazolium salts and antioxidant addition to the culture medium	46

3.2.7	Diffusion of inducible compounds across nylon membranes.....	46
3.2.8	Determination of growth kinetics through microplates assay	47
3.2.9	Siderophores CAS assay.....	48
3.2.10	Statistical Analysis	48
3.3	Results	48
3.3.1	Growth on TTC induces antimicrobial activity of different AEFB species from Bacillales order against <i>R. solanacearum</i>	48
3.3.2	Growth on TTC induces antimicrobial activity of different Gram negative species against <i>R. solanacearum</i>	49
3.3.3	Growth on TTC induces antimicrobial activity of different <i>Bacillus</i> species against other Gram positive and Gram negative strains.....	50
3.3.4	Inducible antimicrobial activity of <i>Bacillus</i> strains is TTC-dose dependent.....	52
3.3.5	<i>R. solanacearum</i> viability is not affect by different concentrations of TTC.....	53
3.3.6	<i>R. solanacearum</i> sensitivity to antibiotics is not affected at 50 mg/L TTC.....	54
3.3.7	TTC is the stronger inducer within other tetrazolium salts tested	55
3.3.8	Inducible compounds are diffusible and produced in the absence of the target pathogen <i>R. solanacearum</i>	56
3.3.9	TTC Induces antimicrobial activity of <i>Bacillus</i> strains in liquid co-cultures and mono-cultures	57
3.3.10	Extracellular TPF does not have antibacterial activity against against <i>R. solanacearum</i>	59
3.3.11	Exploration of the chemical nature of inducible compounds	60
	• Siderophores are deregulated in the presence of TTC.....	60
	• Antioxidants addition does not alter the size of inhibition zones	61
	• Knockout mutants of <i>B. subtilis</i> NCIB-3610 activity against <i>R. solanacearum</i>	62
3.4	Discussion.....	63
3.5	Conclusion	69
4.	Transcriptomic Analysis.....	70
4.1	Introduction.....	70
4.2	Methods	73
4.2.1	Cell cultures for RNA-extraction	73
4.2.2	Total RNA extraction	74
4.2.3	Library construction	75
4.2.4	Sequencing	75
4.2.5	NanoString.....	75
4.2.6	Bioinformatic analysis	76
4.3	Results	77

4.3.1	Total RNA extraction yields are higher in +TTC condition	77
4.3.2	Histidine biosynthesis is upregulated and siderophores synthesis is down-regulated in <i>Bacillus</i> sp. cells growing with TTC in a liquid fermentation	77
4.3.3	Purine and pyrimidine biosynthetic routes are upregulated and siderophores synthesis is downregulated according to nanoString methodology	82
4.3.4	Differentially expressed genes from the two transcriptomic analysis methodologies converge in metabolic pathways.....	82
4.4	Discussion.....	89
4.5	Conclusion	94
5.	Metabolomics.....	95
5.1	Introduction.....	95
5.2	Methodology	97
5.2.1	Microorganisms and culture media.....	97
5.2.2	Inducible compounds extraction	97
5.2.3	Antagonism tests.....	98
5.2.4	Metabolomic data acquirement.....	98
5.2.5	Bioinformatic data treatment	99
5.2.6	Spectral network curation and annotation	99
5.2.7	Data mining	100
5.3	Results	100
5.3.1	Activity is retained in the extract obtained from inducible inhibition zones	100
5.3.2	Spectral networking metabolomic analysis for <i>B. subtilis</i> NCIB-3610 in GNPS platform evidences a complex network with 54 library hits and compounds only present in the active extract.....	101
5.3.3	The active extract presents unique and more abundant compounds than ..	103
	The non-induced control extract.....	103
5.3.4	Spectral networking analysis presents a subnetwork with interrelated unidentified compounds significantly more abundant in the active extracts.....	105
5.3.5	The inducible antagonistic compounds potentially include selected functional groups associated to intermediates or products of the nitrogen metabolism	117
5.3.6	Selected potential compounds from Table 5-5 present activity only against pathogens sensitive to the inducible antagonistic compounds	117
5.1	Discussion.....	119
5.2	Conclusion	123
6.	Concluding remarks and suggestions	124
7.	Supplementary material.....	126

LIST OF ABBREVIATIONS

AEFB: Aerobic Endospore Forming Bacteria
TTC: triphenyl tetrazolium chloride
NPs: natural products
USA: United States of America
USGS: United States geological survey
AMR: antimicrobial resistance
AGP: antimicrobial growth promoters
USDA: US department of agriculture
MRSA: methicillin-resistant *S. aureus*
WHO: World Health Organization
RiPP: ribosomally synthesized and post-translationally modified peptides
OSMAC: one strain many compounds
CPR: candidate phyla radiation
NanoDESI: nanospray desorption electrospray ionization
MALDI-TOF: matrix assisted laser desorption ionization – time of flight
BGC: biosynthetic gene clusters
HTS: high through-put screening
HPLC: high-performance liquid chromatography
UPLC-MS: ultra-performance liquid chromatography – mass spectrometry
HRFT-MS: high-resolution Fourier-transform mass spectrometry
NMR:
GNPS: global natural products social molecular network
CHIKV: chikungunya virus
AUGURA: association of commercial banana producers of Colombia
RSSC: *R. solanacearum* species complex
BN: billion
ha: hectares
MM: millions
NBT: nitroblue tetrazolium
MTT: 3-(4,5-dimethylthiazol-2-yl)-2,5-diphenyltetrazolium bromide
IEA: Intermediate electron acceptors
XTT: sodium 2,3-bis(2-methoxy-4-nitro-5-sulfophenyl)-5-[(phenylamino)-carbonyl]-2H-tetrazolium
TPF: triphenyl formazan

INT: Iodo-nitro phenyl tetrazolium chloride
ppm: parts per million or mg/L
WT: wild type strain
HDTMA: hexadecyltrimethyl ammonium bromide
CAS: cromeazurol S
PIPES: 1,4-piperazinediethanesulfonic acid
MeOH: methanol
CFU: colony forming units
ROS: reactive oxygen species
RNS: reactive nitrogen species
O.D: optical density
CFS: cell-free supernatants
PKs: polyketides
PKS: polyketide synthases
LPs: lipopeptides
NRPS: non-ribosomal peptide synthetases
PBS: phosphate-buffered saline
DE: differential expression
RPKM: reads per thousand nucleotides in transcript per million reads
PCA: principal component analysis
ORF: open reading frames
NCE: normalized collision energy
DNP: dictionary of natural products
NDTs: nucleoside 2'-deoxyribosyltransferases

LIST OF FIGURES

Figure 2-1. Formazan molecular skeleton: open tetrazole ring or azohydrazone group.....	30
Figure 2-2. Tetrazole ring conformations.....	31
Figure 2-3. Molecular structures of oxidized TTC and reduced TFP.....	32
Figure 2-4. AEFB strains antagonistic to <i>S. marcescens</i> and <i>R. solanacearum</i> in TTC presence and absence	37
Figure 2- 5. Inducible antagonism potential in TTC presence of AEFB strains non-belonging to 'operational group <i>B. amyloliquefaciens</i> ' against <i>R. solanacearum</i>	38
Figure 3-1. Effect of TTC on the antagonistic activity of <i>B. subtilis</i> NCIB-3610 (a) and <i>B. cereus</i> EA-CB1047 (b) against several target strains	51
Figure 3-2. Effect of different TTC concentrations in the size of inducible inhibition zones produced by selected AEFB	52
Figure 3-3. <i>R. solanacearum</i> EAP09 viability after 168 h of growth in the presence of different TTC concentrations.....	54
Figure 3-4. Effect of other tetrazolium salts on the inducible inhibition zones generated by <i>B. cereus</i> EA-CB1047	56
Figure 3-5. Inhibition zones produced by <i>B. cereus</i> EA-CB1047 across Nylon membranes against <i>R. solanacearum</i>	57
Figure 3-6. Growth curves of <i>B. cereus</i> EA-CB1047 and <i>R. solanacearum</i> EAP09 in a co-culture in TTC presence (a) and absence (b)	58
Figure 3-7. <i>R. solanacearum</i> EAP09 viability after 93 h of growth in the presence of different TPF concentrations.....	60
Figure 3-8. CAS assay for siderophores production of <i>B. subtilis</i> NCIB-3610 in the presence and absence of TTC.....	61
Figure 3-9. Inhibition zones against <i>R. solanacearum</i> produced by <i>B. cereus</i> EA-CB1047 in the presence of antioxidant compounds.....	62
Figure 3-10. <i>B. subtilis</i> NCIB-3610 Knockout mutants Inducible inhibition zones in TTC presence against <i>R. solanacearum</i> AW1 (a) and <i>R. solanacearum</i> EAP09 (b)	63

Figure 4-1. Differentially expressed genes under TTC presence based on three bioinformatic approaches for <i>B. subtilis</i> NCIB-2610 (a) and <i>B. subtilis</i> SMY (b).....	78
Figure 4-2. <i>B. subtilis</i> SMY and <i>B. subtilis</i> NCIB-3160 differentially expressed genes in the presence of TTC: RNA-seq	80
Figure 4-3. Differentially expressed genes of <i>B. subtilis</i> NCIB-3610 under TTC conditions according to nanostring.....	83
Figure 4-4. KEGG map for L-histidine metabolic pathway	85
Figure 4-5. KEGG map for purines nitrogenous bases metabolic pathway	86
Figure 4-6. KEGG map for pyrimidines nitrogenous bases metabolic pathway.....	87
Figure 4-7. KEGG map for L-aspartate, L-glutamate, L-alanine amino acids metabolic pathways	88
Figure 5-1. Curated and annotated spectral network for <i>B. subtilis</i> NCIB-3610 crude extracts (active and controls)	104
Figure 5-2. Subnetwork-1 of non-annotated and more abundant compounds in from spectral network analysis.....	106
Figure 5-3. Metabolites obtained as candidates from data mining evidence antibiotic activity against <i>R. solanacearum</i> and <i>Staphylococcus</i> sp.....	118

LIST OF TABLES

Table 1-1. New antimicrobial drugs from natural sources reported during the last two decades (2000-2017) and their respective discovery technique	24
Table 2-1. Tetrazolium salts employed in biochemistry: commercial names and molecular structures	33
Table 2-2. Colony appearance of <i>R. solanacearum</i> isolates on BGTA.....	35
Table 2-3. Group of AEFB strains evaluated both in the presence and absence of TTC	37
Table 3-1. AEFB and other Gram negative strains employed as antagonists for the characterization of the antimicrobial inducible behavior	42
Table 3-2. Knockout mutants on selected genes from <i>B. subtilis</i> NCIB-3610 WT	43
Table 3-3. Target bacterial strains tested for their sensitivity to the inducible antimicrobial activity from <i>Bacillus</i> sp.....	44
Table 3- 4. Effect of TTC on the antagonistic activity of selected AEFB strains against <i>R. solanacearum</i>	50
Table 3-5. Effect of TTC on the antagonistic activity of different Gram negative strains against <i>R. solanacearum</i>	51
Table 4-1. <i>B. subtilis</i> NCIB-3610 and <i>B. subtilis</i> SMY RNA extractions yields	77
Table 4-2. RNA-seq - <i>B. subtilis</i> NCIB-3610 and <i>B. subtilis</i> SMY differentially expressed genes, biological function and expression ratios	81
Table 4-3. NanoString - selected differentially expressed and other relevant genes, biological function and expression ratios for <i>B. subtilis</i> NCIB-3610	84
Table 5-1. Antagonistic activity against <i>R. solanacearum</i> AW1 from active and control extracts used in metabolomic analysis	101
Table 5-2. GNPS Spectral networking analysis summary	102
Table 5-3. Selected nodes for data mining from spectral networking analysis of <i>B. subtilis</i> NCIB-3610 extracts.....	107

Table 5-4. Subnetwork-1 and unique precursor ions data mining in Chemspider and Pubchem.....	108
Table 5-5. List of metabolites to which the inducible antagonistic compounds are chemically related.....	11

ACKNOWLEDGMENTS

To my father, who will always be a part of me and cultivated my passion for nature, agriculture, science and technology, with it coming to fruition beyond any of my expectations. “Persevere in the great adventure of knowledge”, he used to say. I now realize that this advice keeps on the track of many things he did well during his life: following it has made me really happy. To my other two musketeers, for their unconditional love, forever thankful.

To my thesis director Valeska, for her amazing guidance and support and for always questioning, which has taught me that it’s the only way to expand the barrier of knowledge. To my other committee members Magally and Javier for their generous guidance and for sharing all their advice and experience.

To professors Roberto Kolter, Mark W. Silby, Matt F. Traxler, and the people working with them (Lucy McCully, Leah Smith, Scott Behie, Rita Pessoti, Nick Lyons), for accepting me as a visitor researcher in their labs, giving me the opportunity to greatly open my perspective in science and the frontier of this particular research.

CHAPTER 1

1. Introduction

Antibiotics, or low molecular size bioactive substances, which inhibit the growth of microorganisms, specially of bacteria, have been largely discovered from microbial sources and until recently, were considered to have a natural defense role for them being mostly produced under stressful circumstances to selectively inhibit the growth of other microbial competitors. Although, several other ecological and evolutionary roles, such as signaling molecules, have been newly suggested for antibiotic substances unveiling the unexplored potential of small-molecule microbial natural products and their multiple functions, and thus raising the interest in them and their value. Its therapeutic versions, or antimicrobials, are widely known as ‘miracle drugs’ and are broadly employed to combat disease-causing or pathogenic microbial agents either in plants or animals. Most of them have been discovered from natural sources, some being afterwards either partially or totally modified by synthetic chemistry methods to achieve higher production levels and enhanced activity. Antimicrobials have been considered for long the therapeutic wonders of the 20th century. Discovery of Penicillin by Alexander Fleming from fungus *Penicillium notatum* in 1928, and its later employment as a curative agent during second world-war II, gripped the interest of scientists all over the world on antibiotic research and discovery. This last event ushered in the golden era of antibiotics from the 1940s until the late 1960’s, during which the majority of life-saving antibiotics were discovered, protecting millions of people from deathly bacterial infections and enhancing food security through the improvement of productivity in crops and farming animals.

Even though multiple drugs addressing different targets emerged during these antibiotic golden era, novel ones appeared with less and less frequency during the following decades until the early 21st century, a tendency that continues up to the present days, along with an over-use of these ‘miracle’ substances taking place. This has derived in a rapid appearance of resistant strains, becoming a world-wide problem of antibiotic microbial resistance (AMR), representing both a clinical and phytosanitary problem. The antibiotic crisis is considered one of the most serious health threats of the XXI century, seriously affecting humans, other animals and crops. It is a multi-faceted issue that everyone has a shared responsibility in limiting its impact and prevent humanity of experiencing a return to the pre-antibiotic era. In this context, the present chapter makes an introduction to new challenges linked to antibiotics discovery as well as an overview of technological advances pointing towards research on novel bioactive substances.

1.1 History of traditional antibiotics discovery and their diverse uses

Over the history of humankind, disease control in both animals and plants has been mainly supported on the use of natural products (NPs) or products derived from natural sources. Antibiotics and pesticides are among these NPs, mainly used to combat animal infections of bacterial origin and to control fungal or bacterial plant diseases, respectively. Even though Penicillin is known to be the first antibiotic discovered (by Fleming in 1928) (1) it was not introduced as a therapeutic agent until several years later, in the 1940s, due to the collaborative work of Howard Florey and Ernst B. Chain, who were able to produce the substance on a large-scale level and make it available for hospitals (2). Parallel to this milestone discovery, other compounds were being introduced to the market, with the synthetic sulfonamides being the first class of antimicrobials used in clinical practice during the 1930's. Their prompt development of resistance later in the same decade, accelerated the discovery of novel antibiotics and research entered the golden area of antibiotics, spanning from the 1940's to the late 60's when most of the antibiotics used today were discovered, among which stand out the largely famous streptomycin, ampicillin or methicillin (2). But shortly after this golden period, during the early 70's, warning signs of greater resistance were observed and research focused on unveiling the foundations of this phenomenon, finding that horizontal gene transfer and other genetic mechanisms, although being natural phenomena in microbial evolution, had increased due to the selective pressure from a higher concentration of antibiotic drugs in the environment (2, 3). Although Fleming had highlighted this since his first observations on Penicillin effect on *Staphylococcus aureus*, as well as his co-worker Chain (4), resistance continued to menace the efficacy of treatments based on antibiotics. Thus, the subsequent years until now have been characterized by an increasing appearance of resistant strains, specially of the three highly common bacteria *Escherichia coli*, *Klebsiella pneumoniae* and *S. aureus*, which cause widespread health care associated and community-acquired infections (5).

The appearance of high resistance in several strains is accompanied by a decrease in programs for discovery of novel antimicrobial compounds from natural sources (6, 7), mainly because of the large funds that are required, the slow return of profit in inventions and various technological limitations (8). This particular situation, has been changing in the last years, due to an updated focus deriving in the development of modern platforms and technologies for screening bioactivity, new methodological approaches pursued in drug and antimicrobials discovery from natural sources and public-private partnerships along with government incentive policies (9, 10), which has made novel antibiotic discovering a trending subject of research nowadays, with the evident necessity for unveiling new small-molecule bioactive compounds and their modes of action, as well as their possible mechanisms of resistance (11, 12).

As NPs, bioactive substances, both disclosed and novel ones, have the challenge of being suitable for diverse uses. For decades now, antibiotics have been intensively used in agriculture as growth promoters, prophylactic agents, pesticides and therapeutics (13). For instance, control and productivity enhancement methods in the control of certain bacterial diseases of high-value fruit, vegetable, and ornamental plants have been based since 1950's on antibiotics. Mainly streptomycin, oxytetracycline, oxolinic acid and gentamicin are employed, with the United States (USA) having implemented this technique on pear, apple, peach and nectarine plantations (14). The effectiveness of antibiotics on human pathogens during these decades of the golden antibiotic-era, made plant pathologists recognize their potential for treating bacterial plant disease and enhance crops productivity, which lead to the screening of nearly 40 antibiotics of natural origin against plant disease control (15). Besides being effective, these natural substances had negligible toxicity toward plants, compared to the metal-based bactericides available to farmers in the 1950s and 1960s. A great amount of antimicrobials has been historically applied in agriculture, with only the US having an estimated annual application that sums 65.227 kg of active ingredient in orchards, according to the US geological survey (USGS) (16, 17). Despite this, larger volumes are needed nowadays due to the appearance of resistant strains of *Erwinia amylovora*, *Pseudomonas syringae*, *P. chichorii*, *P. lachrymans* and *Xanthomonas campestris*, some of the main bacterial phytopathogens causing difficult several important diseases (17).

The USGS (16) measures the amount of pesticides that accumulate up to streams, rivers and groundwater, evidencing accumulation of traces of antimicrobial substances in sediments and streams or water bodies, near agricultural and urban areas. This presence, as a consequence of antimicrobials and antimicrobial-contaminated water use in agriculture, leads to accumulation of these substances in the different trophic levels throughout the terrestrial food web, which means presence in food destined for human consumption (18). Thus, the impact of antimicrobials usage in agriculture goes beyond the appearance of resistant strains of targeted pathogens.

Although the amount of antimicrobials used in plant protection is relatively small, being 0.5% of the total production of antibiotics, it is undeniable that they are an effective preventive strategy and productivity enhancement method in agriculture, and the suspension of its use would greatly affect the productivity of specific high-value plant agriculture sectors (17, 19). Nevertheless, regulating its use is a priority. Starting the use of natural-sourced bioactive substances and narrow spectrum ones in agriculture and food industry, so that resistance occurrence and bioaccumulation can be mitigated, aligns with

the efforts being undertaken to conserve the efficacy of antibiotics in human medicine (5, 12).

Compared to the amounts employed in animal agriculture, the US utilization of antimicrobials in plants is rather small, the situation worldwide being similar (17, 20). Although usage in plants cannot be excluded from the AMR crisis causing activities (17, 19), intensive use of antimicrobials in food animals or livestock production has been widely pointed as an important contributor to the growing AMR crisis and tremendous efforts have been made in studying the links between the actual situation and animal use of antibiotics (19, 21). The amount of these substances used in this industry was estimated in 63.151 tons in 2010 (20), accounting for more than 80% of total sales and distribution of medically important antimicrobial agents in the US (22). The detailed mechanisms of AMR emergence and transmission linked to agricultural practices, especially in the use of antibiotics as feed additives for growth promotion (antimicrobial growth promoters or AGP) and disease prevention, still lacks much information. Although up to date studies in the subject reveal that antimicrobials use, specially within these two activities which use sub-lethal doses of the bioactive substances, has increased the selective pressure of resistant bacteria (19, 23). Thus, the use of antimicrobials in agriculture can be accounted as one of the main reasons of emergence of AMR, where other factors such as microbiota in the animal, the host, the bacterial population and other environmental pressures are influencing the transmissions (5, 19, 24).

Despite these findings, usage of antibiotics in animal husbandry is a practice which has been done more than 60 years worldwide, starting during the 1950s in accordance to the rise in antibiotic utilization, and has largely contributed to the improvement of animal health and productivity of the livestock industry, ensuring growth of global supply of animal products and increasing in about 1.5-2.9% the productions of milk and meat worldwide (19, 20).

In the European Union, antimicrobials used as growth promoters have been banned since 2006 (25), and the USA, has taken a similar action from January 1, 2017. Furthermore, the US department of agriculture (USDA) has developed action plans that propose practical mitigation strategies that will help prolong the effectiveness of antibiotics to treat both people and animals, through collection of science-based, actionable information about antibiotic drug use, its potential role in the development of antibiotic resistance in food-producing animals, and the relationship of drug use and resistance patterns to livestock management practices. But still, a significant proportion of the efforts are concentrated on the development of specific alternatives to antibiotics, such as prebiotics and probiotics,

novel antimicrobial molecules, and immune enhancement products through research (19, 26, 27).

It is evident then, that the diverse uses for which antimicrobials are employed have contributed to the widespread resistance we observe today, as they are still largely employed in the agroindustry (17), posing an additional challenge to the newly discovered substances in overcoming the resistant strains to which the traditional ones have become inactive. The World Health Organization (WHO) emphasizes in two critical strategic objectives that must be achieved in a short-time frame in order to correctly address the AMR crisis: to optimize the use of antimicrobial medicines in human and animal health and to develop the business case for investment in new medicines, diagnostic tools, vaccines and interventions (10). Some of the most recently developed technologies and cutting-edge research strategies, which are leading the discovery of novel natural bioactive compounds, are further discussed in the section below.

1.2 Discovery of novel bioactive compounds

The current problem of AMR is also exacerbated by the shortage of development and discovery of new antimicrobials (11, 12, 26). In fact, the WHO states in its last report on the subject that the world is running out of antibiotics, evidencing a serious lack of new antibiotics under development to combat the growing thread of antimicrobial resistance (28). The report found very few potential treatment options for those antibiotic-resistant infections, which are caused mainly by 12 classes of priority pathogens, or the so-called ESKAPE microorganisms which are increasingly resistant to common antibacterial drugs and include well recognized strains such as methicillin-resistant *S. aureus* (MRSA), *E. coli* ST131, and *Klebsiella* ST258 (29) and pose the greatest threat to health, along with drug-resistant tuberculosis which kills around 250.000 people each year. Of 51 new antibiotics and biologicals in clinical development to treat priority antibiotic seemingly resistant pathogens, as well as tuberculosis and the sometimes deadly diarrheal infection *Clostridium difficile*, only 8 are classed by WHO as innovative treatments that will add value to the current antibiotic treatment arsenal (23).

The main traditional and prolific families of natural antibiotics, in terms of number of compounds, consist mainly of β -lactams, macrolides, tetracyclines, quinolones and oxazolidinones, which are vastly menaced by greater resistance development from highly-occurring pathogens (29, 30). This situation becomes more critical with reports on new classes of natural sourced antibacterial drugs being scarcer every day, with the last renowned reports being the recent success of Teixobactin (31), which seemingly has no

resistance and is highly active against MRSA, Lassomycin which belongs to the ribosomally synthesized and post-translationally modified peptides (RiPP) family of natural compounds and potent against *M. tuberculosis* (32) and Lugdunin, produced by a human commensal microorganism found during human microbiome studies, which prevents *S. aureus* colonization (33). The first two novel compounds have been discovered with the use of innovative and disruptive cultivation technologies and the third one by the screening of original natural environments from which the importance of its microbiome has been accentuated, emphasizing the importance of scientific advancement in this field so that the world can meet the huge need for novel bioactive compounds, for clinical and other uses (13, 28).

Throughout the history of antimicrobials discovery, besides the finding of novel natural compounds, innovation was mainly focused on the use of chemical approaches to improve potency, spectrum of activity, pharmacokinetics and the resistance profiles of existing classes of compounds (11, 13). Most of the drugs currently in the clinical pipeline are modifications of existing classes of antibiotics and represent only short-term solutions; thus the current situation of antibiotic discovery programs is to search for novel structures, families of compounds and mechanisms of action that can address new targets and renew the spectrum of therapeutic solutions (11, 13, 28, 29). Although interest in natural products as a source of innovation in drug discovery has decreased in the last few decades, therapeutics of microbial or plant origin count for more than 30% of the current worldwide human therapeutics (34, 35). About 40% of the top-twenty used antimicrobial medicines come from natural sources, with the genus *Streptomyces* sp. being the largest antibiotic producer plus the genus *Bacillus*, which has had an important place as an outstanding member of the Aerobic Endospore Forming Bacteria group (AEFB) (35). Other important microbial groups from which antibacterial substance have traditionally been isolated are fungi, and nowadays marine microorganisms and other classes as cyanobacteria and myxobacteria (36) are being largely explored, although these seem to offer more promise in areas such as oncology (34, 35).

The production of antimicrobial metabolites by *Bacillus* spp. strains has been a highly studied subject. Moreover, since *Bacillus* spp. are characteristically omnipresent in soils, exhibit high thermal tolerance and rapid growth in liquid culture, they readily form resistant spores and are considered to be a safe biological agent, their potential as biocontrol agents and other environmental applications is considered high (9, 37-40). This scenario occurs not only for antibacterial drugs, but also for anticancer and anti-infective treatment, with even 60% of the approved drugs and the pre-new drug application candidates (excluding biologics) being of natural origin (40). The result of the growing crisis in antibiotic drug

discovery that threatens modern medicine is a re-emergence in the 21st century of natural product research, which is perfectly positioned to fill the antibiotic discovery gap and bring new drug candidates to the clinic, with the support on innovations in genomics, transcriptomics and metabolomics, as well as other diverse techniques, to explore new sources of antimicrobial chemical matter that are revealing new compounds (9, 11). The following subsections discuss the most recent and modern technologies along with areas of research followed nowadays in order to chase the mission for new natural bioactive molecules.

1.2.1 New cultivation techniques

Most naturally sourced antibiotics of microbial origin were detected using ‘The Waksman Platform’ (41). In this strategy, natural product extracts from environmental microorganisms grown under laboratory conditions, are screened for bacterial cell killing effects in the laboratory using simple culture-based assays, but after decades of microbial bioactive substances discovery using this methodology, it has been observed that it frequently re-identifies known compounds from extracts of commonly isolated bacteria (11, 42). It is also widely known that microbial physiology and morphology changes according to cultivation environment, media and conditions, which leads to the conclusion that the chemical arsenal of a specific strain changes as a function of its surrounding environment, since these small-molecules are essentially what operates the metabolism and defines a phenotype, making manipulation of culture conditions a methodology used for decades to improve the outputs from living organisms (43). The term OSMAC (One Strain Many Compounds), coined by Zeek and coworkers (43, 44), defines this observations as the possibility of one single strain to produce diverse compounds when growing under different conditions.

Besides this old-fashioned metabolite discovery method coupled to traditional cultivation techniques, it is well known that our capacity to grow most bacterial species in the lab is quite limited, perceiving that a great number of chemical species are being left uncultured, unnoticed and its genomic potential unexplored, leading to the flourishing of innovative cultivation techniques that aim for the growth of previously uncultured bacteria or to reach directly the bioactive genes, by-passing cell culture through metagenomics approaches (11, 29). According to the review by Overman and collaborators (45), cultivation of bacteria is highly biased toward a few phylogenetic groups, many of which exclude currently underexplored bacterial lineages likely to hold novel biosynthetic pathways and unknown biochemical features. In order to recover and utilize a larger fraction of microbial diversity an improved understanding of the ecology of previously not-cultured bacteria is needed. In

this same trend, Danczak *et al* (2017) (46) reveal new metabolic pathways associated to the largely unexplored candidate phyla radiation (CPR) of the tree of life, that represents more than 15% of all bacterial diversity and potentially contains over 70 different phyla. This study, achieved through metagenomics, clearly exposed the unexplored biochemical potential of unknown and uncultivable microorganisms from this radiation of life forms. Cells from these new species, appear to be leading a symbiotic or syntrophic lifestyle, dependent upon one or more partners for necessary metabolites while potentially providing labile fermentation waste products such as acetate in return (47). Such a co-dependent lifestyle could potentially account for our current lack of cultured CPR members and would highlight the unexplored potential of microbial interactions for the activation of certain metabolites production.

For instance, *In situ* cultivation methods, are grounded on the enrichment of the natural environment or more properly, the chemistry surrounding the microorganism to promote their growth in the presence of a simulated natural environment. Kaeberlein *et al.* (48), were able to isolate from marine environments two previously unreported bacterial strains, designated MSC1 and MSC2 using special diffusion chambers, to whom the closest relatives are *Lewinella persica* and *Acrobacter nitrofigilis*, respectively (29, 48). This technology, taken to the high throughput screening level, has evolved into the so-called isolation chips or iChips (49), which consists of micro diffusion chambers that use the naturally-occurring compounds of the ecosystems from where isolation is taking place, to meet the nutritional requirements of target microorganisms, cultivating them as single colonies in isolated micro-compartments. This way, the microbial battery to search for active metabolites broadens from the traditionally explored bacterial groups: filamentous actinomycetes, myxobacteria, cyanobacteria, *Pseudomonas* sp. and *Bacillus* sp. (50). This technology of *in situ* enrichment cultivation appears greatly promising, since already two of the most recent successful antibiotic discovery research programs, the ones finding Lassomycin and Teixobactin, achieved it by employing this methodology, unveiling new microbial species as a first step and its novel active compounds later, with *Lentzea kentuckyensis* being the producer of lassomycin and *Eleftheria terrae* the alleged producer of teixobactin (29, 31, 32).

Another way of accessing potential antibiotics is through the use of co-culture, which exploits the relatedness of microbial species in natural ecosystems through the exchange of chemical signals (29, 43). Successful cases for the discovery of compounds using this approach are the studies by Wu *et al* (2015), which explored the enhanced chemical diversity of *Aspergillus/Streptomyces* co-cultivation resulting in the isolation of the new alkaloid, aspergicin (51); and the ones by Traxler *et al* (2013), which revealed the altered

secreted metabolome of *Streptomyces coelicolor* when interacting with five other actinomycetes belonging to different species and genera, using emerging instrumental techniques such as nanospray desorption electrospray ionization (NanoDESI) and matrix-assisted laser desorption ionization–time of flight (MALDI-TOF) imaging mass spectrometry, displaying a unique metabolome for each different interaction and some of them rendering a family of unknown compounds, constituting 12 different desferrioxamines with acyl side chains of various lengths, their production triggered by siderophores made by neighboring strains (52).

The strength of this approach has further been shown in one of the first systematic studies, conducted by Schroeckh *et al.* (2009), to investigate the activation of cryptic or silent biosynthetic gene clusters (BGCs), sets of contiguous genes that have the potential to produce drug-like natural substances that are active against a wide variety of biological targets, in the model fungus *A. nidulans* during co-cultivation with different actinomycetes (53). Besides co-cultivation, other methods for unveiling and activating the potentially useful BGCs in microorganisms are further discussed.

1.2.2 Discovery and activation of biosynthetic gene clusters (BGCs)

Over the past decade, bacterial genome sequences have revealed an immense reservoir of BGCs, which as described above, are sets of genes which have the potential to produce drugs or drug-like molecules, with an estimate of each strain having 20-40 of them, with the majority not being expressed under laboratory conditions and thus being absent from the extracts tested on screenings; most of these clusters remain silent or cryptic under normal cultivation techniques, meaning they are inactive or no representative expression levels of them are achieved (11, 54). In the face of the urgent action needed towards discovering new antibiotics, this untapped source of original chemical entities from microorganisms gains much interest, opening the need to identify these new antibiotic chemical scaffolds taking advantage of the techniques that modern ‘Omics’ have to offer, which could even evade the resistance mechanisms circulating in pathogens today (11). In order to follow this strategy, the first inevitable step is to take *in-silico* approaches of assessing potential producers by performing genome mining, which involves looking at the sequenced genomes of microbial species to determine if BGC involved in the production of new antibiotics can be found in these organisms. This has also the potential to fully explore a specific strain’s bioactive NPs potential, under the OSMAC concept (43, 44).

The limitation that traditional active NPs discovery platform has, is supported in the research done during the Danish Galathea 3 global research expedition (2006–2007), which

reinforced the value of the bioinformatic approach by identifying many more clusters than would be possible via bioassay-guided fractionations, by underlining the unusual biosynthetic mechanisms or novel chemistries which would not usually be detected since most of prediction software used such as AntiSMASH, NaPDoS, NP.searcher and BAGEL 3 look only for reported or sequences recognized by their ability to produce bioactive metabolites (29). But the ways to activate the silent BGC in order to fully exploit and decrypt the potential of new natural chemical entities faces still a long way ahead and is being accomplished mainly through innovative cultivation techniques (43, 54).

Besides novel cultivation techniques and co-culturing of strains, activating silent BGC by chemical Interactions is defined by Reen *et al.* (43) as a promising alternative way to unlock the biochemical potential of microorganisms. Rodriguez-Rojas *et al* (7) discuss it as well, questioning what happens when antibiotics are present at very low concentrations which are not sufficient to kill or stop the growth of the susceptible population as those present in many environments?. There has been abundant research recently regarding the role of antibiotics in natural ecosystems as signaling molecules and playing other important roles such as quorum sensing molecules influencing gene expression regulation, revealing the fact that we still remain highly ignorant regarding the ecological context in which these small molecules are made, how they function in natural settings, or how they evolved (55). Many of these compounds which are produced in very low proportions in ecosystems, compared to the already discovered natural molecules, are normally only activated under certain circumstances such as specific interspecies interactions through small-molecule compounds and remain silent under normal laboratory cultivation techniques (54).

In addition to the previously mentioned manipulation of cultivation parameters, external cues have been used to deviate cellular metabolism towards secondary metabolite production. This cues can either be naturally produced small-molecule compounds by interacting microorganisms, physical changes as heat or light, or chemical cues, such as batteries of drugs and therapeutic substances normally used for other purposes (43, 54). More specific chemical cues concern the use of antibiotics, or molecules strictly related to them, to elicit the production of secondary metabolites. Seyedsayamdost *et al* (2014) studies on *Burkholderia thailandensis*, using a collection of 640 well-characterized and biologically active compounds and screening them using a High-Throughput Screening (HTS) platform, proved that sub-inhibitory doses of antibiotic molecules, precisely β -lactam piperacillin, the dihydrofolate reductase inhibitor trimethoprim and two cephalosporins, ceftazidime and cefotaxime, acted as the best chemical elicitors to activate the silent *mal* biosynthetic cluster, responsible for production of the virulence factor malleilactone in the

mentioned bacterial species. Surprisingly, almost all elicitors discovered were antibiotics, suggesting they play an important role in modulating silent biosynthetic pathways (54).

As another case, *Challis* and collaborators (56) described the elucidation of the products of two BGC in the model actinomycete *S. coelicolor* M145. One of them is the siderophores coelichelin, which was induced by creating iron-deficient conditions in the culture media and later detected by modifying the culture medium with ferric ion (Fe^{+3}). Monitoring by HPLC analysis, at 435 nm absorbance which is the maximum absorbance wavelength for ferric tris-hydroxamate complexes, coelichelin was detected as the product of the cryptic or orphan gene cluster *cch*, through comparative metabolic profiling with a mutant lacking the inducible BGC. Its further structure elucidation was achieved, through high-resolution tandem MS.

These examples clearly show how such stresses, as sub-inhibitory doses of antibiotics or modifications in the culture medium, greatly influence the production of secondary metabolites and may allow the induction of otherwise silent BGC, allowing the exploration of their metabolic products (43). This might lead to a possible exploitation of the entire biosynthetic ability of the already explored microorganisms as well as from the less studied ones, opening an alternative path for active compounds discovery in the laboratory or HTS platforms, with innumerable possible combinations for eliciting cryptic clusters. A selection of new microbial-sourced active substances which have been reported or approved for commercial use in the last two decades, some of them using novel discovery techniques, is described in Table 1-1.

1.2.3 Exploring the total chemical space through metabolomics

The chemical space is defined as the multidimensional space occupied by all chemical compounds (9). The main technology used nowadays to study this chemical space or composition of a determined biological sample is metabolomics, described as the systematic, qualitative and quantitative analysis of all metabolites contained or produced in an organism at a specific time and under specific conditions.

Table 1-1. New antimicrobial drugs from natural sources reported during the last two decades (2000-2017) and their respective discovery technique

COMPOUND*	YEAR OF REPORT/APPROVAL	METHOD/TECHNOLOGY	CHEMICAL NATURE	SOURCE	SPECTRUM OF ACTION	REFERENCE
Lassomycin	2014	New cultivation techniques	Lasso peptides (ribosomically encoded cyclic peptides)	<i>Lentzea kentuckyensis</i> isolate IS009804	Mycobacteria (mostly <i>M. tuberculosis</i>)	(32)
Teixobactin	2015	New cultivation Techniques (iChip)	Depsipeptide containing D-aminoacids	<i>Eleftheria terrae</i>	Gram positives (<i>M. tuberculosis</i> , <i>S. aureus</i> , <i>Clostridium difficile</i> , <i>B. anthracis</i>)	(31)
Lugdunin	2016	Exploration of novel ecological niches (microbiome studies)	thiazolidine-containing cyclic peptide (Non-ribosomically synthesized)	<i>Staphylococcus lugdunensis</i>	Strong against Gram positives (<i>S. aureus</i> , <i>Streptococcus pneumoniae</i>), mild against Gram negatives (<i>E. coli</i> , <i>P. aeruginosa</i>)	(33)
Daptomycin	2003	Modified fermentations of soil microorganisms	Lipopeptides	<i>Streptomyces roseosporus</i>	Gram positives (mainly <i>S. aureus</i>)	(57)
Fidaxomycin	2007	Traditional fermentations of soil microorganisms	Macrocyclic lactone	<i>Dactylosporangium aurantiacum</i> subsp. <i>hamdenensis</i>	<i>C. difficile</i>	(58)
Halo-duracin	2006	Activation of silent BGC by heterologous expression	Two component-lantibiotic	<i>Bacillus halodurans</i> C-125	Gram positives	(59)

* All compounds' names are generic

Since the augmentation of methods for studying natural products is on the rise, new instrumental techniques offer alternative ways to directly screen this specific biochemistry produced during a situation of interest, such as an observed inducible bioactivity, a newly isolated species, an interaction evidencing a different phenotype (9). This approach gains more interest as it becomes the ultimate step in supporting insights on the gene function and biochemical status of an organism, acquired through genomics and transcriptomic assays; the ability of an organism to produce secondary metabolites is a phenotype and these metabolic phenotypes have been studied using metabolomics.

Examples of these new platforms started emerging over ten years ago, mainly in the fields of biomedical and agricultural research with the aims of obtaining metabolic profiling data, with the introduction of photo-diode arrays, along with HRFT-MS (high-resolution fourier-transform mass spectrometry) detectors that were coupled with HPLC (high-performance liquid chromatography), used as a pre-fractioning method in order to gain a better resolution of the entire biochemical arsenal obtained in a crude extract (9, 60, 61). Becoming a basic analytical technique, HRFT-MS along with NMR spectroscopy, are being the two mostly technologies used to dereplicate and quantify known metabolites against novel natural products (62, 63), even if dereplication is a massive task because of the complex and diverse atomic arrangements of secondary metabolites and bioactive compounds, which makes elucidating their structure challenging. A combination of analytical methods that includes ultraviolet spectroscopy, tandem mass spectrometry and NMR spectral data is used to ensure the correctness of the identification of the basic structure of dereplicated compounds in crude samples (64).

Although the use of metabolomics along with the active extract fractioning tools can help prioritize fractions for further purification, saving time and resources in isolating target compounds, the identification of the bioactive metabolites cannot always be done directly or by dereplication. Instead, there is a rapid progress on pioneering information technologies or bioinformatic platforms for practical and efficient analysis of large data sets of natural-product libraries (65-67). These innovative approaches to analyze mass spectrometry data such as MZmatch (68), MZmine (69), Global Natural Products Social Molecular Networking (GNPS) (70) and XCMS (71) among others, along with visualization tools like Cytoscape (72) can be used to construct differential expression analysis, with the aid of online databases such as ChemSpider, MarinLit and the Dictionary of Natural Products, or in-house databases as well (73). Differential expression analysis (69) involves a series of processes, including nonlinear retention-time alignment of compounds that are unique to the sample, followed by matched filtration of authentic peaks in mass spectra to the sample and against noise and background peaks (such as those resulting from solvents or media), to finally detect peaks associated to known metabolites and call a match or a chemical similarity to previously identified compounds (9).

While metabolomics is being applied to identify and biotechnologically optimize the production of pharmacologically active secondary metabolites (65), in order to properly attribute a bioactivity to a specific metabolite an obligate step forward is simplifying active extracts and making them more suitable for use in bioassays, by removing compounds that increase complexity; this is achieved through pre-fractionation the sample, from which

small quantities of an increased number of fractions can be later biologically tested using HTS (9, 74) The use of simplified fractions, together with sensitive NMR and HPLC-MS techniques has addressed the isolation and structure-elucidation bottleneck in bioactive natural products discovery (74).

A clear example of a novel bioactive NP discovery using metabolomics is the study by Olivon *et al* (75). The authors prioritized high potential value molecules (the ones with chemical novelty and potential biological activity), from crude extracts of 292 Euphorbiaceae specimens from New Caledonia, using massive molecular networks embedding various informational layers, as taxonomic information and reported bioactivity. Data for networks construction came from NPs extracts library for this botanical family, and the targets for bioactivity where the oncogenic Wnt signaling pathway and the chikungunya virus (CHIKV) replication. Prioritized nodes and clusters from the analysis of the molecular network, led to the selection of various molecular features from two plant species (*Neoguillauminia cleopatra* and *Bocquillonia nervosa*), which were later isolated through guided MS. Some of the Isolated compounds proved to be novel NPs, that exhibited anti-cancer and anti-viral activities in the micro- to nanomolar ranges.

1.3 Conclusion

Given the challenge that discovery of novel antibiotics from microbial sources presents, this thesis describes progress towards the characterization of phenomenon of inducible antibiotic activity observed in *Bacillus* sp. strains against the destructive plant pathogen, *R. solanacearum* and other bacterial species, only in the presence of a chemical inducer, triphenyltetrazolium chloride (TTC) in the culture media. The discovery and first observation of this phenomenon is described in the following chapter and further chapters contain the findings from conducted research towards its biochemical, molecular and metabolomic characterization. Classical microbiology analytical assays were performed, along with diverse techniques as total RNA isolation and sequencing, nanoString transcriptomics, chemical extractions and metabolomics using UPLC-MS followed by bioinformatic analysis through specialized platforms, with the final aim of setting the basis for reaching the further elucidation of the responsible compounds, contributing to the discovery of novel active natural substances with future applications.

CHAPTER 2

2. Background

Abstract

A collection of 1493 aerobic endospore forming bacteria (AEFB), mostly belonging to order Bacillales, was screened for their *in vitro* activity against plant pathogens of *Musa* sp., among which bananas stand out for the social and economic importance derived from its commercialization. Among these pathogens were the saprophyte *Serratia marcescens* and *Ralstonia solanacearum*, the last one being an important phytopathogenic bacterium that affects other crops besides bananas, producing the bacterial wilt disease. Triphenyl tetrazolium chloride (TTC) is a redox indicator used traditionally in culture media as a mild antibiotic against Gram positive bacteria and viability indicator of isolated colonies, as was the case for *R. solanacearum* isolation. In previous steps of this research, the antagonism of the collection of AEFB was determined against *S. marcescens* and *R. solanacearum* in the presence of TTC, observing that almost 99% of the tested strains produced an inhibition zone against either one of the Gram-negative target bacteria. When TTC was removed, only half of the tested strains retained antimicrobial activity, leading to hypothesize that TTC was acting as an inducer of antimicrobial substances in certain AEFB species and setting a start point for the next steps of this research.

2.1 Introduction

In the frame of collaborative research projects between the association of commercial banana producers of Colombia (AUGURA), through its research center (CENIBANANO), and Universidad EAFIT, a collection of 1496 aerobic endospore forming bacteria (AEFB) was established (Humboldt Institute Collection N° 191), isolated from the rhizosphere and phyllosphere of banana and plantain plants in Urabá region, Antioquia during 2009 (76-78). The main objective was to formulate sustainable crop protection solutions for the banana industry based on microorganisms and their metabolites. Thus, the activity of these strains was tested against various phytopathogenic organisms affecting banana crops (79). Until the present day, the majority of natural products discovered has come from organisms that inhabit the soil, among these actinomycetes (e.g. *Streptomyces*) and Firmicutes (e.g. *Bacillus*) are the most important sources, along with filamentous fungi (35, 80, 81). Within Firmicutes, several species of *Bacillus* harbor a high capability of producing bioactive molecules, such as peptide antibiotics, and are capable of growing in varied environments,

exhibiting considerable genomic diversity, especially the highly studied *B. subtilis* (82-84). Besides this, *Bacillus* sp. and other AEFB were selectively isolated through heat shock for this collection, since they are considered a safe biological agent, they have an ability to sporulate and to be later formulated into bioproducts (37, 85).

2.1.1 Importance of the target pathogen: *R. solanacearum* and Moko disease

Bacterial and other soil borne diseases, like the ones caused by *R. solanacearum*, are considered to be more limiting than seed-borne or air-borne diseases in the production of many crops and account for 10–20% of yield losses annually (86). This phytopathogenic species, is the second most devastating bacterial soil pathogen along with other ten bacterial species that are listed based on their scientific and economic importance in plant diseases, these being in order of importance: *P. syringae* pathovars, *R. solanacearum*, *Agrobacterium tumefaciens*, *Xanthomonas oryzae* pv. *oryzae*, *X. campestris* pathovars, *X. axonopodis* pathovars, *E. amylovora*, *Xylella fastidiosa*, *Dickeya* (former *Erwinia*) (*dadantanii* and *solani*), *Pectobacterium* (former *Erwinia*) *carotovorum* and *P. atrosepticum* (87). It causes bacterial wilt disease in over 250 hosts from 54 botanical families in a broad geographic distribution (88). *R. solanacearum* is a pathogen with high genetic diversity, for which it had been traditionally considered a species complex composed of four phlotypes (I to IV), that corresponded to evolutionary and geographic origin, called the *R. solanacearum* species complex (RSSC) (89), but more recent studies by Prior *et al.* (90) confirm through proteomics and genomic comparisons that there is enough evidence to confirm evolutionary distance considering the existence of three different species of this RSSC. This genetic variability makes the control of the pathogen difficult to address in all affected crops as are tomato, potato and other economically important plants belonging to the Solanaceae family, as well as bananas, plantains and ornamental *Heliconia* plants (88, 91); along with its ability to persist in the environment, either in waters, shallow and deep layers of soils or temporary hosts such as weeds, its rapid spread through xylem and endophytic growth, and broad host range (92).

The disease this pathogen causes in *Musa* sp. species like bananas and plantains, called Moko disease, brings severe constraints to crop production in commercial plantations, an activity of high economic and social importance in the world. For instance, bananas constitute the most exported fresh fruit representing an economic activity of US\$10 BN/year (93) and they are an essential source of income for thousands of rural households in developing countries, with top main producers being the Philippines, Ecuador, Costa Rica and Colombia. However, agrochemical-intensive production along with declining producer prices has given rise to many environmental and social challenges (93). In Colombia, 47.000

ha of cultivated land are exclusively destined to bananas production for exportation, deriving in earnings accounting for US\$ 811,6 millions (MM) in 2016 (94) and about 14.000 ha are destined to national consumption (95). The social impact of bananas production is also of great importance providing approximately 120.000 jobs, being the primary source of income for about 100.000 families (96). Plantains are also a relevant agricultural product for Colombia, highly affected by Moko disease, with about 394.000 ha planted and 3.5 MM metric tons being produced during 2016 either for exportation or for supplying national demand, representing an income of US\$46,6 MM coming only from exportations (94, 95, 97).

The control for Moko disease, in the case of Colombia, which has reached 100% of devastation on severe cases (98) is done through the application of a 20% solution of the herbicide glyphosate to the infection foci reaching a final desiccation of the plant after several weeks of decay, killing all living tissue that could be a host for the pathogen. Glyphosate is not only applied to the infected plant but to the near-by ones in a 5 meter radius, as well as to the weeds that could emerge in this “quarantined” zone. The plants inside a 10 m ring from the infection foci are kept under daily surveillance for the appearance of Moko disease symptoms, avoiding the pathogen’s spread around the rest of plantation (99, 100). The costs of maintaining and replanting the quarantined zones reach approximately US\$ 150.000/ha/year plus the loss of earnings which extends for 15 months, from the infection center detection until the next production batch comes out, representing around 2.500 boxes/ha with an economical value of US\$ 8 each one, for a total of US\$ 20.000/ha (98, 100).

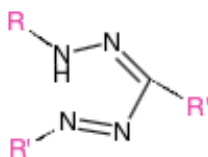
The need for development of sustainable and more efficient solutions for controlling this pathogen is a priority. By focusing research in the discovery of new active molecules or compounds against *R. solanacearum*, which come from different sources like microorganisms, a step ahead is given in the quest for alternative control methods of this devastating pathogen.

2.1.2 Tetrazolium salts

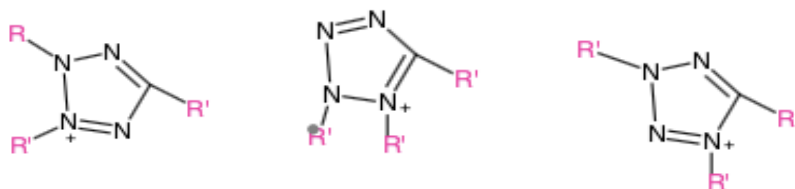
Tetrazolium salts, first described in the last decade of the nineteenth century, which change from colorless or weakly colored aqueous solutions when oxidized, to brightly colored derivatives known as formazans when reduced, have been used as vital dyes in redox histochemistry and in biochemical applications for more than half a century (101). They are synthetically generated from formazans, being then both molecules intimately related (102, 103). Diverse compounds of this class have been employed throughout history in

experimentation comprising cell cultures, ranging from ditetrazolium salts such as nitroblue tetrazolium (NBT) that form insoluble formazans to more favored monotetrazolium salts, the most widely used being 3-(4,5-dimethylthiazol-2-yl)-2,5-diphenyltetrazolium bromide (MTT), which also forms an insoluble formazan (102). In fact, most of the historically used tetrazolium salts form insoluble formazans, so they have been normally applied in endpoint assays; by contrast, most recently developed ones, are used in conjunction with intermediate electron acceptors (IEAs) that facilitate dye reduction. These tetrazolium salts form soluble formazans and consequently can be used in real time assays (104). Intensive interest among biologists, technologists, chemists and other specialists on formazan molecules has been mainly due to their characteristic skeleton (Fig. 2-1) known as azohydrazone group, which has chemical versatility and chelating properties (101, 105) and to their flexible applications in histochemistry, cell biology, biochemistry and biotechnology (104) as an indicator of the respiratory state of the cells given that they measure the integrated pyridine nucleotide redox status of cells, with the reduction of these compounds likely involving reaction with NADH or similar reducing molecules that transfer electrons to the tetrazole molecule (106).

Figure 2-1. Formazan molecular skeleton: open tetrazole ring or azohydrazone group



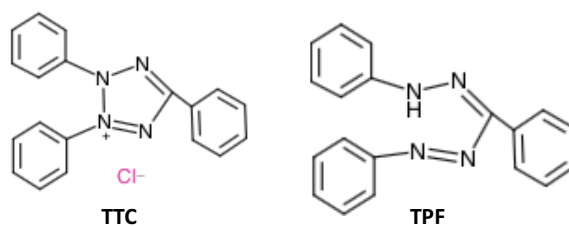
Different from formazans, tetrazolium salts are quaternized tetrazoles and therefore contain a ring of one carbon and four nitrogen atoms, one of which is quaternary, hence being positively charged and having as a result salt-like properties, like dissociation in water and other solvents. The chemical structural possibilities of these tetrazole rings are as diagrammed in Figure 2-2 (102).

Figure 2-2. Tetrazole ring conformations

A wide variety of C-atoms substituents have been introduced chemically to tetrazoles, yielding tetrazolium salts when combined with a halogen atom, like chlorine (Cl) or iodine (I). Most of the reported tetrazolium salts have aryl or chemical functional groups derived from an aromatic ring in this free C-position (R' in Fig. 2-2), as well as in the two others from nitrogen atoms (the two R 's bonded to N in Fig. 2-2). In fact, the term formazan is derived from naming the compound which is derived from the reduction of the tetrazolium salt triphenyl tetrazolium chloride (TTC), having three phenyl groups as radicals in the C-position and in the two nitrogen atoms, deriving the term “phorm-Azyl” or “formazyl” which evolved to formazan (102). The biological properties of tetrazolium salts, depend on the positively charged quaternary tetrazole ring core containing four nitrogen atoms, or in the net charge of the moiety comprising this tetrazole ring (104). The named “second generation tetrazolium dyes” have been modernly synthesized by substituting positions in the original phenyl radicals or by substituting different radicals in the C and N atoms by different chemical groups, as are for instance sulfonates in the compound sodium 2,3,-bis(2-methoxy-4-nitro-5-sulfophenyl)-5-[(phenylamino)-carbonyl]- 2H-tetrazolium (XTT), causing this tetrazolium salt to have a negative net charge (107). In conclusion, all these modifications have resulted in compounds with a range of different properties that cause distinctive responses in the cells and thus, have been applied both qualitatively and quantitatively in an variety of biological measuring systems (Table 2-1) (104).

2.1.3 Triphenil tetrazolium chloride (TTC)

The prototype tetrazolium salt compound is known as triphenyl tetrazolium chloride (TTC), first synthesized more than a century ago (102, 104, 108). It is a white-yellow powder, water-soluble compound when oxidized, but its formazan, namely Triphenyl Formazan (TPF) is highly insoluble in aqueous solvents (Fig. 2-3). This first tetrazolium salt has been modified in many ways over the years by adding nitro, iodo and methoxy groups to the phenyl rings, thus yielding the large diversity of tetrazolium salts available in the present-day (104), some of them exemplified in Table 2-1.

Figure 2-3. Molecular structures of oxidized TTC and reduced TPF.

In respects to its reduction mechanism, it has been deduced by some experimentation in the area that monotetrazolium salts that more readily enter cells, as is TTC as well as MTT and 2-(4-iodophenyl)-3-(4-nitrophenyl)-5-phenyl tetrazolium chloride (INT), are reduced by NADPH-dependent oxidoreductases and dehydrogenases of metabolically active cells, more than by Complex I and Complex II or flavin-containing enzymes, as was thought for a long time (104). As different microorganisms have different dehydrogenase systems, it may be possible that not all dehydrogenase systems are capable of using TTC. Results by Smith & McFeters (109) clearly suggest that the dehydrogenase system of most fungi is not capable of using TTC as an electron acceptor, being its reduction much lower than in bacteria and actinomycetes; a hypothesis for this behavior might be the lower diffusion of this compound inside fungal cells due to the structure of the cell wall and cell membrane.

2.1.4 Traditional use of TTC in microbiology

The biological reduction of tetrazolium derivatives by cellular redox systems to insoluble colored derivatives has been used to measure viability within a number of living systems including seeds (110), frozen vegetables, protoplasts and cultured cell (111) and other vegetables tissues, under various conditions including imposed stresses (112). Its use on microbiology has been reported since the first half of the past century, with Lederberg in 1948 (113) reporting its addition to culture media in order to detect phenotypic changes in *E. coli* mutants. Its subsequent incorporation in other experimental sets, in a varied display of applications, ranging from the rapid detection of phenotypic colony variations and extracellular polysaccharide production to determination of microbial activity in soils (114, 115) as well the monitoring of viability in medically and agriculturally important pathogens (116), was rapidly executed in the subsequent years. Although, its use nowadays limited to cultivatable microbial colonies and sometimes, allows to enhance colony differences so that microbial diversity can be assessed, a specific example of this being BIOLOG plates (117) .

Overall, the main applications of TTC in microbiology are monitoring cell viability through respiratory activity and colony differentiation.

Table 2-1. Tetrazolium salts employed in biochemistry: commercial names and molecular structures

MOLECULE NAME*	COMMERCIAL ABBREVIATION	MOLECULAR STRUCTURE
3-(4,5-dimethylthiazol-2-yl)-2,5-diphenyltetrazolium bromide	MTT	
2,3,5-triphenyl-2H-tetrazolium chloride	TTC	
2-(4-iodophenyl)-3-(4-nitrophenyl)-5-phenyl-2H-tetrazolium chloride	INT	
Nitrotetrazolium Blue	NBT	
5-cyano-2,3-ditolyl tetrazolium chloride	CTC	
sodium 2,3-bis(2-methoxy-4-nitro-5-sulfophenyl)-5-[(phenylamino)-carbonyl]-2H-tetrazolium	XTT	
sodium 5-(2,4-disulfophenyl)-2-(4-iodophenyl)-3-(4-nitrophenyl)-2H-tetrazolium inner salt	WST-1	
5-[3-(carboxymethoxy)phenyl]-3-(4,5-dimethyl-2-thiazolyl)-2-(4-sulfo-phenyl)-2H-tetrazolium inner salt	MTS	

2.1.5 Use of TTC in antagonism screenings against *R. solanacearum*

The traditional isolation of *R. solanacearum* strains from infected tissue, is performed in a medium named BGT, which is originally amended with 50 mg/L of the tetrazolium salt TTC and was first described by Boucher *et al.* (118). This practice has been replicated since then in a large number of studies compromising any of the four phylotypes of the pathogen (92, 119-121). When a bacterial stream of *R. solanacearum*, exuding from infected tissues, is streaked on medium containing TTC, round to oval shape, fluidal colonies with pink or red center can be observed 48 h after incubating at 30 °C (Table 2-2); the unique colony type on TTC is a key for diagnosis and has been used as well for isolating virulent strains of other phytopathogenic bacteria, such as *Erwinia amylovora*, causal agent of fire blight (92, 114). Even though, given this TTC employment for isolation, the media used for screening of growth inhibition or antagonistic activity produced by other bacteria against *R. solanacearum* do not employ this amendment and antagonistic tests are usually performed in BG agar or media of similar composition, without TTC (122, 123). Up to date, there are no previous records of screening of activity from any bacterial species against *R. solanacearum* in the presence of TTC.

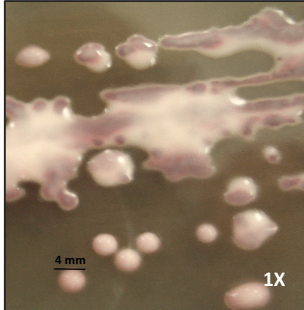
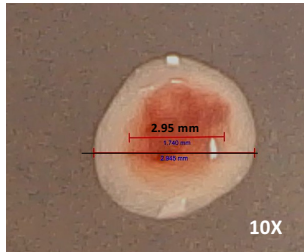
Finally, the main objective of this chapter was to consolidate the information available from previous studies done by the research group, on the observation of an inducible antagonism produced by some AEFB strains uniquely in the presence of 50 mg/L of TTC in the medium, against *S. marcescens* and *R. solanacearum*.

2.2 Methods

2.2.1 Microorganisms

The 1493 AEFB strains that belong to collection N° 191 of Humboldt Institute, stored in TSB (trypticase soy broth, Merck) with 20% v/v glycerol at -80 °C, were activated in TSA (Merck) for 48 h at 30 °C. *R. solanacearum* strain EAP09 (GenBank accession no. KU603426) and *S. marcescens* (GenBank accession no. KU603427), isolated from infected corm tissue of a banana plant, were stored in BG medium (118, 124) with 20% glycerol at -80 °C and activated in BGA (118) (composition for 1 L: 10 g of special peptone (Oxoid), 5 g glucose, 1 g casaminoacids, 1 g yeast extract, 18 g agar) at 30 °C for 48 - 72 h before preparation of the inoculum for activity trials.

Table 2-2. Colony appearance of *R. solanacearum* isolates on BGTA

ISOLATE NAME, ORIGIN AND REFERENCE	COLONY APPEARANCE IN BGT AGAR
<p>AW1 strain, a N^x derivate of a wild-type (WT) tomato isolate (Dr. Timothy Denny, University of Georgia, Athens) (125)</p>	
<p>EAP09 strain, isolated from infected banana plant tissues (María Ramirez, Universidad EAFIT)</p>	

N^x: Nalidixic acid resistant

2.2.2 Activity Trials

The screenings of AEFB against strains of *R. solanacearum* and *S. marcescens*, on which the phenomenon for the present research was observed, were performed following a modified methodology previously described (126). Briefly, 100 μ L of the target strain suspension in distilled sterile water containing 10^6 CFU/mL was spread on BGTA (BG medium plus 1.6% agar and 50 mg/L (ppm) TTC). Afterwards, a 5 mm disc of each AEFB, grown in TSA for 48 h at 30 °C, was transferred onto the BGTA and incubated at 22 °C. Inhibition growth was assessed by measuring the radius (mm) of the growth inhibition zone after incubation for 48 h in the case of *S. marcescens* and 72 h for the case of *R. solanacearum*, using 2 replicates per treatment. The strains that reported a positive activity on BGTA were later assessed in BGA (with no TTC) as well.

2.3 Results

2.3.1 Screening of AEFB strains collection against *Musa* sp. pathogens

During the screening of the collection of AEFB, the ability of all strains to inhibit other Gram negative bacteria, was first assessed against *S. marcescens* EAD-005, in a medium containing TTC as a redox indicator as described above. Results suggested that 47 strains, representing 3.1% of the total number of strains of the AEFB collection were antagonist of *S. marcescens* EAD005 in BGTA. The same 47 strains plus 28 added strains, corresponding to different morphologies, were screened against *Musa* sp. pathogen *R. solanacearum*, proving that 98.7% of them produced growth inhibition zones against this phytopathogen. The initial 47 strains which were active in TTC presence both against *S. marcescens* and *R. solanacearum* shared the same morphology in 50% TSA, and amid the identified ones, the majority belonged to 'operational group *B. amyloliquefaciens*' (supplementary material Table S-1). Given the high percentage of antagonists encountered in TTC presence, the redox indicator was removed from the medium. When growth inhibition was tested in the absence of TTC in the medium (BGA), for the initial 47 strains plus 57 different ones from the collection, belonging to different morphologies, the number of antagonistic strains decreased to 58.7% (Figure 2-4).

The group of 58 strains which retained activity against *R. solanacearum* even in the absence of TTC, includes the initial 47 active strains and thus, probably the majority of them belong to 'operational group *B. amyloliquefaciens*' (127), recognized for its lipopeptides producing capacities (128). Among the other 46 strains which were not active in TTC absence, a group of 8 strains had been evaluated both in the presence and absence of TTC and evidenced antagonistic capacity only when TTC was present in the medium (Table 2-3, Figure 2-5). These strains belong to other *Bacillus* species; among the identified ones are *B. subtilis* and *B. cereus* group species (Table 2-3, supplementary material Table S-1). Is within these species then, that the production of inducible antimicrobial compounds in TTC presence is stronger and more evident (Fig. 2-5).

Figure 2-4. AEFB strains antagonistic to *S. marcescens* and *R. solanacearum* in TTC presence and absence

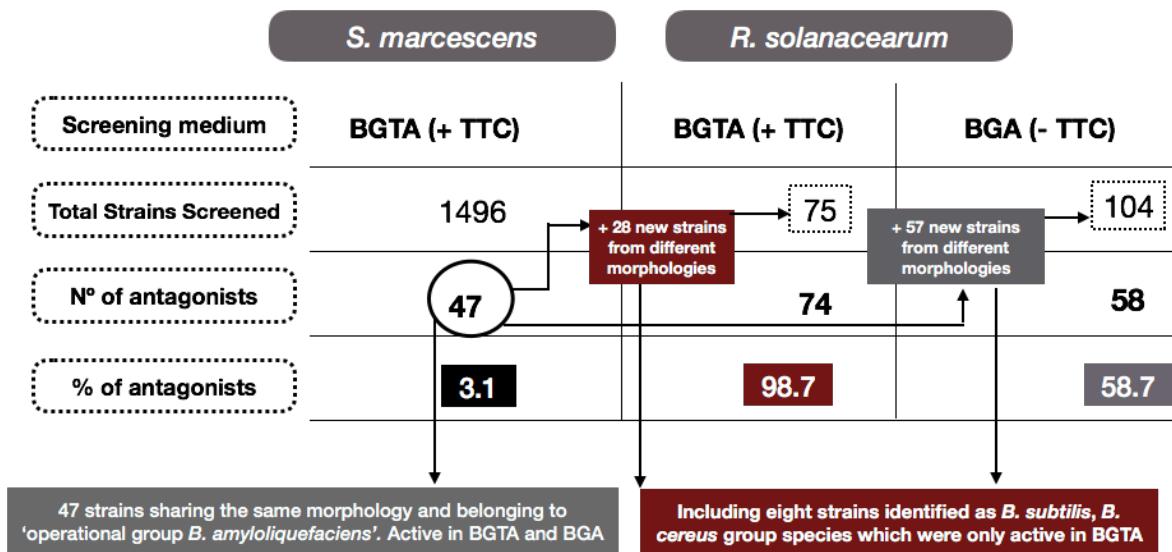
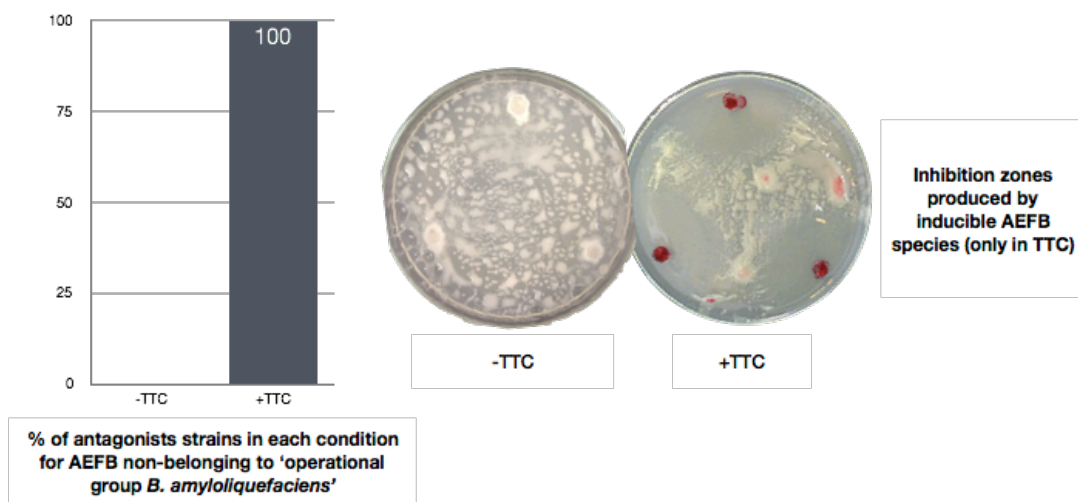


Table 2-3. Group of AEFB strains evaluated both in the presence and absence of TTC

STRAIN	MOLECULAR ID BY 16S rDNA	INHIBITION ZONE		
		AGAINST	INHIBITION ZONE AGAINST	
		<i>S. marcescens</i> (mm)	<i>R. solanacearum</i> (mm)	
		BGTA (+TTC)	BGTA (+TTC)	BGA (-TTC)
EA-CB0575	<i>B. subtilis</i>	0.0 ± 0.0	11.0 ± 0.0	0.0 ± 0.0
EA-CB0015	<i>B. subtilis</i>	0.0 ± 0.0	6.0 ± 0.0	0.0 ± 0.0
EA-CB0586	<i>B. subtilis</i>	0.0 ± 0.0	8.0 ± 2.0	0.0 ± 0.0
EA-CB1047	<i>B. cereus</i>	0.0 ± 0.0	12.0 ± 1.0	0.0 ± 0.0
EA-CB1465	NI	0.0 ± 0.0	≥ 25.0	0.0 ± 0.0
EA-CB1473	NI	0.0 ± 0.0	≥ 25.0	0.0 ± 0.0
EA-CB1486	<i>B. subtilis</i>	0.0 ± 0.0	13.0 ± 1.0	0.0 ± 0.0
UA321	<i>B. subtilis</i>	0.0 ± 0.0	12.0 ± 1.0	0.0 ± 0.0

NI: strain not yet identified

Figure 2- 5. Inducible antagonism potential in TTC presence of AEFB strains non-belonging to ‘operational group *B. amyloliquefaciens*’ against *R. solanacearum*



2.4 Conclusions

The phenomenon of induced antimicrobial activity produced by AEFB, especially from *Bacillus* species different from the ones belonging to ‘operational group *B. amyloliquefaciens*’ in the presence of TTC, suggests either an induction in the production of antibiotic substances in these bacterial species or a biotransformation of this molecule or its reduced product TPF, by AEFB, into antimicrobial compounds.

A series of trials were performed to characterize the biological systems producing the inducible antagonistic activity against *R. solanacearum* and other target species. All of these results are exhibited in the following chapters.

CHAPTER 3

3. Characterization of the Inducible Antagonism System

Abstract

A series of strains, mostly AEFB belonging to different *Bacillus* species, were tested for their production of inducible inhibition zones only in the presence of TTC, against several potentially target species, with *R. solanacearum* as main target. Even though all the strains tested belonging to the order Bacillales evidenced a capacity for producing inducible inhibition zones against *R. solanacearum* and other Gram negative and Gram positive strains, *B. cereus* EA-CB1047 and *B. pumilus* EA-C0009 stand out for having the highest inducible potential, observable both in solid and liquid media but stronger in solid media, thus the rest of trials were performed in this last media. Kinetics analysis among other assays demonstrated that the main target pathogen, *R. solanacearum*, does not have increased sensitivity in the presence of the inducer and that its presence is not needed for *Bacillus* cells to produce an inhibition zone, observable instead due to the secreted inducible substances diffused to culture medium by *Bacillus* cells. TTC acts as the main inducer among other chemically similar substances and has an inhibitory effect on certain *Bacillus* species at concentrations above 100 ppm. Knockout mutant strains of *B. subtilis* NCIB-3610, silenced on the central genes for the synthesis of some of the most studied secondary metabolites from *Bacillus*, were tested for their inducible inhibition zones production capacity, with none being defective or significantly overinduced. This indicates that the chemical nature of the inducible antimicrobial substances may not belong to these well-characterized biosynthetic routes and that TTC, when applied at sub-inhibitory concentrations to the medium, acts as an inducer of antagonism, perhaps by accumulation of intracellular TPF or activation of silent biosynthetic gene clusters or non-characterized ones.

3.1 Introduction

Besides being a species with versatile applications due to its ability to form endospores, the resistant structures which confer them survival capacity over long periods and prolonged shelf life, *Bacillus* sp., above other AEFB, are widely known for their capacity for producing diverse bioactive secondary metabolites (37, 82). The vast majority of secondary metabolites produced by *Bacillus* sp. are antibiotic peptides which possess diverse functions, including the capacity of being effective chemotherapeutic agents in the

treatment of animal diseases. Some of these metabolites are involved in the distinctive morphological, physiological and habitat survival traits of the microorganism (81, 129, 130). Besides peptide antibiotics, several species of *Bacillus* sp. produce other non-peptide compounds such as polyketides, which are the basis of numerous human and veterinary drugs; plant-growth hormones, terpenoids, isocoumarins, all of them being compounds that have proven to be effective agents against molds and yeasts (81) and could also express activity towards other microbial or nonmicrobial infective agents of plants and animals. Other renowned substances produced by *Bacillus* sp. are lipopeptides, which represent the family of peptide antibiotics that are synthesized by large nonribosomal peptide synthetases (NRPS) (131) and are composed of a hydrocarbon chain linked to a short cyclic oligopeptide. *Bacillus* sp. strains coproduce various families of lipopeptides such as surfactin, iturin and fengycins (83). These NPs are active against a broad spectrum of biological targets, with iturins evidencing strong *in vitro* activity against fungi and yeasts, as well as fengycins which are strong antifungals highly employed in plant protection against filamentous fungi. But are surfactins the ones with the broadest reported bioactivity, being active *in vitro* against Gram positive and Gram negative bacteria, virus, mycoplasmae and larvae (132).

In addition to these families of compounds, Bacillales species still hold a great explored potential for discovery of new bioactive substances, with about 4–5% of a *B. subtilis* genome considered to be devoted to secondary metabolites production (130), indicating that there is still potential for novel compounds to lie undiscovered in the genomes of microorganisms belonging to families such as Bacillaceae and Paenibacillaceae. Beyond the already known sets of biosynthetic genes, there could be plenty more classes of compounds to look into through modern bioactive compounds discovery techniques.

The collection of NPs which have been isolated from Bacillales, have demonstrated to be active *in vitro* against important Gram negative pathogens, as are phytopathogenic strains of *Xanthomonas* sp. and *Pseudomonas* sp (133). Specifically, lipopeptides from *Bacillus* sp., have broad-spectrum antibiotic properties against some multi-drug resistant bacteria (128) and other human pathogens as *S. enterica* (130). Among Gram negative bacterial species, several stand out because of their harmful effects to plants and/or animals, among them *X. campestris* (134), *P. carotovorum* (135), *P. syringae* (129), *Agrobacterium tumefaciens* (136) in agriculture, as well as *K. pneumoniae*, *E. coli*, *Salmonella* sp., *P. aeruginosa*, *S. marcescens* and *S. aureus* in humans and other animals, with important strains from these species considered as priority pathogens by the World Health Organization (23) due to their high antibiotic-resistance and for being considered common community bacteria, in most cases. According to this WHO report, prioritization of these pathogens should guide research and

development of new antibiotics. Accordingly, strains of selected species belonging to this list were tested for their susceptibility to the inducible antimicrobial compounds from *Bacillus* sp.

The main objective of this chapter was to perform biochemical and microbiological analysis in order to identify the main traits which define the observed inducible antagonism phenotype and the most favorable conditions for its production.

3.2 Methods

3.2.1 Strains screened for inducible antagonism potential

Selected species of the 1496 AEFB strains collection (Humboldt Institute Collection N° 191) were chosen among the ones identified by 16S rDNA gene sequencing. Strains from selected Gram negative species were also included, with the aim of testing the specificity of the inducible antagonism (Table 3-1). All strains were stored in TSB (trypticase Soy Broth Merck) and glycerol (20% v/v) at -80 °C. Further activation in 50% TSA (Merck) and incubation for 48 h at 30.0 ± 0.5 °C was done before any experimental use. WT of *B. subtilis* strains 3610, SMY, PY79 (Table 3-1) and 3610 knockout mutants (Table 3-2) were employed in a series of trials, donated by Dr. Roberto Kolter from Harvard Medical School. These strains were activated in LB agar (composition for 1 L: tryptone (Oxoid) 10 g, NaCl (Merck) 10 g, yeast extract (Oxoid) 5 g, agar (BD) 15 g), conserved and activated in the same way as the rest of strains.

3.2.2 *R. solanacearum* and other target strains

R. solanacearum EAP09 was isolated from infected tissues of banana plants as previously described (137) and identified by 16S rDNA gene sequence (GenBank accession no. KU603426). Stored in BG medium (118, 124) with 20% glycerol at -80 °C, it was activated in BGA (118), and incubated at 30.0 ± 0.5 °C for 72 h before preparation of inoculums. *R. solanacearum* AW1, a nalidixic acid resistant strain derived from a WT isolate from tomato, was donated by Dr. T. Denny from University of Georgia (125), conserved and activated in the same way as strain EAP09. Other target strains comprised *P. putida* UA-0095, *Xanthomonas* sp. UA-1539, *B. cepacea* UA-1541, *S. marcescens* UA-1538, donated by Dr. Camilo Ramirez from Universidad de Antioquia; *Salmonella* sp. ATCC 14028, *S. aureus* and *E. coli* DH5 were part of the biotechnology lab at Universidad EAFIT strains collection and *Pectobacterium* sp. strain was donated from the Kolter Lab at Harvard Medical School. These target strains evaluated are listed in Table 3-3.

Table 3-1. AEFB and other Gram negative strains employed as antagonists for the characterization of the antimicrobial inducible behavior

SPECIES/GENUS	STRAINS	ORIGIN	COLLECTION /DONATOR
Gram positives			
<i>B. cereus</i>	EA-CB 1047	P	Humboldt Institute Collection N° 191
	EA-CB 0012	R	Humboldt Institute Collection N° 191
<i>B. pumilus</i>	EA-CB 0009	R	Humboldt Institute Collection N° 191
	EA-CB 0177	P	Humboldt Institute Collection N° 191
<i>B. megaterium</i>	EA-CB 0185	R	Humboldt Institute Collection N° 191
	EA-CB 1057	P	Humboldt Institute Collection N° 191
<i>Paenibacillus pasadenensis</i>	EA-CB 840	P	Humboldt Institute Collection N° 191
<i>B. subtilis</i>	EA-CB 0015	P	Humboldt Institute Collection N° 191
	EA-CB 0575	R	Humboldt Institute Collection N° 191
	NCIB 3610	N	BGSC
	SMY	N	BGSC
<i>B. amyloliquefaciens</i>	EA-CB 0959	P	Humboldt Institute Collection N° 191
<i>B. altitudinis</i>	EA-CB1450	P	Humboldt Institute Collection N° 191
	EA-CB 0686	R	Humboldt Institute Collection N° 191
<i>B. licheniformis</i>	ATCC14580	So	Kolter Lab strains collection
<i>B. simplex</i>	ZK5093	N	Kolter Lab strains collection
<i>B. thuringiensis</i> subsp. <i>Darmstadiensis</i>	ZK5165	N	Kolter Lab strains collection
<i>B. coagulans</i>	ZK5189	S	Kolter Lab strains collection
<i>B. lentus</i>	ZK5173	Si	Kolter Lab strains collection
<i>Marinibacillus marinus</i>	ZK5187	N	Kolter Lab strains collection
<i>B. firmus</i>	ZK5172	So	Kolter Lab strains collection
<i>Aeribacillus palidus</i>	ZK5191	N	Kolter Lab strains collection
Gram negatives			
<i>Delftia tsuruhatensis</i>	UA-1537	B	Dr. Camilo Ramírez. Universidad de Antioquia
<i>Herbaspirillum seropedicae</i>	UA-1542	B	Dr. Camilo Ramirez. Universidad de Antioquia
<i>Burkholderia cepacea</i>	UA-1541	B	Dr. Camilo Ramirez. Universidad de Antioquia
<i>Pseudomonas putida</i>	UA-0095	B	Dr. Camilo Ramirez. Universidad de Antioquia
<i>Serratia marcescens</i>	UA-1538	B	Dr. Camilo Ramírez. Universidad de Antioquia

P: phylloplane of banana plants from commercial plantations. R: Rhizosphere of banana plants from commercial plantations. B: Moko infected tissues from banana plants. BGSC: Bacillus Genetic Stock Center, Columbus, OH. N: Unknown. S: sediments. Si: Symbiont of gram negative *Xenorhabdus*. So: soil.

Table 3-2. Knockout mutants on selected genes from *B. subtilis* NCIB-3610 WT

GENOTYPE	STRAIN CODE	* KNOCKOUT GENE MAIN FUNCTION
<i>spo0A::erm</i>	ZK385	Stage 0 sporulation protein
<i>kinA::mIs, kinB::kan, KinC::cat</i>	ZK3706	Sporulation kinases A, B, C
<i>KinA::mIs</i>	ZK5157	Sporulation kinase A
<i>KinB::cm</i>	ZK5158	Sporulation kinase B
<i>KinC::cm</i>	ZK5159	Sporulation kinase C
<i>degS::tet</i>	ZK3737	Signal transduction histidine-protein kinase/phosphatase DegS
$\Delta degU$	HV1130	Transcriptional regulatory protein DegU
<i>abrB::tet</i>	ZK4279	Transition state regulatory protein
$\Delta pksX$: <i>specR</i>	ZK3640	Polyketide synthase involved in bacillaene production
<i>sinI::spc</i>	ZK4200	Transcriptional regulator. Nutrient depletion and development
<i>ppsB</i> Ω <i>Tn10</i> : <i>specR</i>	ZK3639	Biosynthesis of the lipopeptide antibiotic plipastatin
$\Delta bacA$	NL363	Synthesis of dipeptide antibiotic bacilysin
<i>srfAA::erm</i>	ZK3858	Surfactin synthase subunit-1
<i>comA::cat srfA-lacZ</i>	ZK3863	Transcriptional regulator (quorum-sensing and competence)
<i>sunA::erm</i>	NL384	Bacteriocin sublancin
<i>eps :: tet tasA :: km comX :: spc</i>	ZK3771	Competence pheromone (quorum-sensing system)
<i>skf :: cm</i>	ZK3748	Sporulation killing factor (toxin)
<i>sdp :: spc</i>	ZK3749	Sporulation delaying protein (toxin)
<i>codY::spc</i>	NL3864	Transcriptional repressor. Nutritional limitation sensor
$\Delta sigH$	NL161	RNA polymerase sigma-H factor. Transcriptional regulator
$\Delta sigD$	NL165	RNA polymerase sigma-D factor. Transcriptional regulator
$\Delta sigE$	NL166	RNA polymerase sigma-E factor Transcriptional regulator
$\Delta sigX$	NL167	RNA polymerase sigma-X factor Transcriptional regulator
$\Delta sigY$	NL361	RNA polymerase sigma-Y factor Transcriptional regulator
$\Delta sigW$	NL362	RNA polymerase sigma-W factor. Transcriptional regulator

*Source: (www.uniprot.org/uniprot/P08874) (138)

Table 3-3. Target bacterial strains tested for their sensitivity to the inducible antimicrobial activity from *Bacillus* sp.

SPECIES/GENUS	STRAINS	ORIGIN	COLLECTION/ DONATOR
<i>Xanthomonas</i> sp.	UA-1539	B	Dr. Camilo Ramirez. Universidad de Antioquia
<i>Ralstonia solanacearum</i>	AW1	T	Dr. Tim Denny. University of Georgia
<i>Ralstonia solanacearum</i>	EAP09	B	Universidad EAFIT strain collection
<i>Escherichia coli</i>	DH5 α	CGSC	Universidad EAFIT Biotechnology LAB
<i>Staphylococcus</i> sp.	G	W	Universidad EAFIT Biotechnology LAB
<i>Salmonella enterica</i>	ATCC 14028	A	Universidad EAFIT Biotechnology LAB
<i>Ralstonia eutropha</i>	H16	N	UMass Darmtouth
<i>Pectobacterium</i> sp.	N	N	Kolter Lab

B: *R. solanacearum* infected tissues from banana plants. T: *R. solanacearum* infected tissues from Tomato plants. N: Unknown. CGSC: laboratory engineered strain from the Coli Genetic Stock Center at Yale University. A: Animal tissue. W: sewage water samples

3.2.3 Culture media

BGT agar medium (BGTA), composed by special peptone (10 g/L, Oxoid), glucose (5 g/L), casaminoacids (1 g/L, Amresco), yeast extract (1 g/L, Merck), bactoagar (18 g/L, BD), TTC (50 mg/L, Merck) was used for antimicrobial testing against *R. solanacearum*. Several other TTC concentrations were employed for other trials. BG agar (BGA), with the same composition as BGTA without TTC (114, 118) was employed as the negative control for inducible antagonism production. TS10 medium, composed by TSA (10% w/v) and sucrose (1 g/L), with or without TTC depending on the test, was employed for other *R. solanacearum* trials.

3.2.4 *In vitro* antagonism tests

3.2.4.1 Antagonistic activity by agar plug diffusion method

The agar plug diffusion method was employed to evaluate the inducible antagonism capacity of different bacterial strains (Table 3-1) against different target strains (Table 3-3) (139). Briefly, 100 μ L of an inoculum of approximately 1×10^6 CFU/mL of the target strain were plated onto BGTA and BGA plates. In another version, the target strain was submerged into molten BGA or BGTA at a desired final concentration and mixed well. On top of the target strain, a 0.5 cm disc (diameter) containing the antagonistic strain grown in the appropriate medium (50% TSA, LB, BG) was placed. After 72 h of incubation under

environmental conditions or room temperature ($RT = 22 \pm 1$ °C), the presence and radius size of inhibition zones were registered. Each condition was performed in three replicates.

3.2.4.2 Antagonistic activity by agar well diffusion method

The agar well diffusion method was employed to determine the inducible antagonism capacity of strains belonging to *Bacillus* sp. and of *B. subtilis* NCIB 3610 knockout mutants against two strains of *R. solanacearum*, EAP09 and AW1. On BGTA and BGA plates containing the target strain, either submerged or plated, wells were opened with a sterile Pasteur pipette followed by the addition of 50 µL of an overnight inoculum, grown at 30.0 ± 0.5 °C, and 150 rpm, of the antagonistic strain. After incubation at 30.0 ± 0.5 °C for 48 h, three measures of the radius of inhibition zones were registered. Three different plates of the assay were established for each treatment (a specific strain or an extract).

3.2.4.3 Antagonistic activity in liquid co-cultures

Co-cultures of a specific *Bacillus* sp. strain and *R. solanacearum* EAP09 or *R. solanacearum* AW1, were prepared by inoculating both strains, at an approximate initial concentration of 1×10^6 CFU/mL each, to a 500 mL erlenmeyer flask containing 100 mL of the corresponding liquid medium and incubated for 24 h at 30.0 ± 0.5 °C and 150 rpm in an orbital shaker in the dark. Fermentations were performed in liquid media amended (BGT) and not amended with TTC (BG). 2 mL samples were taken at specific times from each fermentation to determine cell density in CFU/mL by the spread plate technique. Briefly, serial dilutions were performed for each sample and 100 µL of each dilution were plated onto BGA medium amended with 0.5 ppm of nalidixic acid (Nx), in order to count only *Bacillus* sp. colonies and onto BGTA medium amended with 0.5 ppm of ampicillin and 5 ppm of chloramphenicol in order to count only *R. solanacearum* colonies. Two replicates per treatment were established.

3.2.4.4 Antagonistic activity in liquid monocultures

Liquid mono-cultures of each selected *Bacillus* sp. strain were performed by inoculating each strain, at an approximate initial concentration of 1×10^6 CFU/mL each, to a 500 mL erlenmeyer flask containing 100 mL of the corresponding liquid medium, amended (BGT) and not amended with TTC (BG). Fermentations were incubated for 24 h at 30.0 ± 0.5 °C and 150 rpm in an orbital shaker in the dark. 2 mL samples were taken at specific times from each fermentation to determine cell density in CFU/mL, by the spread plate technique, and

cell-free supernatant activity (obtained by centrifugation at 14.000 rpm for 10 min and filtrations through 0.2 μm pore-size acetate membranes) by agar well diffusion method.

3.2.5 Antibiotics sensitivity tests

R. solanacearum sensitivity to antibiotics in the presence and absence of TTC was determined by establishing an antagonism test through the agar disk-diffusion methodology or Kirby–Bauer antibiotic testing (140). Antibiotic stock solutions of rifampicin, ampicillin, streptomycin and kanamycin (all from Sigma-aldrich) were added to sterile paper discs placed over a plated inoculum of *R. solanacearum* EAP09 on BGA and BGTA plates, to achieve final concentrations of 20 mg/L of each antibiotic. Incubation at RT followed for 48 h, after which three measures of inhibition zones were taken. Three replicates for each treatment were established.

3.2.6 Other tetrazolium salts and antioxidant addition to the culture medium

Antagonism plates were established according to agar plug method in culture media modified by the addition of either antioxidant compounds to the medium or by replacing the main inducer compound TTC by other tetrazolium salt. For the first experiment with antioxidants, final concentrations were of 100 mg/L for ascorbic acid (vitamin C, ECAR), 10 mg/L for α -tocopherol (vitamin E, Sigma-Aldrich) and uric acid (Sigma-aldrich), and 18 mg/L for L-glutathione (Alfa-Aesar, USA) were achieved in plates containing culture media amended (BGTA) and not amended (BG) with TTC. For other tetrazolium salts, final concentrations of 25, 50 and 100 mg/L were used for NBT (Sigma-aldrich), INT (Sigma-aldrich) and XTT (Sigma-aldrich) by adding stock solutions to BG agar before solidifying. Controls for these trials consisted of non-antioxidants containing BGTA and BGA plates, and BGTA and BGA plates for other tetrazolium salts evaluation. Three replicates were established for each treatment.

3.2.7 Diffusion of inducible compounds across nylon membranes

For determining the ability of *Bacillus* sp. strains to produce the inducible compounds without the presence of the target pathogen, polyamide (nylon) membranes discs (Sartorius) of 47 mm of diameter and 0.2 μm of pore size, were sterilized and placed on top of BGA and BGTA plates. 5 mm discs of *Bacillus* sp. previously grown on 50% TSA for 24 h at 30.0 ± 0.5 °C, were settled on top of the membranes and incubated at RT for 48 h. After this time, membranes were carefully taken out and 100 μL of the inoculum of the

pathogen were applied. Positive controls for this experiment consisted of: a positive control of the antagonistic activity of *B. cereus* EA-CB1047 growing without nylon membranes (positive control); a normal agar plug antagonistic test but placing *B. cereus* plugs over a sterile membrane after plating *R. solanacearum* (membranes control). Two negative controls were established: a membrane without *Bacillus* placed on top of the agar before plating *R. solanacearum* and a membrane with agar-plugs of a non-antagonistic strains placed on top, in order to prove that neither membrane presence or nutrients depletion by the growth of another microorganisms were causing the observed inhibition zones. Besides this last control, another treatment was established where nutrients were restored in the culture medium by applying 100 μ L of concentrated solution of sterile BG liquid medium where the membrane had been previously located, before inoculation of the pathogen (diffused compounds + nutrients reposition). Incubation followed for 48 h at RT after which inhibition zones radius was measured. Three replicates were established for each treatment and control.

3.2.8 Determination of growth kinetics through microplates assay

Microplate assays were used in order to assess the effect of different TTC concentrations, as well as those from its reduction product TPF, in the growth kinetics of the main target pathogen, *R. solanacearum* EAP09 and the antagonistic microorganisms. 96-wells microplates were prepared by adding 90 μ L of BGT liquid medium to each well, to reach final concentrations ranging from 25 to 400 ppm of the inducer TTC, increasing 2-fold each time, with eight replicates per treatment. A positive growth control consisted of BG medium with 0 ppm of TTC and the blank (values corresponding to O.D = 0) consisted on BGT medium without any bacterial inoculation. Addition of TTC to BG medium, which gives BGT medium as result, does not alter its O.D when registered at 600 nm, thus BGT without any microbial inoculation can be used as the blank for all treatments. After every TTC concentrations was prepared in each column, 10 μ L of either *R. solanacearum* EAP09 adjusted to an O.D (600 nm) = 0.1 - 0.15 or *Bacillus* sp. strains adjusted to an O.D = 2 inoculums, which correspond to 1×10^6 CFU/mL, were added to each well, in order to complete a total volume of 100 μ L in each well. Effects of TPF (Sigma-adrich) concentrations on microorganisms was done in the exact same way as formerly described for TTC, but replacing the tetrazolium salt by its reduction product dissolved in methanol (Honeywell®). O.D values were recorded at a wavelength of 595 nm, in a microplate reader (Bio-Rad®) every 4 h, until 72 h of growth were completed for *Bacillus* sp. strains and 160 h for *R. solanacearum*. Data was processed in order to construct growth kinetics curves.

3.2.9 Siderophores CAS assay

Siderophores production by *Bacillus* sp. strains in the presence and absence of TTC was determined by the previously described colorimetric assay established by Schwyn and Neilands (141). Briefly, pre-solutions of 10 mM hexadecyltrimethyl ammonium bromide (HDTMA), 10 mM Iron III in 1 N HCl and 0.12% Chrome Azurol S (CAS) were prepared. Afterwards, blue agar plates were prepared by mixing in a 1:5 ratio of Iron III acid solution with the aqueous CAS solution, before addition of a diluted (5 mM) HDTMA in a 1:1.5 ratio. 100 mL of this final solution were added to 900 mL of blue agar (15 g agarose, 32.24 g PIPES, 12 g NaOH) and left at incubation for maintaining at semi-solid temperature (40 ± 2 °C). The trial consisted of placing agar discs of the strain to test for siderophores production on top of BGA and BGTA plates, incubating for 24 h at optimal growth temperature (37 °C) and afterwards overlay with 15 mL of previously prepared blue agar. These plates were dried for 2 h on biosafety cabinet and incubated for 24 h at 30°C, until orange zones were visible around colonies of producing strain.

3.2.10 Statistical Analysis

All datasets for each experiment were analyzed in R package (142) and Microsoft Excel, this last only for Student t-test for two conditions datasets. As a first step for R package analysis, datasets were tested for their fitting to ANOVA (analysis of variance) assumptions: independence of observations, normal distribution of residuals and homoscedasticity or homogeneity in variance of residuals. If assumptions were met, a one-way ANOVA analysis followed, finding statistically significant differences across means of treatments if P -value ≤ 0.05 . Tukey multiple range test was applied in order to find homogeneous groups. If ANOVA assumptions were not met, a Kruskal-wallis non-parametric test was performed, and homogeneous groups were found if P -value ≤ 0.05 , by applying Dunn post-hoc analysis.

3.3 Results

3.3.1 Growth on TTC induces antimicrobial activity of different AEFB species from Bacillales order against *R. solanacearum*

Representative strains belonging to diverse AEFB genera (Table 3-1) were tested for their ability to produce inducible inhibition zones in the presence of TTC (Table 3-4). Antagonistic activity was tested in BGA medium as well (0 mg/L of TTC), as a negative control. From overall results, an inducible activity is observed in a great variety of Bacillales genera, evidencing no inhibition zone production when TTC is absent in the medium (0 mg/L TTC) and finding statistically significant inhibition zones when TTC is present (50 mg/L)

(supplementary material Fig. S-1). A greater inducible activity was observed in *B. cereus* and *B. pumilus* strains above others, with inhibition zones produced by them being larger to species and genus like *B. megaterium*, *M. marinus* and *P. pasadenensis*, according to statistical analysis. It is interesting to note that the only exception of antagonistic activity in the absence of TTC, meaning a non-TTC inducible activity, was observed for *B. amyloliquefaciens*, with no statistically significant difference found when comparing inhibition zone sizes in of negative control to the ones produced when TTC was present. Although *B. subtilis* strains evidenced low inhibition zones without inducer, its dimension was significantly different to the ones produced under TTC presence according to statistical analysis.

3.3.2 Growth on TTC induces antimicrobial activity of different Gram negative species against *R. solanacearum*

In order to assess if inducible antimicrobial behavior against *R. solanacearum* was exclusive to AEFB species, other Gram negative strains (Table 3-1) were randomly selected to assess their ability to produce inhibition zones in the presence (BGTA) and absence of TTC (BGA) (Table 3-5). *B. cereus* EA-CB1047 was used as a positive control for its high production of inducible inhibition zones. Results suggest that the phenomenon of induced antimicrobial activity may not be exclusive to AEFB genera, since strains of species like *S. marcescens* and *B. cepacea* produce larger halos in the presence of the inducer and no activity or small inhibition zones in the absence of it. Although further trials are needed in order to assure that inducible antagonistic potential is restricted to some microbial families, it is indeed observable that some species, are as for instance *D. tsuruhatensis* and *P. putida*, produce smaller or equally large halos when the inducer compound is present in the medium, indicating either a repression in the production of non-induced antibiotic substances or a non-induction by TTC in certain species. Such is the case for *H. seropedicae* which displays no antibiotic potential against the target pathogen neither in the presence or absence of TTC, although it grows normally in both culture media, BGA and BGTA. But even for the Gram negative strains which exhibit inducible inhibition zones as is the case for *S. marcescens*, potential remains low when compared with *B. cereus* EA-CB1047, which presents statistically significant differences when comparing the size of its inducible inhibition zones against the ones from other tested species. These result, indicate an intrinsic capacity of *Bacillus* species, for being more strongly induced than Gram negative species, in the production of these specific antimicrobial substances in the presence of TTC.

Table 3- 4. Effect of TTC on the antagonistic activity of selected AEFB strains against *R. solanacearum*

SPECIES	STRAIN	0 mg/L TTC	50 mg/L TTC
		INHIBITION ZONE (mm)	INHIBITION ZONE (mm)
<i>B. cereus</i>	EA-CB1047	0.0 ± 0.0 *	22.7 ± 1.4 abc
	EA-CB0012	0.0 ± 0.0 *	21.2 ± 0.0
<i>B. pumilus</i>	EA-CB0009	0.0 ± 0.0 *	22.6 ± 0.4 a
	EA-CB0177	0.0 ± 0.0 *	26.8 ± 0.6
<i>B. megaterium</i>	EA-CB0185	0.0 ± 0.0 *	14.0 ± 0.4 e
	EA-CB1057	0.0 ± 0.0 *	15.0 ± 0.0 f
<i>P. pasadenensis</i>	EA-CB0840	0.0 ± 0.0 *	7.3 ± 0.6
<i>B. subtilis</i>	EA-CB0015	4.7 ± 0.8 *	16.3 ± 0.0
	EA-CB0575	2.8 ± 0.8 *	12.8 ± 2.5
	NCIB-3610	3.2 ± 0.8 *	15.5 ± 0.4 cdef
	SMY	0.0 ± 0.0 *	15.3 ± 0.5
<i>B. amyloliquefaciens</i>	EA-CB0959	18.0 ± 1.3	19.7 ± 0.4 b
<i>B. altitudinis</i>	EA-CB1450	0.0 ± 0.0 *	21.0 ± 3.5 abcd
	EA-CB0686	0.0 ± 0.0 *	16.8 ± 0.5
<i>B. licheniformis</i>	ATCC14580	0.0 ± 0.0 *	22.4 ± 2.9 abcdef
<i>B. simplex</i>	ZK5093	0.0 ± 0.0 *	17.2 ± 0.2 cdef
<i>B. thuringiensis</i>	ZK5165	0.0 ± 0.0 *	19.2 ± 2.8 abcdef
<i>B. coagulans</i>	ZK5189	0.0 ± 0.0 *	22.0 ± 0.0 abcdef
<i>B. lentus</i>	ZK5173	0.0 ± 0.0 *	16.2 ± 1.2 cdef
<i>M. marinus</i>	ZK5187	0.0 ± 0.0 *	13.7 ± 0.0 def
<i>B. firmus</i>	ZK5172	0.0 ± 0.0 *	15.0 ± 2.0 cdef
<i>A. palidus</i>	ZK5191	0.0 ± 0.0 *	22.2 ± 2.8 abcdef

Intervals represent standard errors of the mean (n = 3). * denote a statistically significant difference (P < 0.05) between the conditions 0 mg/L and 50 mg/L for each strain, according to Student t-test. Species sharing letters do not differ statistically in their values at 50 mg/L, by Kruskal-Wallis and Post-hoc Duncan-test for multiple comparisons. Treatments which do not present letters were tested independently from the group and not included in the statistical test.

3.3.3 Growth on TTC induces antimicrobial activity of different *Bacillus* species against other Gram positive and Gram negative strains

Expanding the spectrum of action of potentially novel antimicrobial compounds is crucial for determining is further exploration and research. Thus, the spectrum of activity of the inducible antagonism produced by two of the most inducible species, *B. cereus* and *B. subtilis*, was determined against other strains of diverse genera. Although in smaller

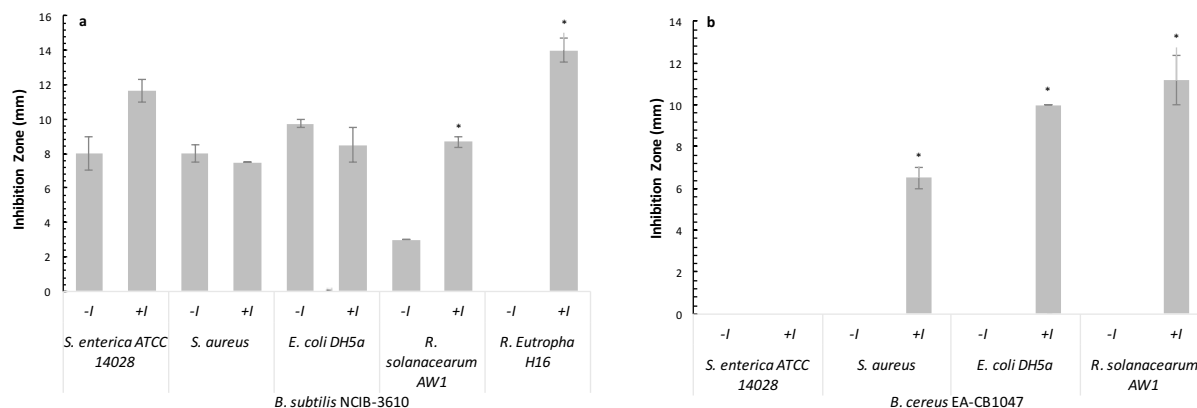
magnitude than against *R. solanacearum*, activity of these compounds can be expanded beyond the genus *Ralstonia* sp. to *E. coli*, *S. aureus* and *S. enterica* (Fig. 3-1).

Table 3-5. Effect of TTC on the antagonistic activity of different Gram negative strains against *R. solanacearum*

SPECIES	STRAIN	0 mg/L TTC	50 mg/L TTC
		INHIBITION ZONE (mm)	INHIBITION ZONE (mm)
<i>D. tsuruhatensis</i>	UA-1537	13.8 ± 2.1 *	9.5 ± 1.3 b
<i>P. putida</i>	UA-0095	11.6 ± 1.9	11.4 ± 2.8 b
<i>S. marcescens</i>	UA-1538	7.0 ± 0.3	11.8 ± 0.1 b
<i>B. cepacea</i>	UA-1541	0.0 ± 0.0 *	9.3 ± 1.0 b
<i>H. seropedicae</i>	UA-1542	0.0 ± 0.0	0.0 ± 0.0 c
<i>B. cereus</i>	EA-CB1047	0.0 ± 0.0 *	20.8 ± 2.8 a

Intervals represent standard errors of the mean (n=3). * denote a statistically significant difference ($P < 0.05$) between the conditions 0 mg/L and 50 mg/L for each strain, according to Student t-test. Species sharing letters do not differ statistically in their values at 50 mg/L, by one-way ANOVA and Tukey multiple range-test.

Figure 3-1. Effect of TTC on the antagonistic activity of *B. subtilis* NCIB-3610 (a) and *B. cereus* EA-CB1047 (b) against several target strains

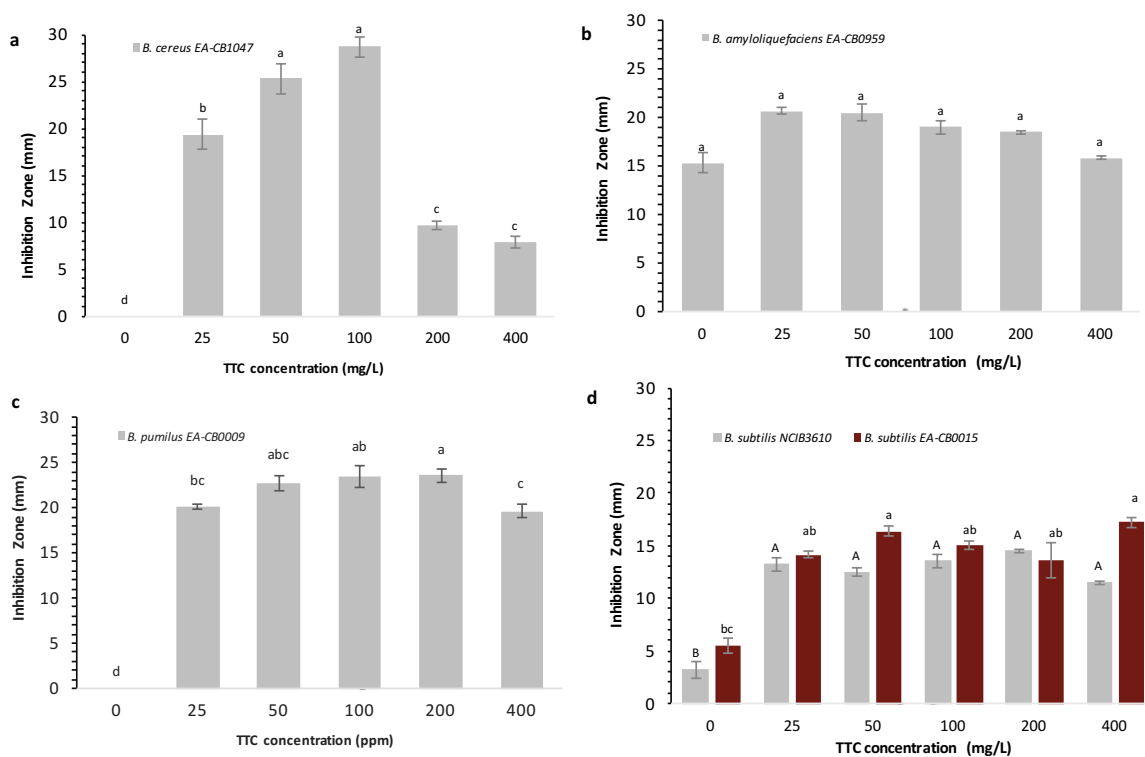


Intervals represent standard errors of the mean (n = 3). +I denotes 50 mg/L TTC amendment in the medium, -I denotes TTC absence in the medium. * denote a statistically significant difference ($P < 0.05$) between the conditions -I and +I for each antagonistic strain, according to Student t-test.

3.3.4 Inducible antimicrobial activity of *Bacillus* strains is TTC-dose dependent

The strains that evidenced higher inducible antimicrobial activity, these being *B. cereus* EA-CB1047 and *B. pumilus* EA-CB0009, were tested to determine if the inducible activity was TTC dose dependent (Fig. 3-2), in BGTA plates with different TTC concentrations ranging from 0 to 400 ppm, increasing 2-fold each time. Other well studied *Bacillus* species were also tested (*B. amyloliquefaciens* EA-CB0959, *B. subtilis* EA-CB0015 and *B. subtilis* NCIB-3610) in order to verify their antagonistic behavior under different TTC doses.

Figure 3-2. Effect of different TTC concentrations in the size of inducible inhibition zones produced by selected AEFB



Intervals represent standard errors of the mean (n = 3). Bars sharing capitalized or non-capitalized letters do not differ statistically in their values, by Kruskal-Wallis rank test and Post-hoc Duncan-test for multiple comparisons.

From Fig. 3-2, it can be deduced that both species, *B. cereus* EA-CB1047 and *B. pumilus* EA-CB0009, have the highest antimicrobial inducible potential when compared to other AEFB and do not produce any antimicrobial activity against *R. solanacearum* in the absence of TTC, supporting the hypothesis that the inhibition zones are a consequence of inducible antimicrobial compounds being produced. Besides, their highest inducible potential is between 50-100 mg/L of TTC, which denotes a dose-dependent capacity for inducible compounds production. Above concentrations of 100 mg/L of TTC, *B. cereus* specifically,

suffers an inhibition which is evidenced as an impaired growth at concentrations of 200 - 400 mg/L of TTC (supplementary material Fig. S-2), thus resulting in lower inducible inhibition zones (Fig. 3-2a) statistically different in size to the ones produced at 50 - 100 mg/L of TTC, denoting that the optimum dose for producing inducible antagonism falls within this range.

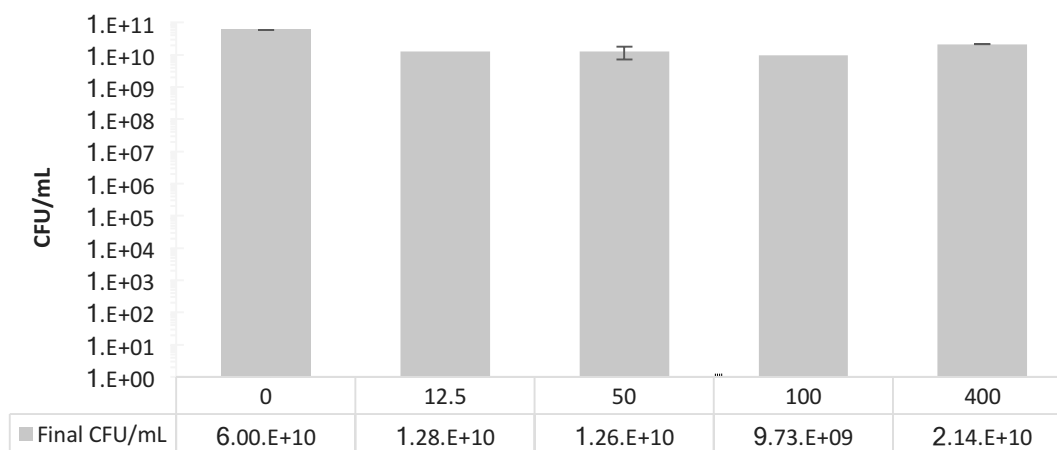
Regarding the other three tested strains of well-studied *Bacillus* species, significant differences were found for both of *B. subtilis* strains between zones produced at 0 ppm and the rest of TTC concentrations (Fig. 3-2d), but not for *B. amyloliquefaciens* (Fig. 3-2b). These results suggest, that *B. subtilis* generates both naturally produced antagonistic compounds and inducible ones against *R. solanacearum*, but inducible ones have higher activity against *R. solanacearum*. In the other hand, *B. amyloliquefaciens* evidences a strong production of naturally crafted antibiotic substances that have high probability of belonging to the lipopeptides families of compounds, as we have previously demonstrated (data not shown and under publication). These substances appear to have the same strong activity against *R. solanacearum* as the inducible compounds have, since no statistical differences are found for the size of inhibition zones in the presence or absence of TTC. Otherwise, these naturally crafted substances could be mixed with the inducible compounds in the inhibition zones, without a synergy between the two classes of substances happening, thus not creating larger inhibition zones against the target pathogen. Another hypothesis would be a non-induction of *B. amyloliquefaciens* strains by TTC. A suppression in the production of naturally crafted antagonistic compounds in the presence of TTC could be occurring as well, and the inhibition zones generated at 0 ppm by naturally crafted compounds are being replaced by the inducible compounds at higher TTC concentrations. Nonetheless, all inducible inhibition zones are TTC dose-dependent, the higher production observed within the range of 50 - 100 mg/L for all *Bacillus* species tested.

3.3.5 *R. solanacearum* viability is not affect by different concentrations of TTC

Growth curves of *R. solanacearum* EAP09 in the presence of different concentrations of TTC were established (supplementary material Fig. S-3) and their biomass concentration in CFU/mL determined at the end-point of each fermentation (Fig. 3-3). Results shown in Fig. S-3 indicate that *R. solanacearum* EAP09 has an exponential growth between 8 and 96 hours of fermentation in the presence of different TTC concentrations ranging from 0 - 400 ppm, reaching stationary phase at 140 h. During exponential phase, specific growth rate (μ_x), was estimated finding that it oscilates between 0.0589 h^{-1} (36.7 h of doubling time) and 0.0892 h^{-1} (32.4 h of doubling time) for 0 ppm and 400 ppm TTC respectively. Eventhough different in value and appearing to have a faster growth when TTC concentration is higher,

differences are not significant across the two conditions. Maximum O.D reached for each TTC concentration differs as well, the highest being reached under the highest TTC concentration (400 ppm). This result suggests that higher TTC concentrations could affect growth or that TTC reduction into TPF is incrementing the O.D measurement, given that TPF absorbs at 595 nm. Due to these observations, CFU/mL was determined at the end of each fermentation (168 h) finding that values do not differ statistically among conditions and thus, differences found between O.D and μ_x values could be attributed to TPF absorption. As previously stated, Fig. 3-3 evidences that a homogeneous biomass production is reached at the end of all *R. solanacearum* fermentations under TTC values from 0-400 ppm.

Figure 3-3. *R. solanacearum* EAP09 viability after 168 h of growth in the presence of different TTC concentrations



Intervals represent standard errors of the mean (n = 3). No statistically significant differences were found (P -value >0.05) according to Kruskal-Wallis test

3.3.6 *R. solanacearum* sensitivity to antibiotics is not affected at 50 mg/L TTC

Antibiotic sensitivity of *R. solanacearum* EAP09 was measured qualitatively, in the presence of 50 ppm of TTC (BGTA medium) and in the absence of it (BGA medium) through the application of four antibiotics active against Gram negative bacteria: streptomycin, ampicillin, rifampicin and kanamycin B, reaching a final concentration of 20 ppm of each one. It was observed that *R. solanacearum* was not sensitive to three of the drugs tested (streptomycin, ampicillin and kanamycin B) neither in presence nor absence of the inducer, suggesting that its sensitivity to the antibiotics tested was not increased by TTC presence. Besides, rifampicin tested at 20 ppm, evidenced inhibition zones of similar magnitude across both conditions (Supplementary material Fig. S-4). Although a broader spectrum of concentrations and antibiotic substances should be tested to clearly assess *R. solanacearum* sensitivity in TTC presence, this result indicates that it is not increased. Besides this trial,

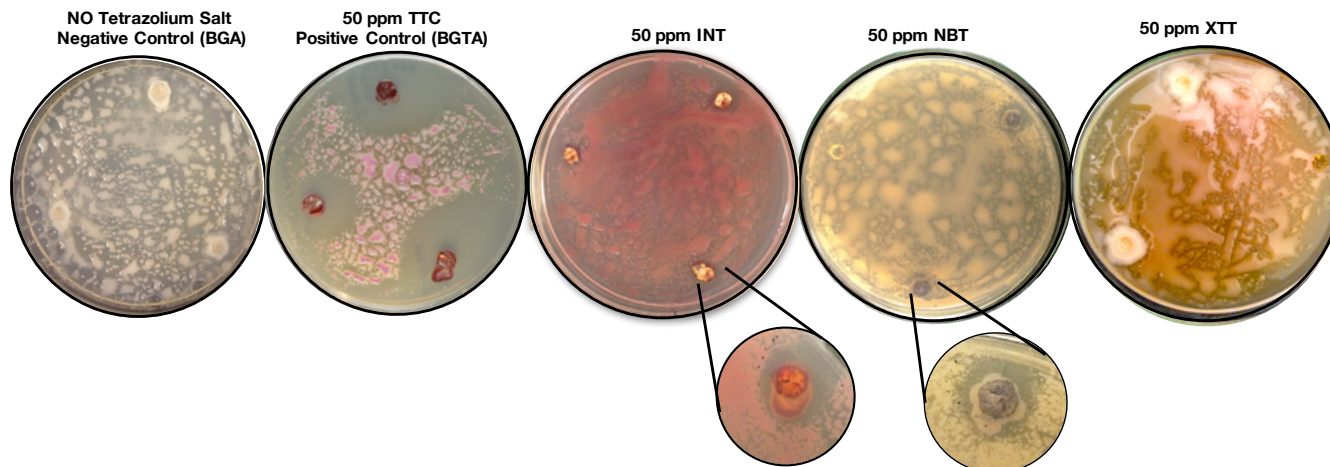
another test was performed where a concentrated TTC solution was applied in the wells of a well-diffusion antagonism test, before cell suspensions of *B. cereus* EA-CB1047 were inoculated. After incubation for 48 h, inhibition zones of 19.5 ± 0.9 mm against *R. solanacearum* were observed for this treatment compared to 23.7 ± 1.3 mm for a normal antagonism test in BGTA, where TTC was present in an homogeneous concentration across the medium (Supplementary material Fig. S-5). These results altogether indicate that inhibition zones produced by *Bacillus* sp. strains in the presence of TTC are not due to an increased sensitivity of *R. solanacearum* in the presence of TTC.

3.3.7 TTC is the stronger inducer within other tetrazolium salts tested

In order to assess the role of TTC as an inducer in the culture medium, within this observed phenomenon of inducible antimicrobial substances production, other compounds of the same family of tetrazolium salts were added one a time to the culture medium, on the same concentrations that were previously evaluated for TTC. The tested tetrazolium salts were XTT, INT and NBT (names and structures in Table 2-1) which form orange, purple and blue formazans respectively. By the observation of the antagonism trials and the color of the colonies of *B. cereus* EA-CB1047 growing in the presence of each tetrazolium salt (Fig. 3-4), it can be concluded that specifically TTC, INT and NBT are being reduced to its respective formazans. Besides, the three of them are considered monotetrazolium salts with a net positive charge (Table 2-1), a trait that allows them to enter the cells, due to a naturally occurring negative charge in the internal part of the plasma membrane which creates a difference in electric potential (membrane potential), making the incorporation of positive ions of certain size take place through ion channels (143).

Although not in the magnitude of TTC, small inhibition zones produced by *B. cereus* EA-CB1047 against the target pathogen are observed in the presence of INT and NBT, indicating a low induction of activity in the presence of these compounds. Although, TTC remains the stronger inducer of antimicrobial substances, as the first observations of this phenomenon suggested. Respects to its reduction mechanism, it has been deduced by some experimentation in the area that monotetrazolium salts that more readily enter cells, as are TTC, MTT and INT, are reduced by NADPH-dependent oxidoreductases and dehydrogenases of metabolically active cells, more than by Complex I and Complex II or flavin-containing enzymes. In the other hand, XTT salt, which has a negative net charge, does not appear to be activated by cells since they remain white and no inducible inhibition zones against *R. solanacearum* were observed.

Figure 3-4. Effect of other tetrazolium salts on the inducible inhibition zones generated by *B. cereus* EA-CB1047

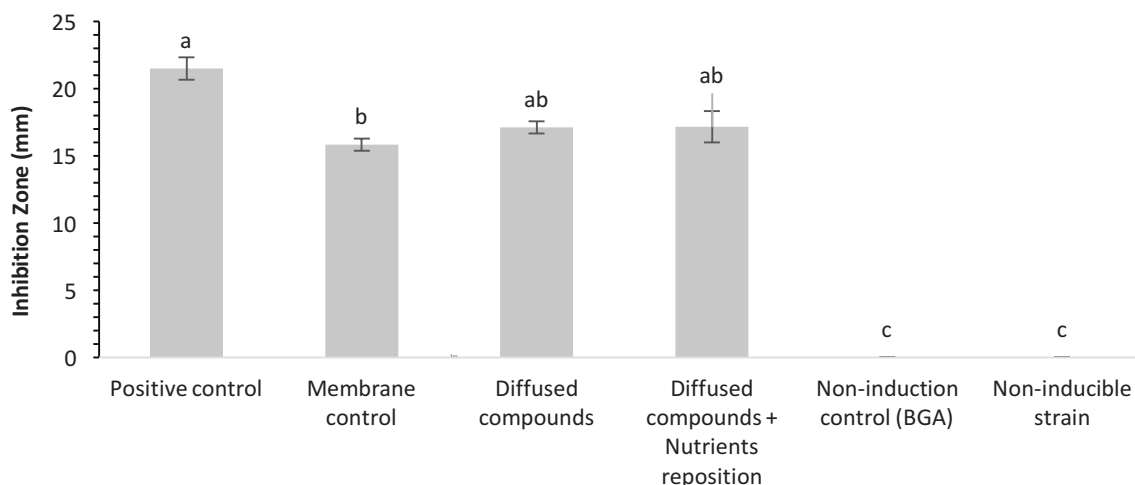


3.3.8 Inducible compounds are diffusible and produced in the absence of the target pathogen *R. solanacearum*

In order to determine if inducible antagonistic activity was dependent of the target pathogen, so that an interspecies interaction would be the one triggering the antibiotic behavior, the ability of *B. cereus* EA-CB1047 to produce inhibition zones before entering in contact with *R. solanacearum* was established by growing *B. cereus* EA-C1047 and *B. pumilus* EA-CB0009 on top of polyamide (Nylon) sterile membranes placed over BGTA and BGA. Fig. 3-5 evidences that inhibition zones of *R. solanacearum*, are still observable after removing *Bacillus* sp. strains growing on top of nylon membranes for 24 h (supplementary material Fig. S-6). Besides, the size of these inhibition zones does not differ from the ones produced by the positive control. These results suggest that the inducible compounds are diffusible, since the formation of an inhibition zone is observable were *Bacillus* cells grew over nylon membranes and that the inducible antagonistic behavior is probably not due to an interaction of *Bacillus* cells with the target microorganism, *R. solanacearum*. Besides, nylon membranes could be impeding to a certain extent the diffusion of the inducible compounds produced by *Bacillus*, as membranes control treatment produces a reduced inhibition zone against *R. solanacearum*. An additional treatment with nutrients reposition, indicates that the cause of observed inhibition zones is the presence of diffused inducible antibiotic compounds produced by *Bacillus* cells, and not due to a nutrients deprivation in the culture medium. It appears then, that inducible antimicrobial compounds are in fact

being diffused through the culture medium by *Bacillus* cells in the presence of TTC. In order to see if this phenotype was only observable in solid cultures, liquid co-cultures and mono-cultures were established.

Figure 3-5. Inhibition zones produced by *B. cereus* EA-CB1047 across Nylon membranes against *R. solanacearum*



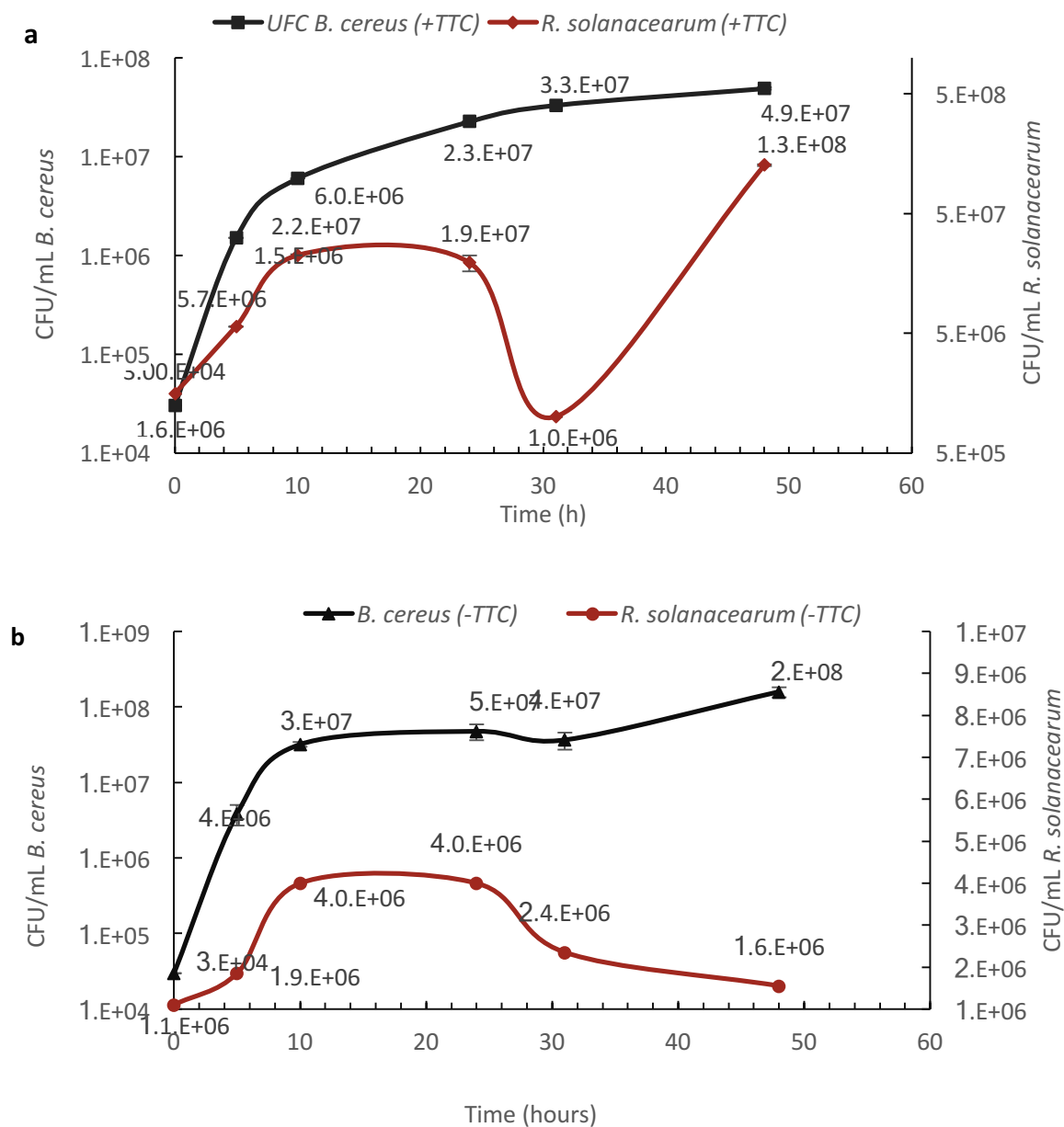
Intervals represent standard errors of the mean (n = 3). Bars sharing letters do not differ statistically in their values, by Kruskal-Wallis rank test and Post-hoc Duncan-test for multiple comparisons. Positive control: normal antagonism test with *B. cereus* EA-CB1047. Membrane control: *B. cereus* EA-CB1047 growing over nylon membranes for 48h over plated target strain. Diffused compounds: *B. cereus* EA-CB1047 growing for 48h over nylon membranes before plating target strain. Diffused compounds + nutrients reposition: diffused compounds treatment + 100 μ L of concentrated fresh medium were membrane was placed. Non-induction control (BGA): *B. cereus* EA-CB1047 growing over nylon membranes in a medium without TTC before plating target strain. Non-inducible strain: *H. seropedicae* UA-1542 growing over nylon membranes in BGTA medium.

3.3.9 TTC Induces antimicrobial activity of *Bacillus* strains in liquid co-cultures and mono-cultures

As inducible antimicrobial activity was well evidenced in solid media containing TTC (BGTA) and it was observed that *Bacillus* sp. strains produce inducible inhibition zones that inhibit *R. solanacearum* growth, the ability of *B. cereus* EA-CB1047 to inhibit *R. solanacearum* in liquid medium was tested. As a first step, growth in co-cultures with *R. solanacearum* was assessed. In Fig. 3-6a, a typical bacterial growth curve with exponential and stationary phases is evidenced for *B. cereus*, while the target pathogen *R. solanacearum* evidenced a decrease of 19-fold in its population that matches the start of stationary phase for *B. cereus*. Such a pronounced decrease in the population was not observable for *R. solanacearum* in control fermentations where the inducer compound was not present, only decreasing 1.6-fold (Fig. 3-6b). These results, altogether with the ones illustrated in supplementary material Fig. S-2, evidence that *B. cereus* is not affected in its growth at a concentration of 50 mg/L of TTC, and remains unaffected until 100 mg/L as well as in the presence of up to

400 mg/L of extracellular TPF (supplementary material Fig. S-7), which is TTC intracellular reduction product. The production of inducible antimicrobial activity in liquid medium when TTC is present, and the punctual decrease of *R. solanacearum* populations suggest that inducible compounds can be produced in TTC presence both in liquid and solid media.

Figure 3-6. Growth curves of *B. cereus* EA-CB1047 and *R. solanacearum* EAP09 in a co-culture in TTC presence (a) and absence (b)



Mono-cultures of *B. cereus* in the presence (+) and absence (-) of TTC in BG medium were established as well, in order to recover cell-free supernatants (CFS) and test their activity against *R. solanacearum*. An inhibition zone of 8 mm approximately, was observed when recovering CFS from *B. cereus* growing in TTC presence, but no activity was observed from CFS of *B. cereus* growing without TTC (supplementary material Fig. S-8).

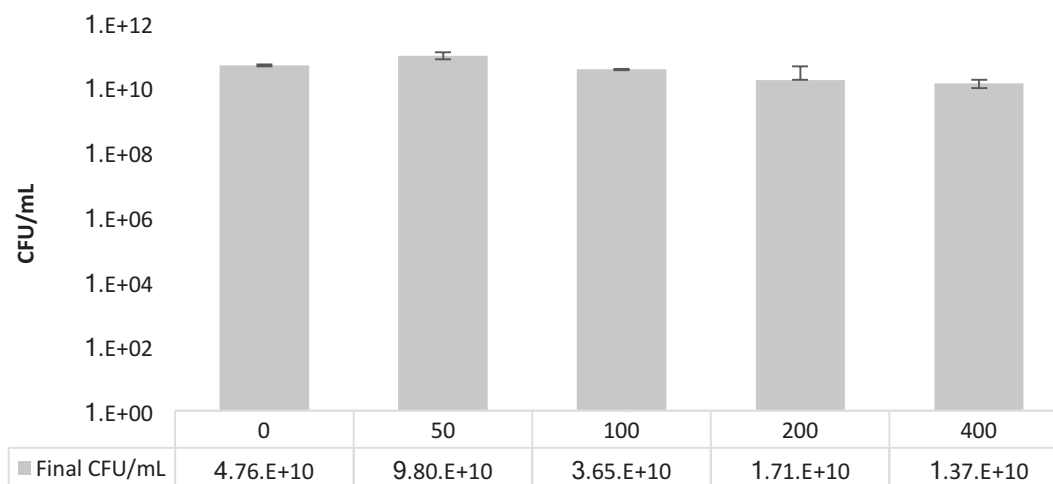
Therefore according to observations, the production of inducible antimicrobial activity in liquid takes place before the antagonistic *B. cereus* enters the stationary phase, decreasing the population of *R. solanacearum* in more than 19 fold. This observation suggests that albeit inducible antimicrobial compounds are being produced intracellularly, they can be secreted and liberated extracellularly. The onset of stationary phase is characterized by a lysis of cells and a liberation of intracellular compounds, which could be allowing a further liberation of antimicrobial compounds into the medium. The behavior of *R. solanacearum*, which restarts its growth after being inhibited, suggests a short-lived or liable nature of inducible compounds, which should be constantly secreted into the medium in order to maintain inhibition of the pathogen. *R. solanacearum* cells lysis could also be liberating nutrients into the already spent medium, which could allow the remaining viable cells to thrive again. This observations overall suggest that although *R. solanacearum* inhibition by *Bacillus* sp. cells growing under TTC presence is observed both in solid and liquid media fermentations, the variability observed in the obtention of active CFS suggests once more that inducible active compounds are sensible and susceptible to degradation. For that reason, further exploration of the phenomenon was performed in solid media (BGTA and BGA).

3.3.10 Extracellular TPF does not have antibacterial activity against against *R. solanacearum*

Growth curves of *R. solanacearum* EAP09 were constructed in the presence and absence of extracellular TPF in order to determine its effect on the growth of this microorganism (supplementary material Fig. S-9). From the curves, it can be observed that even though O.D values become higher as TPF concentrations increase, reaching a maximum at 93.5 h with 400 ppm of TPF, total CFU/mL counts at the end of fermentations of 93.5 h for *R. solanacearum* (Fig. 3-7), do not report statistically significant differences among treatments. Higher O.D measures are due to TPF absorbance a 595 nm and not to a higher biomass concentration of the microorganisms. Antagonism tests by well-diffusion assay with application of concentrated TPF solutions (100, 200 and 400 ppm) dissolved in 100% methanol (MeOH), confirmed that this compound has no antimicrobial activity against *R. solanacearum* or any diffusion is observed along the culture medium (supplementary

material Fig. S-10). These results altogether, strongly suggest that external presence of TPF, is not directly responsible for the observed inducible antagonism, although by contrary, its formation inside *Bacillus* cells, due to TTC reduction, is possibly involved in triggering the induced antagonism, something that is further broaden in discussion section.

Figure 3-7. *R. solanacearum* EAP09 viability after 93 h of growth in the presence of different TPF concentrations



Intervals represent standard errors of the mean (n = 2) and no statistically significant differences were found among treatments (p-value \geq 0.05) by Kruskal-Wallis test.

3.3.11 Exploration of the chemical nature of inducible compounds

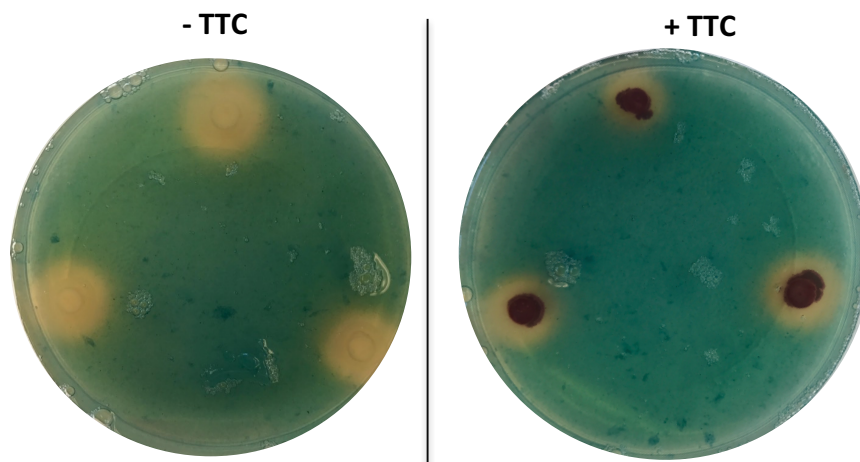
In order to give a step closer into unveiling the chemical nature of the substances produced under the presence of the inducer, several trials were performed (Fig. 3-8 to Fig. 3-10). Testing for siderophores presence in the inhibition zones observed against *R. solanacearum*, the effect of adding antioxidant compounds and the assessment of the inducible antagonistic capacity of knockout mutants from *B. subtilis* NCIB-3610, give more insight on the chemical nature of the active substances.

- **Siderophores are deregulated in the presence of TTC**

Since *Bacillus* sp. species have been widely studied for their active metabolites production, and siderophores such as bacillibactin and other chatecolate-type metabolites are part of the bioactive molecules produced by these microbial species, CAS assay (method 3.2.9) was set with strain *B. subtilis* NCIB-3610 (Fig. 3-8) in order to evaluate in a qualitative manner its capacity to produce siderophores under the presence and absence of the inducer. Siderophores production by a microbial species has been proven to be able to produce

inhibition zones of other bacterial species in certain cases, thus the involvement of these substances in the inducible antagonism was tested. By observation of Fig. 3-9, it can be concluded that siderophores from *B. subtilis* NCIB-3610, are being produced both under the presence and absence of the inducer compound, since the characteristic orange halos in blue agar from CAS assay, are visible across both conditions. Even a suppression of the siderophores producing capacity can be suggested in the presence of TTC for *B. subtilis*, due to the observed smaller halos. This leads to the suggestion of siderophores not being the chemical family to which the inducible compounds belong, though it will be further and more rigorously demonstrated in further chapters.

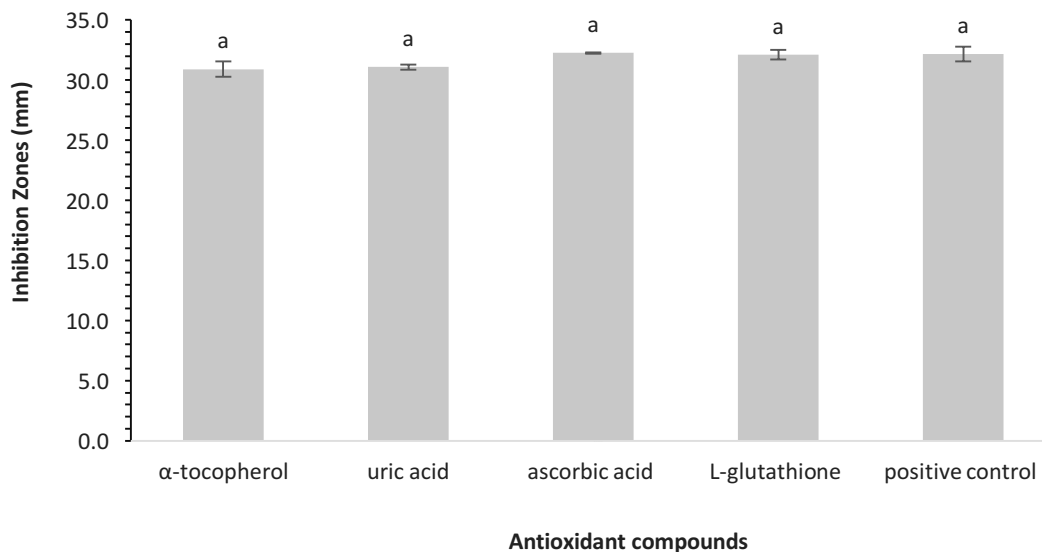
Figure 3-8. CAS assay for siderophores production of *B. subtilis* NCIB-3610 in the presence and absence of TTC



- **Antioxidants addition does not alter the size of inhibition zones**

Free-radicals, reactive oxygen species (ROS) or reactive nitrogen species (RNS), such as superoxide ion, hydroxyl radical, hydrogen peroxide, are well known for its cell damaging effects. Since high reductive activity is taking place inside the cells due to TTC reduction to formazan, ROS and RNS production could be happening and producing the inhibition of *R. solanacearum*. Antioxidant compounds were then added to the culture medium were antagonism trials were performed, to test if inhibition zones were altered by their presence. No statistically significant differences were reported for inhibition zones in the presence of these four strong antioxidants (Fig. 3-9), indicating that inducible compounds probably do not belong to these classes of compounds.

Figure 3-9. Inhibition zones against *R. solanacearum* produced by *B. cereus* EA-CB1047 in the presence of antioxidant compounds

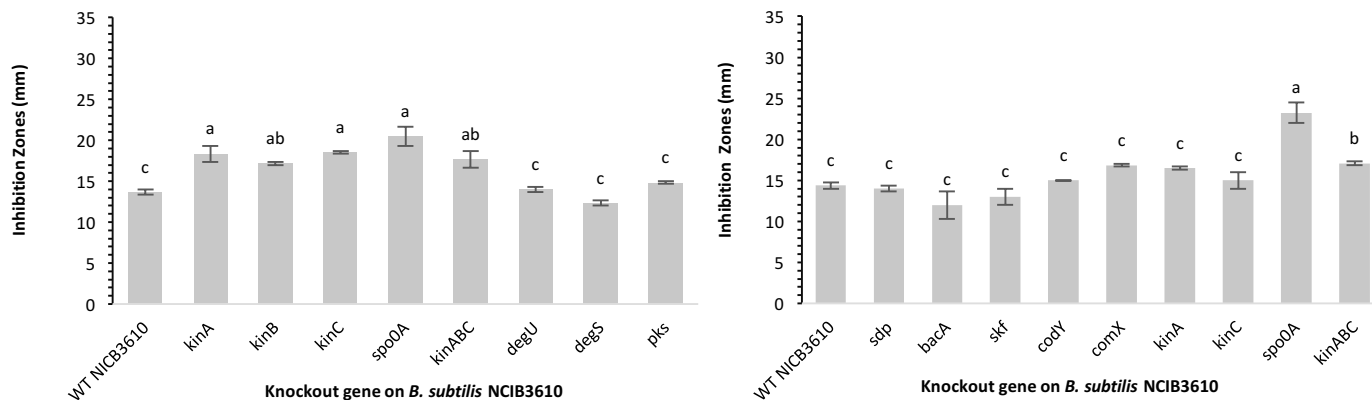


Intervals represent standard errors of the mean (n =3) and no statistically significant differences were found among treatments (p-value \geq 0.05) by one-way ANOVA. Final concentrations in culture medium for antioxidant compounds are: 10 ppm for α -tocopherol and uric acid, 100 ppm for ascorbic acid and 18 ppm for L-glutathione. Positive control consisted on a BGTA plate with 0 ppm of antioxidants.

- **Knockout mutants of *B. subtilis* NCIB-3610 activity against *R. solanacearum***

In order to assess the role of other well studied BGC or antibiotic metabolites naturally crafted by *Bacillus* sp. in the inhibition zones produced under the presence of the inducer, selected strains from a collection of mutants of *B. subtilis* NCIB-3610 strains (Table 3-2) were screened against two strains of *R. solanacearum*, AW1 and EAP09 (Fig. 3-10). Although no strain was defective in producing the phenotype of inducible antagonism, results suggest that statistically larger inhibition zones are being produced by *B. subtilis* NCIB-3610 *spo0A::erm* and by *B. subtilis* NCIB-3610 *kinA::mIs*, *kinB::kan*, *KinC::cat*, indicating an involvement of these genes in metabolic routes that repress the inducible antagonism, since their activation in the WT strain is producing smaller inhibition zones and thus, less concentration of inducible antimicrobial compounds.

Figure 3-10. *B. subtilis* NCIB-3610 Knockout mutants Inducible inhibition zones in TTC presence against *R. solanacearum* AW1 (a) and *R. solanacearum* EAP09 (b)



Intervals represent standard errors of the mean (n = 3) and no statistically significant differences were found among treatments (p-value \geq 0.05) by one-way ANOVA.

3.4 Discussion

A general observation of the results from this chapter, allows the suggestion of various important traits about the inducible antagonism: *Bacillus* sp. have more inducible antagonistic capacity than other strains from Gram negative genera (Tables 3-4 and 3-5), inducible antagonism is observed against other bacterial species beside *R. solanacearum* (Fig. 3-1), the observed inducible antagonism is TTC dose-dependent (Fig. 3-2) and insight into the chemical nature of the inducible antimicrobial compounds indicate that they are diffused in the culture medium (Fig. 3-5) produced as well in liquid cultures (Fig. 3-6 and supplementary material Fig. S-8), and are not related to siderophores (Fig. 3-8), ROS or other oxidative stress substances (Fig. 3-9) or traditionally active compounds such as PKs and LPs previously identified in *Bacillus* sp. (Fig. 3-10), as knockout mutants in central routes to some of these NPs from *Bacillus* sp. were no defective in producing inducible inhibition zones.

When zeroing in on results from Tables 3-4 and 3-5, strains from *B. cereus* group species (*B. cereus* EA-CB1047, *B. thurigiensis* ZK5165) and *B. pumilus* outstand as the ones with the higher inducible antagonism potential. As different microorganisms have diverse dehydrogenase systems, it may be possible that not all dehydrogenase systems are capable of using TTC, or not be able to use it as electron acceptor (115). The case for *B. cereus* groups species or *B. pumilus* strains would be the opposite, suggesting that their special dehydrogenases can more readily reduce TTC and thus, trigger the induction promptly,

evidencing larger inhibition zones than other species. This higher potential for producing inducible substances in these strains highlights a possible novel chemical nature for these inducible compounds, since specifically these two species, *B. cereus* and *B. pumilus*, are not renowned for being the greatest producers of the already characterized collection of NPs from Bacillales, which have been mostly isolated from *Paenibacillus*, *B. subtilis* and *B. amyloliquefaciens* species (144).

In the same line, specifically *B. cereus* EA-CB1047 is the most affected strain in its development under TTC concentrations above 100 ppm (Fig. 3-2a). *B. pumilus* EA-CB0009 evidenced toxicity as well beyond 200 ppm of TTC (Fig. 3-2b), instead *B. amyloliquefaciens* EA-CB0959 and *B. subtilis* strains EA-CB0015 and NCIB-3610 (Fig. 3-2 c-d) proved to be more tolerant, evidencing growth and development up to 400 ppm of TTC and producing no statically different inhibition zones across all these TTC values. But regardless of *Bacillus* strains evidencing a dose-dependency of TTC for producing inducible inhibition zones, a higher sensitivity of *R. solanacearum* in the presence of TTC is not observed, as growth control curves of this microorganism denote similar kinetics (supplementary material Fig. S-3) and end-point CFU/mL measurements prove no differences under TTC concentrations ranging from 0-400 ppm (Fig. 3-3).

Subsequently and in accordance with the stated above, *R. solanacearum* is among the species of phytopathogenic bacteria that tolerates some of the higher TTC concentrations in the medium, up to 5 g/L (5000 mg/L) according to the study from Lovrekovich & Klement (1960) (145) and with no evidence of developmental inhibition at conditions of up to 400 mg/L in this study. This result draws interest on the great magnitude of the inhibition zones produced against this pathogen by *Bacillus* sp. strains in TTC presence (Fig. 3-1, supplementary material Fig. S-1), denoting a powerful antagonism taking place. The report from Lovrekovich & Klement (145) provides evidence as well for other Gram negative strains tolerating high concentrations of TTC, as are pathogenic *Pseudomonas* species like *P. aeruginosa* and *P. syringae* var. *capsici* and *Erwinia chrysanthemi* var. *philodendroni*. Even though, other reports (146) provide support for the opposite behavior happening for Gram positive strains as the ones belonging to *Bacillus*, reporting a certain toxicity happening above 100 ppm of TTC. Activity trials against *R. solanacearum* of various *Bacillus* sp. strains in the presence of TTC concentrations ranging from 0 - 400 mg/L (Fig. 3-3 a-d) show that nearly all species have a maximized inhibition zone production between 50 - 100 ppm of the inducer compound, but decreased growth and inhibition zone sizes are observed for concentrations above 100 - 400 ppm of TTC, depending on the species.

It is well known, that due to plasma membrane potential (104), positively charged tetrazolium salts, the functional group to which TTC belongs (Fig. 2-3) enter the cells and are reduced to colored formazans by respiratory activity (115). This happens due specially to dehydrogenases activity in the respiratory chain, at different extents depending on the bacterial species, since there is a relatively variable nature of prokaryotic respiratory chains compared to eukaryotes, allowing for differences in tetrazolium reduction between organisms to be expected (109). As tetrazolium salts act as an electron acceptor in the respiratory chain (115), insoluble formazan crystals accumulate inside the cells as their reduced product; although its effect on cells has not been characterized and literature reports on formazan detection inside cells are only limited to quantifying and monitoring respiratory activity (109, 147). Given this and the observed behavior of induced antagonism produced by TTC-reducing *Bacillus* cells, it is suggested here that TTC could be acting as the indirect inducer of the production of the diffused antimicrobial substances. This could be happening as a consequence of its reduction process to TPF and the accumulation of the later inside cells.

Chained with results presented above and despite toxicity of TTC happening at certain concentrations for *Bacillus* sp. cells, end-point CFU/mL measurement of *B. cereus* EA-CB1047 demonstrate no statistically significant difference on the behavior or number of viable cells growing with extracellular presence of TPF, at concentrations from 0 - 400 ppm (supplementary material Fig. S-7 and Fig. S-11). These results indicate that extracellular accumulation of the reduction product of TTC may not be the cause of toxicity, even though the effect of intracellular accumulation of the formazan, possibly forming crystals, could be causing toxicity and inducing the antagonistic response from *Bacillus* cells.

Afterwards, other tetrazolium salts were tested in order to assess the effect of intracellular reduction of compounds with chemical similarity to TTC. The compounds that are reduced in an intracellular fashion because of the positive net charge of the molecule (NBT and INT; Table 2-1) appear to have low antagonism inducer effect on *B. cereus* EA-CB1047 (Fig. 3-5) and *B. subtilis* NCIB-3610 strains against *R. solanacearum* EAP09 and *R. solanacearum* AW1. Even though as measured by the size of the inhibition zones they produce against the pathogen (less than 5 mm), it can be concluded that they are negligible and it can be suggested that TTC is acting as the strongest inducer.

Furthermost, inhibition zones are observable when *Bacillus* cells are grown over polyamide (nylon) membranes placed on top of BGTA plates, and nutrients are restored after removing them but before plating *R. solanacearum* (Fig. 3-5, supplementary material Fig. S-6). These results suggest that a diffusion of compounds produced by *Bacillus* cells in the presence of

TTC is taking place, and specifically the membranes assay demonstrates that an interaction between *Bacillus* sp. strains and *R. solanacearum* is not needed for the production of inducible inhibition zones. As demonstrated in various studies (148, 149), microbial interactions by chemical exchange of signals might trigger the production of antagonistic substances in another species. Although, these results suggest that it is not the case for this particular antagonism and support the hypothesis of the antimicrobial substances induction in *Bacillus* cells be either mediated by intermediate products of TTC reduction or by its reduction product, TPF.

Bacillus sp. strains and related genera in the Bacillales within the Firmicutes, as *Paenibacillus* sp., are widely known for being one the most prolific antimicrobial or bioactive compounds producing microorganisms, harboring a variety of secondary metabolite gene clusters or BGC in their genomes and producing substances suitable for medical and agricultural applications (150). These compounds comprise diverse secondary metabolites with a wide spectrum of antibiotic and other bioactive properties, among the most notable are polyketides (PKs) and lipopeptides (LPs), produced by encoded polyketide synthases and non-ribosomal peptide synthetases respectively, and being molecules of modular architecture, formed by these enzymes by adding together building blocks until forming a larger multi-functional compound (151, 152). The repertoire of bioactive components, of chemically diverse structures, produced by strains of these genera includes other peptide antibiotics produced by NPRS, as bacilysin and other D-aminoacid residues containing dipeptides (diketopiperazines or DKPs); other non-peptide products by PKS synthases as bacillaene and macrolactins; ribosomically synthesized compounds, as L-antibiotics, and diverse bioactive proteins, as cell-wall degrading enzymes (CWDE) (132). Bacteriocins are proteins produced by prokaryotes that are bactericidal and/or bacteriostatic against organisms related to the producer strain (153). Species belonging to Bacillales produce known bacteriocins as are cerein 7 (154) and cerein 8A (155) from *B. cereus*, thuricin 7 (156) and thuricin 17 (157) from *B. thurigiensis*.

But could the inducible substances be an overproduction of already known metabolites from *Bacillus* species? It is well known that the Bacillales, specially *Bacillus* sp. and *Paenibacillus* sp. are considered a gold mine that represents a rich source for diverse secondary metabolite gene clusters and produce a great range of active compounds. Specifically, PKs and LPs have played an essential role for applications in agriculture. They are vital for bacterial activities in suppressing disease pressure in plants by their production of antimicrobial substances and by activating plant defense, as well as being important for biofilm formation and root colonization of crop plants (82, 158). Bacteriocins, which are

mostly active against Gram positive strains, have not been as highly employed in agriculture, but are employed as food preservatives (157).

As a first observation for answering the question, it can be noted that *B. amyloliquefaciens* strains are inducible and producing inhibition zones against *R. solanacearum* EAP09 and *R. solanacearum* AW1 at different TTC concentrations (Table 3-4), but their antagonistic potential in TTC absence is equally large. This particular species is reknown as being the most prolific from the point of view of LPs and PKSs production (144), and it's interesting to note that it is not outstanding in this particular form of antagonism (Table 3-4). On the contrary, *B. subtilis* species are highly inducible (Table 3-4, Table 3-5, Fig. 3-3 c-d), with *B. subtilis* SMY and *B. subtilis* NCIB-3610 being indeed used as model organisms for molecular and metabolomics analysis in further chapters of this research. Even if *B. subtilis* natural antibiotics production capacity has been well documented in the literature (130), the inhibitory capacity of these natural substances against *R. solanacearum* is significantly lower than the one produced by TTC –inducible ones, demonstrating that the inducible compounds may have a different chemical nature and that traditional NPs from *Bacillus* sp. are not the main responsible substances for this particular class of antagonism. Thus, complementary to these observations, the inducible antimicrobial activity of mutant strains from *B. subtilis* NCIB-3610 (Table 3-3) was tested, revealing that mutants on some of the most widely known biosynthetic routes for *Bacillus* (*surfA*, *pksX*, *bacA*, *sunA*, *ppsB*, among others) are not defective in the production of the inducible antagonism (Fig. 3-10), suggesting that the chemical nature of these inducible compounds may not be attributed to these families and that new biosynthetic routes not being detected or taken into account may be triggered by the reduction of TTC, an accumulation of TPF inside the cells or a greater nitrogen availability in the cytoplasm.

Besides this, other two genes displayed a greater inhibition zone against *R. solanacearum* EAP09 and *R. solanacearum* AW1. These are *spo0A* and the triple mutant *kinABC*, both of them intimately related, since these kinases, specifically *kinA*, phosphorylate the sporulation-regulatory proteins Spo0A and Spo0F through a phosphotransfer pathway, known as the phosphorelay, composed of Spo0F, Spo0B, and at least four histidine kinases, KinA, KinB, KinC, and KinD (159). This same study by Quisel *et al.* (2001) reveals that in order for *spo0A* to be activate and initiate sporulation, it highly depends on the phosphorylating activity of these kinases. This explains why these two mutants are presenting the same behavior of increased induced activity, since they are different steps from the same pathway of the onset of sporulation, suggesting that sporulation might repress the production of inducible substances and that they are generated during the exponential growth phase or before entering stationary phase, a result observed as well in the co-

cultures of *B. cereus* EA-CB1047 with *R. solanacearum* EAP09 (Fig. 3-6). This result could indicate that genes downstream of this pathway, which are repressed by *spo0A*, might be involved in the production of the inducible compounds; as Molle *et al* (2001) identified 81 genes under its negative control (160). Interestingly, some of these genes encode components of the DNA replication machinery and govern flagellum biosynthesis and chemotaxis, among other important transcriptional regulators as *abrB*, which is an essential regulator in the transition between vegetative growth and the onset of stationary phase and sporulation.

While many of the active compounds from *B. subtilis* and *B. amyloliquefaciens* have been already identified and some of them are deeply studied as are LPs and PKSs, there is still a great amount of their metabolites producing potential that remains unexplored as well as the one from other Bacillales species (151). Most of these products have been studied and isolated from *B. subtilis*, *B. amyloliquefaciens*, *P. polymyxa*, *B. thurigiensis* strains (144), and identified using traditional natural products discovery methods as the Waksman platform, also employed for the discovery of a large amount of the known active compounds from microbial sources (41). It is estimated that more than 31% of the known Bacillales species have the ability to produce bioactive metabolites, although many of these microbes remains untapped, undiscovered and unexploited (151). This pool of novel active metabolites can be even broader taking into account that other genes responsible for many common secondary metabolite classes (e.g. oligosaccharides) are not even detected by widely used prediction tools from genomes, such as antiSMASH (161).

In the other hand, the effect of TTC presence in the medium on the production of other intermediate metabolites and important organic compounds, as are free radicals and siderophores, was tested. Antioxidant addition to the culture medium (Fig. 3-9) proved that the inhibition zones produced by *B. cereus* EA-CB1047 in the presence of TTC were not affected in its size compared to a control not growing in the presence of any antioxidant substance, indicating that an overproduction of ROS, that could be being produced as by-products of intracellular reduction of TTC, may not be the ones causing the antagonism, and in fact, tetrazolium salts are known for acting as neutralizers of superoxide and other free radicals, as they act as intermediate electron acceptors (104).

Besides, the production of other bioactive substances such as siderophores, has been observed to produce large inhibition zones when in conjugation with other metabolites, depending on the nature and the producing strain of the iron-chelating substances (162). *Bacillus* specifically, produce a wide variety of siderophores such as bacillibactin, pyoverdine, pyochelin, schizokinen, petrobactin, which play a crucial role in its existence

(163), although the most studied ones are catechol-type siderophores with variant hydroxylation patterns, these being bacillibactin first identified in *B. subtilis* (164) and petrobactin, inherent but not exclusive to the *B. cereus* group species (165). In this research, siderophores production from *B. subtilis* was tested through the CAS assay (Fig. 3-8), suggesting not only that siderophores are not the ones responsible for halo production, since an observable orange halo characteristic of siderophores production is observable around non-TTC exposed cells as well as in TTC growing ones, but that, siderophores production in the presence of TTC might be repressed since halo size is smaller than the control condition.

3.5 Conclusion

Redox indicator TTC is acting as a dose-dependent inducer of diffusible antagonistic compounds in *Bacillus* sp. strains belonging to *B. cereus*, *B. pumilus* and *B. subtilis* species. These compounds are highly active against *R. solanacearum* and mildly active against other bacterial strains belonging to pathogenic genera. Result from this chapter suggest that the chemical nature of these substances apparently differs from other well-studied natural compounds produced by *Bacillus* and the induction of different biosynthetic gene cluster or a biotransformation of TPF could be occurring, due to its intracellular accumulation.

CHAPTER 4

4. Transcriptomic Analysis

Abstract

Aiming to establish changes in the overall gene expression of *Bacillus* sp. cells during the production of inducible antimicrobial substances, the transcriptomic profiles of *B. subtilis* NCIB-3610 and SMY strains, under the presence and absence of the inducer TTC were established. Data obtained by two differential gene expression techniques, evidences two distinct but interconnected results. According to total-RNA sequencing, the L-histidine biosynthetic pathway is highly upregulated in *B. subtilis* NCIB-3610 cells exposed to TTC, with expression ratios of genes *hisB*, *hisD*, *hisIE*, *hisF*, *hisH* being more than 4-fold higher in TTC exposed cells. Nanostring gene expression analysis, evidenced that pyrimidine and purine nucleotides *de novo* synthesis (genes *pyrC* and *pyrP*) and salvage and interconversion routes (*xpt*), display expression ratios between 1.6 to 3 fold higher on TTC induced *Bacillus* sp. cells compared to others growing under non-TTC conditions. These results strongly imply an increased production of nitrogen-derived compounds, from central nitrogen metabolism biosynthetic pathways in the cells. Transcriptomic profiling results merge with biochemical characterization, specifically in siderophores production down-regulation and characterized antimicrobials from *Bacillus* sp. not being induced in cells growing under TTC presence. Siderophores biosynthesis appears to be under-expressed in *B. subtilis* SMY cells, as genes *yxkB*, *dhbB* and *dhbC* central to bacillibactin production are 4 to 5 fold downregulated when growing in TTC presence. Most of the central genes of known antimicrobials biosynthetic routes appear to be non-altered in TTC presence, supporting the suggestion of lipopeptides and other known antimicrobials from *Bacillus* sp. not being responsible for the induced antagonism.

4.1 Introduction

Microorganisms produce a wealth of structurally diverse specialized metabolites, which are used either in their natural, semisynthetic derivatives form or synthetic analogues in a remarkable range of applications in medicine and agriculture, such as the treatment of infectious diseases and cancer, and the prevention of crop damage (80, 166). Genome sequencing reveals that each strain of actinomycetes can produce around 20–40 secondary metabolites, many of which have not yet been characterized and have high probabilities of presenting antibiotic activity (11). Most of these are not readily produced under laboratory

settings and are therefore not tested in traditional assays of extracts. Efforts to awaken these so-called 'cryptic' or 'silent' BGC have been pursued including altering the growth conditions, the overexpression of genetic regulators, the addition of chemical elicitors, and the capture of BGC for expression in heterologous hosts (11).

Thus, in these modern days, antibacterial drug discovery is highly influenced by genomic data, technology and innovation. This influence started in the early 2000s when complete genome sequences became more accessible and several ones obtained for actinobacteria and filamentous fungi, the two major microbial sources for clinically approved and agriculturally used antibiotics, began to reveal a far greater potential to produce structurally complex, specialized metabolites than suggested by traditional bioactivity-based screening approaches (167, 168). These genome wide studies are based on search for sequences of gene clusters that encoded enzymes typically involved in specialized metabolite biosynthesis, such as nonribosomal peptide synthetases (NRPSs), polyketide synthases (PKSs), terpene synthases and NRPS-independent siderophore synthetases (56).

Complete genome sequences of several other actinobacteria have revealed that they contain, besides the characterized ones, numerous cryptic BGCs that probably encode novel specialized metabolites (169), broadening the perspective for discovery of microbial natural products and setting a start for what is now called the new field of genomics-driven natural product discovery (170). A widely used tool through which this type of analysis can be readily made is antiSMASH (antibiotics and secondary metabolite analysis shell) (171). But although this and similar platforms perform well in the identification of BGCs encoding ubiquitous classes of biosynthetic enzymes (such as PKSs and NRPSs), are less reliable for the identification of BGCs that encode pathways involving more enigmatic or less explored enzymes and final products (172).

Bacillus species have not escaped the exploration of their active metabolite producing potential from the perspective of this modern technique, that allows for a whole genome exploration of potential metabolites. Since many *Bacillus* draft genome sequences as well as the ones for several other prokaryotes have been performed over the years (161) it is easy nowadays to obtain these type of analysis. In example, the study by Cheng *et al.* (173) analyzed the pan-genome of 44 *B. amyloliquefaciens* strains, using the workflow BGDMDocker, and revealed its BGC content and features. Main findings suggest a total of 997 known BGC for the entire pan-genome of this species and 553 unknown ones, evidencing that more than 30% of the total BGC of *B. amyloliquefaciens* strains, one the most prolific species in producing active NPs, remains uncharacterized and unexplored by traditional methods.

In the same line, the transcriptome, which is the complete set of transcripts in a cell and their quantity, for a specific developmental stage or physiological condition, has been largely used as a target for studies looking to understand what are the essential causes for a determined phenomenon (174) either in prokaryotic or eukaryotic cells. The quantity of mRNA produced of a specific gene is quantified and that is called the gene expression for that specific genomic portion under those conditions (175).

In accordance, measuring the expression of genes in bacterial genomes has a very broad range of applications, from developing treatments for infections to creating synthetic genomes (176). Gene expression studies in bacteria have been used to study metabolic pathways, identify properties of mutants, and otherwise better understand the molecular processes in their genomes (177).

For instance, the study by Pavlidi *et al* (178), exemplifies the use of transcriptomics for deciphering the molecular processes taking place during an interspecies interaction. In this particular case, the interaction between *Bactrocera oleae*, a fly that constitutes olive crops' most devastating pest, and its host, was investigated at the molecular level in the study by Pavlidi *et al* (178). Authors used both microarray and sequencing techniques to determine the genes which enabled the fly to cope with high levels of toxic phenolic compounds, as Oleuropein (179), present in green olives. Findings, point to the production of detoxification and digestive enzymes in *B. oleae* larvae, indicating a potential association with the ability of the insect larval stage, to cope with green olives toxic environment. Besides, several biological processes seem to be activated in *Ca. Erwinia dacicola*, an uncultivated gut obligate symbiotic bacterium of *B. oleae*, during the development of larvae in olives, with the most notable being the activation of amino-acid metabolism, which probably influence the larvae's nitrogen utilization and aid in development

But besides transcriptomics use to uncover the principal molecular processes taking place during a biological interaction in a living organism, one of the principal uses of transcriptomics in drug discovery is based on its ability to provide information on the effect of a determined compound once it enters in contact with an organism, providing data that conveys more information about its properties and allows lead optimization in pharmaceutical discovery projects (180). This is called a multi-dimensional assay, meaning that it measures a wide diversity of biological effects during lead optimization stage of bioactive candidate compounds screening. The focus of these multidimensional assays that use RNA as response variable, is to decode the gene expression profile of a living organism during the interaction with the drug candidate and give a comprehensive snapshot of the

biological state of the living system (180). In fact, the popularity that transcriptomics has acquired in the last decade in drug discovery platforms is due to the ability of gene expression to be measured in a high throughput fashion and to identify drug-induced genes in the target which allow drug repurposing and discovery among a battery of tested compounds, refining the uses of lead substances and detecting novel active ones (181).

The first step in a differential gene expression analysis process is to quantify gene expression for all the genes expressed in a particular experiment (176). For this matter, diverse techniques have been devolved and employed over the years, with hybridization or sequence-based approaches being the most prolific ones (174). Hybridization-based approaches typically involve incubating fluorescently labelled cDNA with custom-made microarrays or commercial high-density oligo microarrays, which makes them suitable for high throughput analysis and are relatively cost-efficient (182). They have several limitations as well, as the reliance upon the existence knowledge on a determined genome sequence, the high background levels due to cross-hybridization or saturation of signal (183). Meanwhile, RNA sequencing (RNA-seq) has been rapidly adopted for the profiling of transcriptomes in many areas of biology, including studies into gene regulation, development and disease, but there are a number of subtle yet crucial aspects of these analyses, such as read counting, appropriate treatment of biological variability, quality control checks and appropriate setup of statistical modeling that difficult the reaching of conclusions (184). Besides, for properly analyzing datasets of such volume and complexity as the ones generated from RNA-seq, scalable, fast and mathematically principled analysis software or bioinformatic pipelines are fundamentally needed (185), compared to the easy access and readily analysis offered by the companion software of hybridization platforms (186).

The main objective of this chapter was to establish a differential gene expression profile and derived analysis of *B. subtilis* NCIB-3610 and *B. subtilis* SMY, two model strains of a TTC-inducible *Bacillus* species, growing in the presence and absence of TTC in the culture medium.

4.2 Methods

4.2.1 Cell cultures for RNA-extraction

B. subtilis NCIB-3610 and SMY both belong to BGSC collection and a copy of each one was stored in 0.5X TSB plus 20% glycerol at -80 °C. The strains were activated in 50% TSA (Merck) or LB agar (composition for 1 L: tryptone (Oxoid) 10 g, NaCl (Merck) 10 g, yeast extract (Oxoid) 5 g, agar (BD) 15 g) and incubated for 48h at 30 °C before any experimental use.

For liquid cultures destined for total RNA extraction used in RNA-seq technique, two colonies of each strain were inoculated into 2 mL of BG medium on a 15 mL tube and incubated at 30 °C until an O.D (600 nm) of 1 was reached, approximately for 15 h. Afterwards, 1 mL of this pre-inoculum was inoculated into each 50 mL flasks containing either fresh BGT (+TTC) or BG (-TTC) media. Two flasks were used per conditions and incubation was performed at 150 rpm and 30 ± 2 °C for 14h.

For solid cultures, destined to extract total RNA for NanoString expression profiling, preinoculums of *B. subtilis* NCIB-3610 antagonistic strain were prepared by resuspending two colonies into 2 mL of BG medium on a 15 mL tube, and incubating overnight at 37 °C at 150 rpm. Afterwards, antagonism tests by well diffusion assay (method 3.2.4.2) were prepared in BGTA (+TTC) and its respective negative control BGA (-TTC). After 24 h of RT (22 ± 1 °C) incubation two colonies were scraped from each plate for total RNA extraction. Three biological replicates were established per condition each time the experiment was performed, twice in different times.

4.2.2 Total RNA extraction

500 µL of liquid cultures of *Bacillus* sp. strains growing under each condition (+TTC/-TTC) were harvested at 14h post-inoculation, at O.D (600 nm) of 1.6 and 2.0, respectively for +TTC and -TTC cultures, measured at 600 nm. Fermentations samples were immediately treated with 2 volumes (2v) of RNAprotect cell reagent (Qiagen, Netherlands), in order to provide RNA stabilization without removing culture medium. Afterwards, every step of the RNeasy RNA isolation kit (Qiagen, Netherlands) was followed, with a modification in the cell disruption procedure, employing sonication (Branson, Emerson, USA) at 30% amplitude with 1s on, 1s off pulses, performing a total of 25 pulses, on ice. RNA yields after isolation and purification were determined by Nanodrop (ThermoFisher, USA) and total DNA digestion followed using Turbo DNA-free (ThermoFisher, MA) DNase treatment.

A PCR amplification was done following DNase treatment in order to check DNA absence. 5F (5'- AGAGTTTGATCCTGGCTCAG-3') and 519R (5'-GWATTACCGCGGCKGCTG-3') primers (187) were employed. Genomic DNA from *B. subtilis* NCIB-3610 and *B. subtilis* SMY strains was extracted with Wizard genomic DNA Kit (Promega, USA) and used as positive control for DNA presence. The PCR mixtures (50 µL) contained 2 µmol of each appropriate primer, 200 µM of each deoxynucleoside triphosphate, Taq extender PCR buffer diluted to 1X of original concentration, 1.5 mM of MgCl₂, and 0.5 U of Taq polymerase (Qiagen, Netherlands). Approximately 25 ng of genomic DNA were added to each PCRs mix. Reaction

conditions were: initial denaturing at 96 °C for 2 min, followed by 40 cycles at 94 °C for 20s, 64 °C for 20s, 72 °C for 30s and a final extension period at 72 °C for 5 min in a thermal cycler (Biorad). PCR products were visualized by agarose gel electrophoresis. After checking DNA absence RiboZero ribosomal RNA removal kit (Illumina, USA) was employed to remove other RNA types besides mRNA.

4.2.3 Library construction

Library construction for RNA sequencing (RNA-seq) was performed using the purified mRNA from steps above and using the RNA library prep kit for illumina NEBNext (New England Biolabs, USA). The starting material for this kit was 5 ng – 1 µg and briefly, the steps followed were: RNA fragmentation, priming and cDNA synthesis, followed by purification of double stranded cDNA, end repair and adaptor ligation, with a final step of PCR enrichment and purification of product. Quality was checked through bioanalyzer before sequencing.

4.2.4 Sequencing

Libraries were sequenced at TUCF Genomics (Tufts University Core Facility). All samples (two samples per condition in two time-independent replicates, for a total of 8 samples) were submitted in bar coded tubes to ensure accurate sample handling and tracking and sequenced at an HiSeq 2500, rendering single-end reads of 51 nucleotide and getting an average coverage of 1000X for each sequence, of either *B. subtilis* SMY or *B. subtilis* NCIB-3610, under each condition (+TTC/-TTC).

4.2.5 NanoString

The quantification of mRNAs in cell lysates of *B. subtilis* NCIB-3610 was performed *via* the nanoString nCounter analysis system (NanoString technologies, USA) (186). Cell cultures were established as described above (4.2.2). Afterwards, two colonies of each sample from each condition were scraped with a pipet tip from each plate at the edge of growth and immediately suspended in 250 µL RNeasy lysis buffer (Qiagen, USA; diluted 1:1 in water). Cell clumps were mechanically disrupted with mortar at RT for 15 min and followed by sonication on ice bath with 30% amplitude with 25 pulses, 1s on, 1s off. Cells were then centrifuged at 13.000 rpm for 1 min and washed with 500 µL PBS buffer. After another centrifugation, pellets were resuspended in 100 µL of 15mg/mL lysozyme (Qiagen, 37.5mM in 2mM Tris-EDTA, pH7.5), pipetting thoroughly to resuspend cells and incubating at RT for 1 h. Finally, 200 µL of RLT buffer (Qiagen, Netherlands) + 2 µL β-mercaptoethanol were added to each tube and 1 µL of a 1:10 dilution in RLT buffer was used for hybridization.

Probe hybridization was done overnight. Briefly, 10 μL of hybridization buffer were mixed with 10 μL of reporter probe from original codeset (codeset names: Pascale2, Traxler1) and 4 μL water, per reaction. A master mix was prepared for all reactions and aliquoted into each tube, to finally add 1 μL of cell lysate to each, with minimal pipetting to avoid probe degradation. Tubes were taken to pre-heated thermocycler (65 °C) and 5 μL of capture probe were added to each one, inverting to mix and briefly spinning, before letting them for overnight incubation (approx. 16 h).

For the nCounter to assess gene-expression, preparation plates with 6 reactions were stabilized to RT and centrifuged for 2 min at 1800 rpm to collect liquid. Cartridges were also stabilized to RT before applying solution from hybridization tubes and setting the nCounter run (3 h). After nCounter, cartridge was transferred to reader (4 h) and results datasets were collected for further analysis.

4.2.6 Bioinformatic analysis

RNA-seq data was downloaded from TUCF server onto Apolo computational center at EAFIT university. Afterwards, analysis were performed through a bioinformatic pipeline which employed three different methodologies: Tuxedo suite, specifically CuffDiff tool (185), R-package DE-seq (188) and EDGE-pro (176) in order to calculate differential gene expression (DE) through the normalized parameter RPKM (read per million reads per million bases sequenced). Fold change was calculated by finding the ratio of the RPKM parameter on TTC presence vs TTC absence, and its significance was evaluated by the statistic *p-adj* value. Statistical analysis using PCA (principal component analysis) and Venn diagrams was performed prior and after analysis, respectively. PCA was done to assess replicates dispersion and Venn diagrams to find common DE genes across methodologies.

Nanostring results were analyzed in its companion software nSolver package (nanoString technologies, USA). Briefly, total transcript counts were normalized using internal controls with background subtraction. Transcript counts for housekeeping genes *def*, *folB*, *glpF*, *gsaB*, *ptsG* were used for normalization to correct for differences in total mRNA concentration. All data were collected from three biological replicate. Two time independent experiments were done for Pascale2 codeset and one for Traxler1 codeset. Gene expression was considered significantly altered if LOG2 of expression-ratio counts were 1.5 units above or below zero (189).

4.3 Results

4.3.1 Total RNA extraction yields are higher in +TTC condition

Following RNA extraction, total transcriptional material was quantified (Table 4-1). The main observation from these results, coming from two time-independent extractions, relies on the higher average of total RNA from strains growing under +TTC condition. This result is further discussed in the next section, but could be attributed to higher concentrations of nucleic acids that are being produced in TTC induced cells, or other related compounds such as nucleotides, which absorb at a wavelength close to the one used for measuring double stranded nucleic acids concentration (260 nm) (190) in a Nanodrop spectrophotometer. This result could be also associated to membrane permeabilization in TTC exposed cells, allowing major quantities of nucleic acid material to be extracted. This scenario is further considered in discussion section.

Table 4-1. *B. subtilis* NCIB-3610 and *B. subtilis* SMY RNA extractions yields

STRAIN	+I (ng/ μ L)	-I (ng/ μ L)
<i>B. subtilis</i> NCIB-3610	157.8 \pm 94.5	60.8 \pm 13.1
<i>B. subtilis</i> SMY	307.7 \pm 41.4	19.3 \pm 1.4

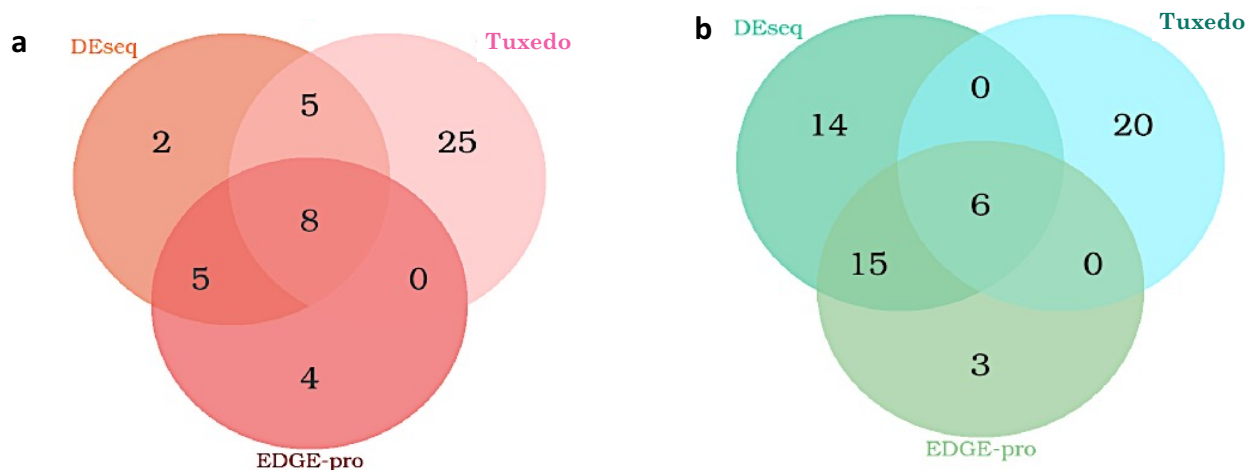
Intervals represent standard errors of the mean (n=3).

+I denotes 50 mg/L TTC amendment in the medium -I denotes TTC absence in the medium.

4.3.2 Histidine biosynthesis is upregulated and siderophores synthesis is down-regulated in *Bacillus* sp. cells growing with TTC in a liquid fermentation

The results obtained from total RNA-seq followed by bioinformatic analysis using three different bioinformatic packages, as stated in methods section 4.2.6 section, are summarized in Fig. 4-1, 4-2 and Table 4-2. In a general fashion, eight common genes were found differentially expressed across the three methodologies for *B. subtilis* NCIB-3610 (Fig 4-1a), while six were found for *B. subtilis* SMY (Fig 4-1b).

Figure 4-1. Differentially expressed genes under TTC presence based on three bioinformatic approaches for *B. subtilis* NCIB-2610 (a) and *B. subtilis* SMY (b).



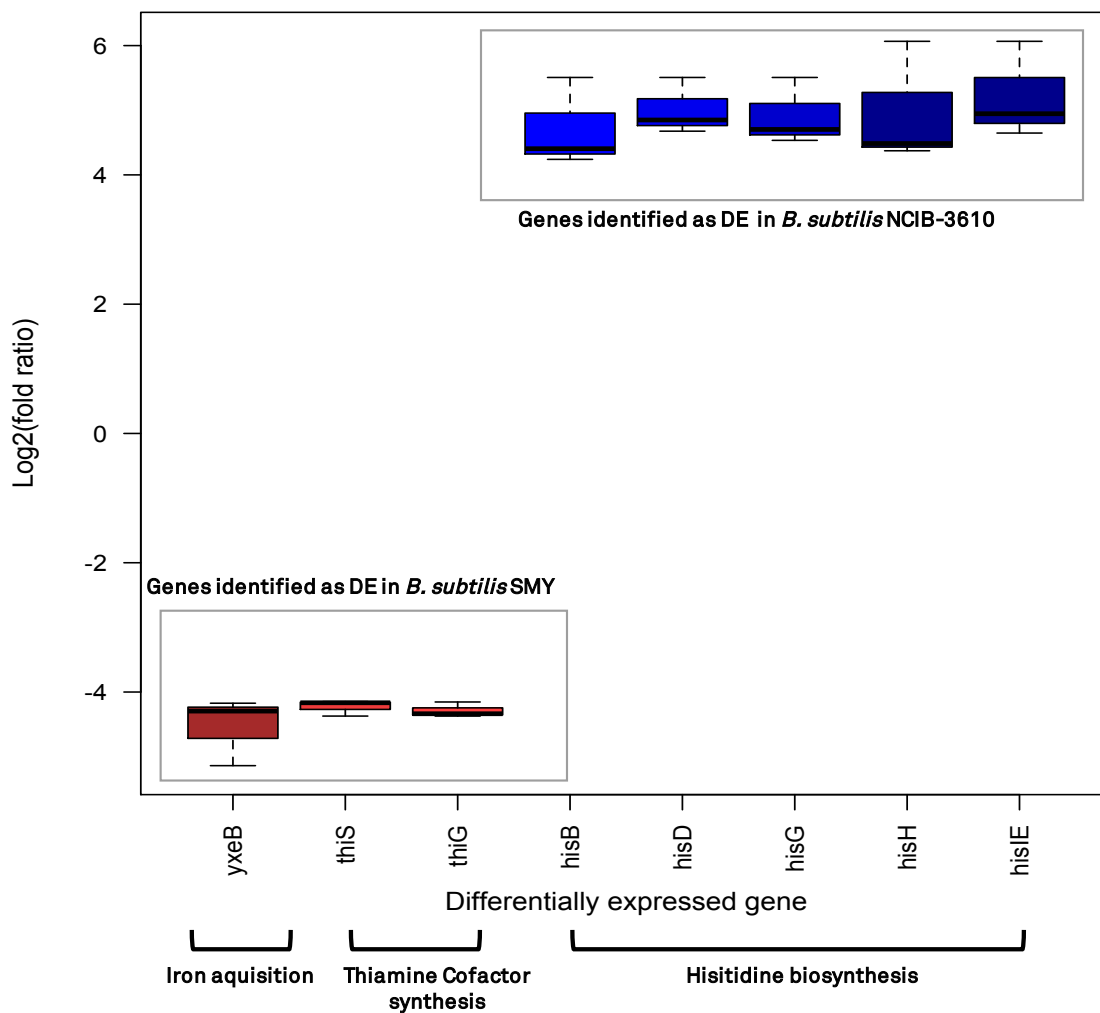
Data dispersion (supplementary material Fig. S-13), quality check and correction prior to analysis support the statistically significant difference in expression levels stated for the group of common DE genes of each strain, leading to confidently compare expression ratios among methodologies (Table 4-2). Besides the significantly expressed genes common across the three bioinformatic packages used, expression ratio values for other genes, independently found to be significant by each methodology (Fig. 4-1, supplementary material Table S-2), serve as reinforcement of the observed alterations in specific metabolic pathways.

Differentially expressed genes suggest that histidine biosynthetic pathway is upregulated in *B. subtilis* NCIB-3610 cells (Fig. 4-2, Table 4-2), since all the major *his* biosynthetic genes (*hisB*, *hisD*, *hisI*, *hisF*, *hisH*) are overexpressed with values for log₂ of fold-ratios ranging from 4.7 to 5.2, when TTC is present in the culture medium and thus, when producing the inducible antagonistic compounds. As for *B. subtilis* SMY, iron transport appears to be downregulated in cells growing under TTC presence (Fig. 4-2, Table 4-2), since the *yxkB* gene, responsible for processes involving iron 3⁺-hydroxamate complex import and required for transport of siderophore desferrioxamine (138, 191), is notably under-expressed. Another important result is the under-expression of genes *thisS* and *thisG*, which produce synthase proteins involved in the biosynthetic pathway of thiamine diphosphate, which is itself part of the larger cofactor biosynthesis (138).

Besides these differentially expressed genes represented in the figure (Fig. 4-2) and table (Table 4-2), which outstand the major functions in the cells that are being affected in either over or under-expression when the cells are subjected to growth in TTC presence, there are other genes which reinforce the suggestion of alteration for these pathways. These genes have been independently found to be significant by each methodology (supplementary material Table S-2). For instance, in *B. subtilis* NCIB-3610 the gene *hisA*, which is also part of histidine biosynthetic pathway (138, 192) was found to be significantly over-expressed from DE-seq and Tuxedo methodologies (supplementary material Table S-2). The gene *trxA* responsible for thioredoxin, a protein crucial in various redox reactions, regulation of oxidative stress in the cells and part of electron transport chain (193), was found significantly underregulated by DE-seq tool and *nadB*, responsible for L-aspartate oxidase involved in NAD⁺ and cofactor biosynthesis (194) was found underregulated as well by EDGE-pro methodology (supplementary material Table S-2). As for *B. subtilis* SMY, *dhbB* and *dhbC* genes, responsible for isochorismatase and thus, involved in bacillibactin and other catechol-type siderophores production (164) appear under-expressed (supplementary material Table S-2).

These results overall reinforce the previously observed alteration in the pathway of catechol-type siderophores biosynthesis, as well as in nitrogen metabolism through histidine over production and cofactor biosynthesis. Besides these results, other genes relevant to diverse cellular processes in both strains, *B. subtilis* NCIB-3610 and *B. subtilis* SMY, as are membrane transport systems (inositol transporter *IoT*), DNA repair (p-450, DNA repair protein) and redox equilibrium in the cell appear to be negatively altered when TTC is present, according to RNA-seq results (supplementary material Table S-2). Specifically, the major inositol transporter *IoT* is interesting since it is in charge of transporting alternative carbon sources inside the cells, as is sugar alcohol *myo*-inositol, but this gene product has significant similarity with many bacterial sugar transporters in the databases (195)

Figure 4-2. *B. subtilis* SMY and *B. subtilis* NCIB-3160 differentially expressed genes in the presence of TTC: RNA-seq



** Colors indicate under (red tones) or over (blue tones) expression of the gene.

Table 4-2. RNA-seq - *B. subtilis* NCIB-3610 and *B. subtilis* SMY differentially expressed genes, biological function and expression ratios

STRAIN	GENE	FOLD RATIO (+/-)				STANDARD ERROR	BIOLOGICAL FUNCTION*
		TUXEDO	EDGE-PRO	DE-SEQ	AVERAGE		
<i>B. subtilis</i> SMY	<i>thiS</i>	-4,4	-4,2	-4,2	-4,2	0,1	Sulfur carrier protein ThiS adenylyltransferase (thiamine metabolism)
	SMY_RS11645	-4,4	-4,2	-4,3	-4,3	0,1	Hypothetical protein
	SMY_RS11695	-4,4	-4,0	-4,0	-4,1	0,1	Hypothetical protein
	SMY_RS11655	-4,4	-3,8	-3,9	-4,1	0,2	Hypothetical protein
	<i>yxkB</i>	-5,1	-4,2	-4,3	-4,5	0,3	Iron(3+)-hydroxamate-binding protein yxB
	<i>thiG</i>	-4,4	-4,2	-4,3	-4,3	0,1	Thiazole synthase ThiG (thiamine metabolism)
<i>B. subtilis</i> NCIB-3610	BS3610_RS12370	-4,1	-4,3	-4,4	-4,3	0,1	Hypothetical protein
	<i>hisH</i>	6,1	4,4	4,5	5,0	0,6	Imidazole glycerol phosphate synthase subunit HisH
	<i>hisD</i>	5,5	4,7	4,9	5,0	0,3	Histidinol dehydrogenase HisD
	<i>hisG</i>	4,7	4,5	5,5	4,9	0,3	ATP phosphoribosyltransferase HisG
	<i>hisH</i>	ND	4,6	ND	4,7	0,0	Imidazole glycerol phosphate synthase subunit HisH
	<i>hisI</i>	6,1	4,6	5,0	5,2	0,4	Histidine biosynthesis bifunctional protein HisI
	<i>hisB</i>	5,5	4,2	4,4	4,7	0,4	Imidazoglycerol-phosphate dehydratase HisB
BS3610_RS12405	-4,0	-3,9	-4,1	-4,0	0,1	Hypothetical protein	

*Source: uniprot <http://www.uniprot.org/uniprot>

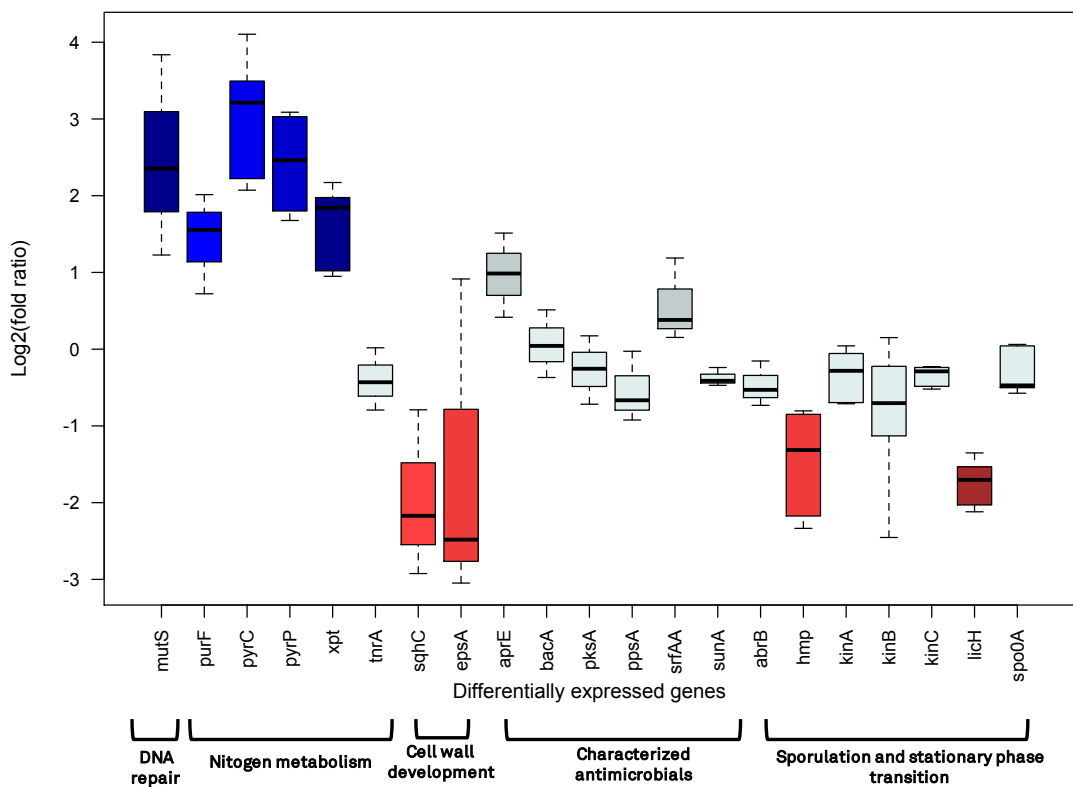
4.3.3 Purine and pyrimidine biosynthetic routes are upregulated and siderophores synthesis is downregulated according to nanoString methodology

Transcriptomic profiling from nano-String analysis is displayed in Fig. 4-3 and Table 4-3, where significantly altered genes evidence an upregulation of the nitrogen metabolism mainly through the genes involved in pyrimidines and purines *de novo* synthesis and salvage and interconversion routes (*pyrP*, *pyrC*, *purF*, *xpt*), as well as an onset on the DNA damage-machinery (*mutS*), which is related to DNA repair during oxidative stress. The utmost under-expressed genes, mainly related to exopolysaccharide synthesis (*epsA*) and membrane fluidity and stability (*sqhC*), denote a diminished biofilm production in TTC presence, as evidenced by *epsA* repression, as well as a diminished squalene (*sqhC*) and thus, hopanoids production, these being the sterol homologs in bacteria and its under-expression denoting membranes structural perturbations in *Bacillus* growing under TTC presence. Other non-significantly expressed genes, when comparing expression levels for the two conditions of presence and absence of TTC, are related to traditional natural products already characterized in *B. subtilis* strains, precisely bacillaene (*pks*), sublancin (*sunA*), surfactin (*urfAA*), plispastatin (*ppsA*), subtilisin (*aprE*) and bacilysin (*bacA*), demonstrating that these pathways are not over nor under expressed and probably are not directly involved in the inducible antagonism observed.

4.3.4 Differentially expressed genes from the two transcriptomic analysis methodologies converge in metabolic pathways

RNA-seq and nanoString techniques, the two transcriptomic analysis methodologies performed for *Bacillus* cells growing under TTC presence, report results which converge in the upregulation of a specific metabolic route: the purines and pyrimidines biosynthesis (Fig. 4-2 and 4-3). RNA-seq results, highlight the upregulation of the aminoacid L-histidine biosynthesis (Fig- 4-2, Table 4-2), while nanoString evidences an over-expression of the purine and pyrimidine biosynthetic and salvage routes (Fig- 4-3, Table 4-3). The highly upregulated metabolic pathways are represented in the KEGG maps (196) under Figs. 4-4, 4-5 and 4-6, where upregulated genes identified by transcriptomic analysis are highlighted in red boxes. Observation of the interconnectedness of L-histidine (Fig. 4-4) and other amino acids biosynthesis (Fig. 4-7) with purine and pyrimidine nitrogenous bases biosynthesis (Fig. 4-5; Fig. 4-6) is highlighted in blue boxes, expressing a common end for much of the cell pool or excess of nitrogen.

Figure 4-3. Differentially expressed genes of *B. subtilis* NCIB-3610 under TTC conditions according to nanostring



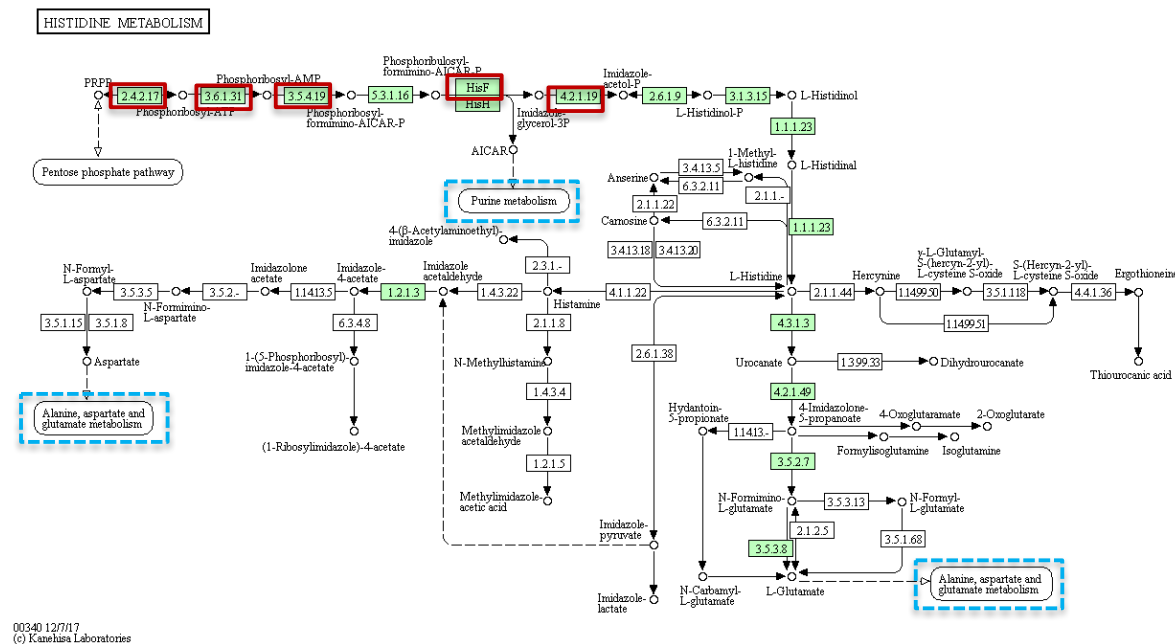
*Colors indicate under (red tones), over (blue tones) or non-altered (grey) expression of the gene

Table 4-3. NanoString - selected differentially expressed and other relevant genes, biological function and expression ratios for *B. subtilis* NCIB-3610

METABOLIC PATHWAY	GENE NAME	* BIOLOGICAL FUNCTION	**LOG2 (FOLD RATIO)
Nitrogen	<i>mutS</i>	DNA damage machinery	2,8
	<i>purF</i>	purine biosynthesis	1,5
	<i>pyrC</i>	Dihydroorotase from de novo pyrimidine metabolism.	3,0
	<i>pyrP</i>	Uracil transporter from pyrimidine salvage pathway	2,4
	<i>tnrA</i>	Transcriptional repressor, active under N-limitation	-0,4
	<i>xpt</i>	Xanthine phosphoribosyltransferase from purine salvage pathway	1,6
Development	<i>epsA</i>	Polysaccharide component of matrix	-2,2
	<i>sqhC</i>	Hopanoid metabolism involved in membrane synthesis	-1,9
Antimicrobials production	<i>pksA</i>	Bacillaene production	-0,3
	<i>sunA</i>	Sublancin lantibiotic precursor peptide	-0,4
	<i>bacA</i>	Bacilysin; first gene in operon	0,1
	<i>ppsA</i>	Plipastatin synthetase	-0,6
	<i>aprE</i>	Subtilisin E serine alkaline protease	1,0
	<i>srfAA</i>	Surfactin production and competence	0,6
Sporulation & stationary phase general regulators	<i>abrB</i>	Regulation of transition state genes, pleiotropic	-0,5
	<i>spo0A</i>	Stage 0 sporulation protein (central role in sporulation)	-0,3
	<i>kinA</i>	Sporulation Kinase A	-0,3
	<i>kinB</i>	Sporulation Kinase B	-0,9
	<i>kinC</i>	Sporulation Kinase C	-0,3
Other processes	<i>hmp</i>	flavo-hemoglobin: involved in nitric oxide stress	-1,5
	<i>licH</i>	6-phospho-beta-glucosidase	-1,7

Source: uniprot <http://www.uniprot.org/uniprot>

Figure 4-4. KEGG map for L-histidine metabolic pathway

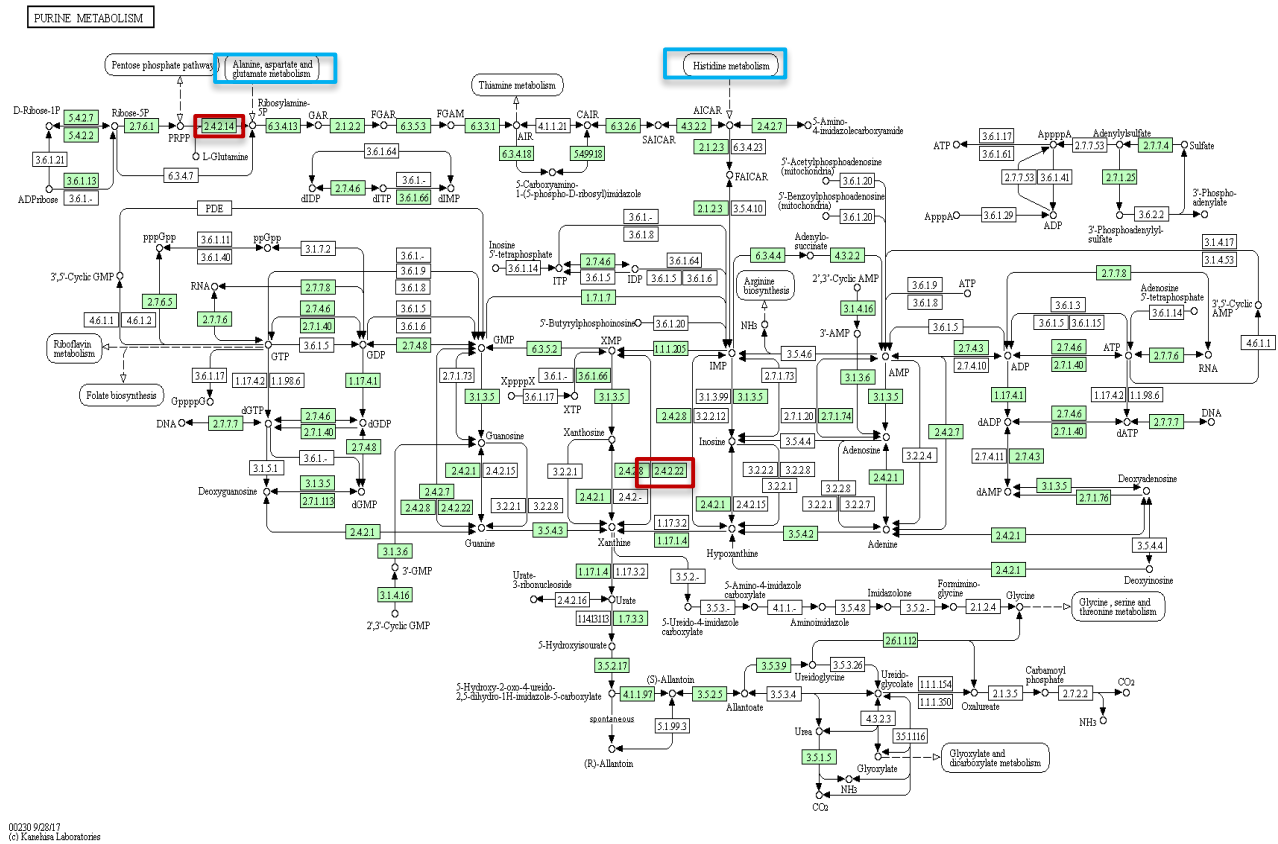


Red boxes-continuous border: upregulated genes identified by transcriptomic analysis.

Blue boxes-dashed border: interconnectedness of biosynthetic pathway represented in KEGG map with other nitrogen metabolism pathways

The metabolism of some amino acids, as L-histidine, glutamate and alanine appears to be destined to feed the highly upregulated purine and pyrimidine biosynthesis. While other metabolic routes, which appear as well connected to these nitrogen derives compounds from KEGG maps observation (Fig. 4-5, 4-6), are evidenced as downregulated from transcriptomic analysis, these being thiamine cofactor biosynthesis (*thiS*, *thiG*) (Fig. 4-2) and pentose phosphate pathway (*licH*) (Fig. 4-3).

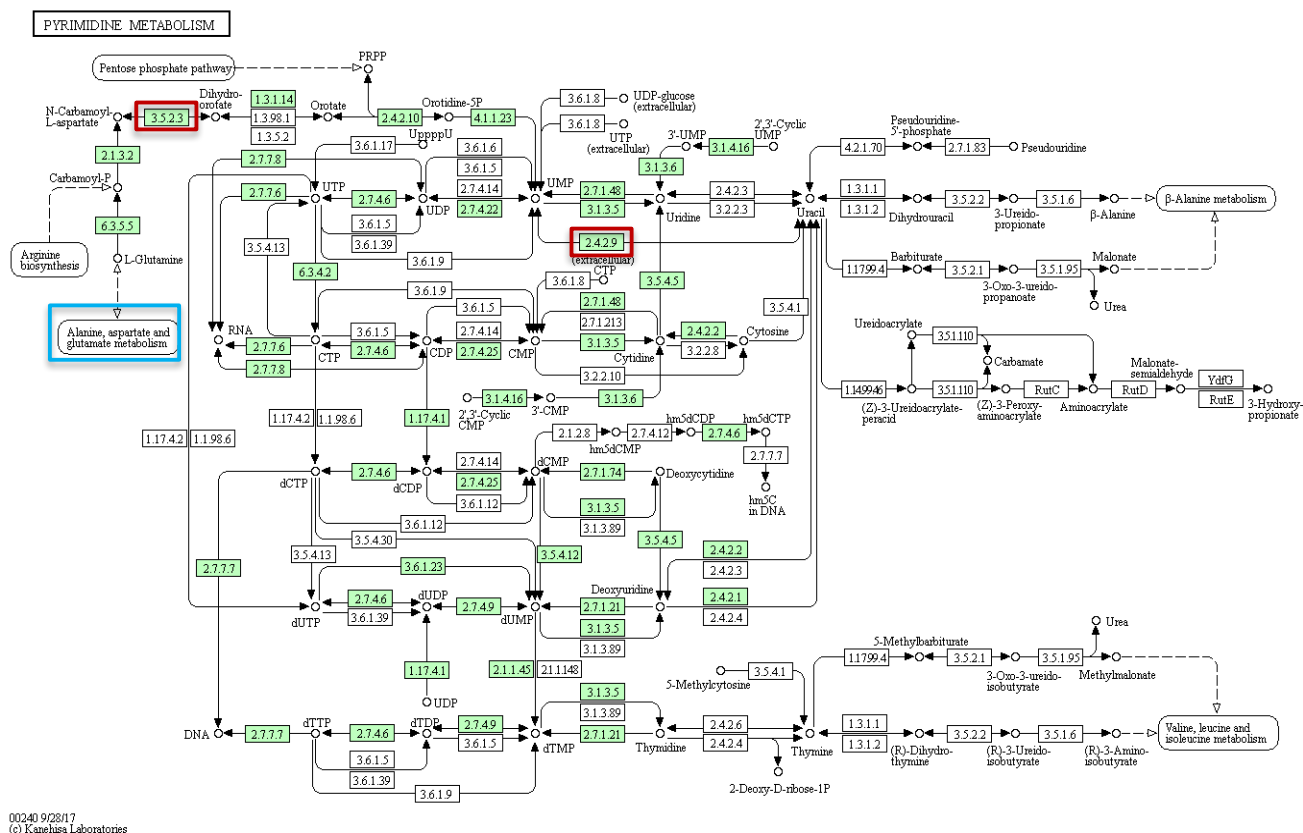
Figure 4-5. KEGG map for purines nitrogenous bases metabolic pathway



Red boxes-continuous border: upregulated genes identified by transcriptomic analysis.

Blue boxes-dashed border: interconnectedness of biosynthetic pathway represented in KEGG map with other nitrogen metabolism pathways

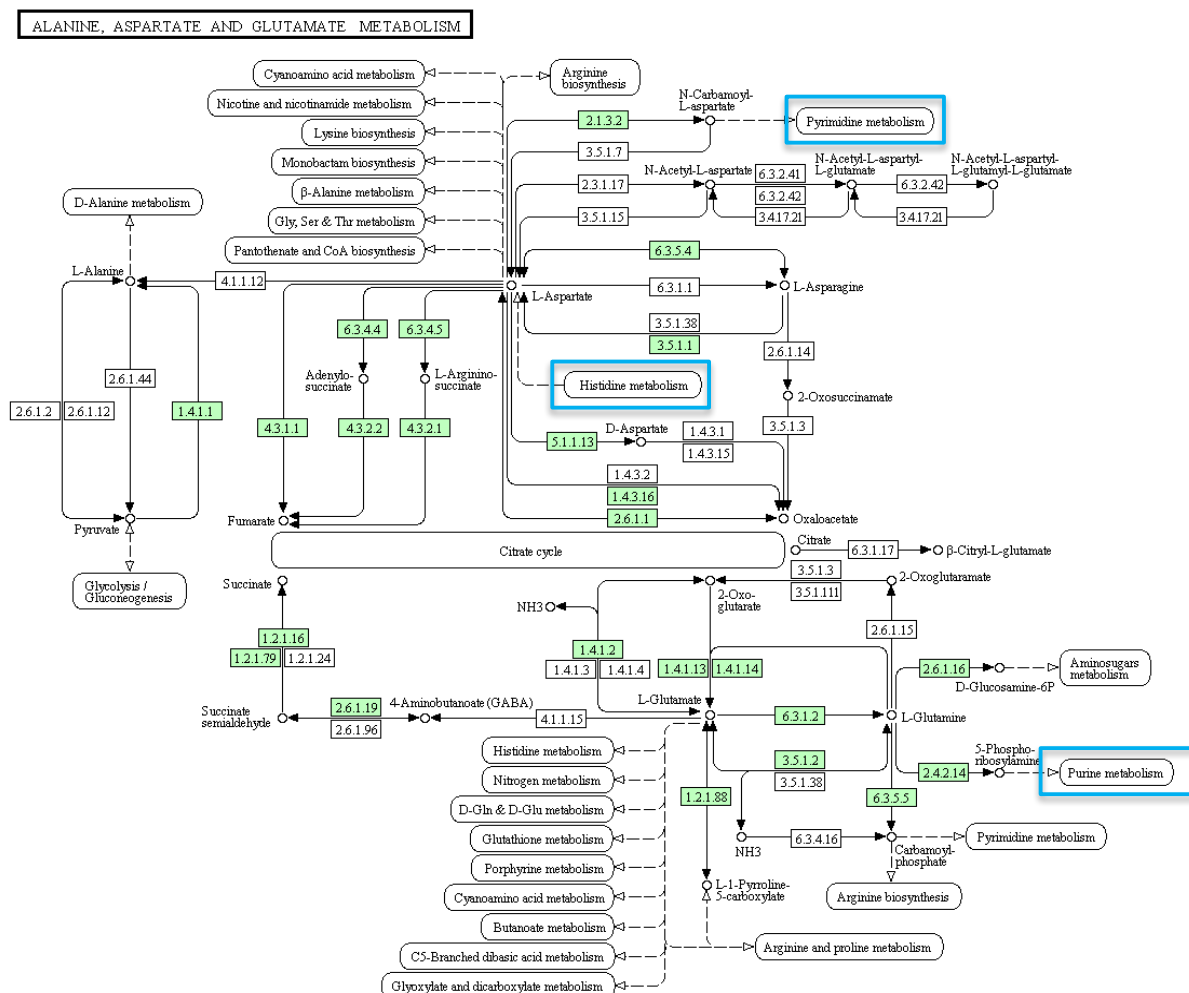
Figure 4-6. KEGG map for pyrimidines nitrogenous bases metabolic pathway.



Red boxes-continuous border: upregulated genes identified by transcriptomic analysis.

Blue boxes-dashed border: interconnectedness of biosynthetic pathway represented in KEGG map with of other nitrogen metabolism pathways

Figure 4-7. KEGG map for L-aspartate, L-glutamate, L-alanine amino acids metabolic pathways



00250 10/30/15
 (c) Kanehisa Laboratories

Blue boxes-dashed border: interconnectedness of biosynthetic pathway represented in KEGG map with of other nitrogen metabolism pathways

4.4 Discussion

Results from this chapter clearly suggest an increased expression of two principal metabolic routes in *B. subtilis* NCIB-3610 cells when growing in TTC amended media and a repressed expression in two routes of *B. subtilis* SMY cells under the same condition. For the first strain, synthesis of amino acid L-histidine (Fig. 4-2, Table 4-2), and pyrimidines and purines *de novo* synthesis, salvage and interconversion (Fig. 4-3, Table 4-3) are highly up-regulated.

When specifically regarding all kingdoms of life, cellular replication relies on the presence of nucleosides and nucleotides, the building blocks of nucleic acids and the main sources of energy (197). Both types of molecules, have as structural basis a nitrogenous base, either of purine or pyrimidine type, a deoxyribose sugar and a phosphate group, in the case of nucleotides, with nitrogenous bases being nitrogen-rich molecules with 5 atoms of nitrogen in the case of purines, and 2 atoms per molecule, in the case of pyrimidines (198). The two classes of molecules can serve both as nitrogen and carbon sources for growth in a variety of microorganisms (199, 200) and are constantly being formed and degraded in the biosphere by all living organisms (200). Specifically in bacteria, purine nucleotides are synthesized *de novo* from phosphoribosylpyrophosphate, amino acids, CO₂, and formate and when nucleotides are degraded, either aerobically or anaerobically to nucleobases and nucleosides, they may be reutilized via purine salvage pathways or further degraded (201). Oxidative purine degradation in microorganisms involves up to seven transformation steps before release of the end products, either urea or allantoin (198). Specifically in *Bacillus*, catabolism of purines takes place through the involvement of xanthine dehydrogenases, expressed by the operon *pucABCDE* and several other genes (200).

For pyrimidines, according to Vogels & van der Drift (201), some bacteria possess reductive pathways for its degradation into NH₄⁺ and amino acid or its derivative β-alanine and β-aminoisobutyric acid, but the reactions are energy-demanding and require NADPH. Alternatively, other bacteria utilize oxidative pathways in which pyrimidines are degraded to NH₄⁺, urea and organic acids, but only in the absence of NH₄⁺. This last is the most common pathway, forming orotic acid or orotate and then following subsequent oxidative steps which render L-aspartic acid as a final product.

In the other hand, the biosynthetic route for pyrimidines in bacteria parts from glutamine and L-aspartate and is followed up by enzymatic conversion of dihydro-orotate to orotate (202). It is usually a constitutive route, for instance in *E. coli* it has been demonstrated to be composed of particle-bound enzymes, linked with the respiratory chain (202). For both types of nitrogenous basis the biosynthetic routes are presented below, adopted from KEGG platform (196).

It also has been proven that the expression of enzymes and proteins involved in purine salvage, biosynthesis, and uptake in bacteria are directly regulated by the availability of metabolites or small-molecules, through riboswitches; these are portions of mRNA that can control gene expression by conformational changes in response to ligand binding (197). Besides this, closely related to purines metabolism is the co-factor Nicotinamide adenine dinucleotide (NAD⁺ in its oxidized form) or NADH in its reduced form, a low-molecular-weight substance discovered more than 100 years ago (203) that plays a central role in cellular respiration, the cascade of reactions that generate adenosine triphosphate (ATP) from nutrient breakdown, by acting as a coenzyme for oxidoreductases and dehydrogenases (204). This molecule is composed by a purine base (adenine) and nicotinamide bonded by two phosphate groups; its biosynthesis is done either *de novo* from media supplemented nutrients as tryptophan and nicotinic acid plus several enzymes involved, or by a salvage pathway from intracellular recovered nicotinamide dinucleotide (205).

From observation of KEGG metabolic pathway maps of these mentioned routes (Fig. 4-4, 4-5 and 4-6), it becomes evident that other amino acids metabolisms are interconnected with nucleotides biosynthesis, as amino acids are themselves precursors of nucleotides, a trait very conserved among all forms of life (206). For instance, biosynthesis of L-aspartate is narrowly related with L-histidine synthesis, and L-aspartate itself is an essential precursor of pyrimidine *de novo* synthesis, with the action of dihydroorotase (*pyrC*) acting directly on N-carbamoyl-L-aspartate to produce dihydroorotate (207) (Fig. 4-6). Consequentially, L-alanine, L-glycine, L-asparagine, L-lysine, L-arginine, L-serine, L-threonine, which are interconnected to L-aspartate synthesis (Fig. 4-7), are possibly presenting alteration in their concentrations in *B. subtilis* NCIB-3610 cells, this being suggested as a downstream consequence of *his* genes overexpression. In the same line, L-histidine intermediate 5-aminoimidazole-4-carboxamide ribonucleotide (AICAR, Fig. 4-4, 4-5) is an essential precursor of purines biosynthesis (143), and PRPP (5-phosphoribosyl diphosphate) is a key intermediate in the *de novo* synthesis of purines, pyrimidines nucleotides and histidine (Fig. 4-4, 4-5, 4-6) (206) these facts supporting the overall interconnectedness of these routes. In the same line, Bazaruto *et al.* (208) demonstrated in bacteria, that pyrimidine moiety of central metabolites, as cofactor thiamine for instance, is derived from aminoimidazole ribotide (AIR), an intermediate in purine biosynthesis. The same authors provide other findings to demonstrate that these intermediates in purines and pyrimidines biosynthetic routes are produced from various and diverse metabolic routes, which are sometimes redundant but essential for nucleotide and coenzyme biosynthesis (208).

These results suggest either an accumulation of intermediates in these routes, which can be possibly causing an antagonism due their large concentrations. Results as the ones attained by Bazaruto *et al* (208) suggest, that accumulation of AICAR is known to affect diverse areas of bacterial and animal cells metabolism, including adenosine homeostasis and gluconeogenesis (209, 210). In *Salmonella enterica*, AICAR has been shown to indirectly inhibit thiamine synthesis at the ThiC step (211) and directly inhibit pantothenate synthesis at the PanC-catalyzed step (208). This connects with observations by Andrade-Dominguez *et al* (212) on the antagonistic effect of other nucleotides biosynthetic routes intermediates as orotic acid, produced by a yeast strain of *Saccharomyces cerevisiae* and acting as a growth inhibitor of bacterium *Rhizobium etli* CE3 during liquid co-cultures. All these results suggest that the possible accumulation of intermediates, specifically imidazoles, aminoimidazoles, from the overexpressed routes, could be causing the observable induced antagonism, since presence of imidazole nucleus in several categories of therapeutic agents such as anti-microbials, anti-virals, anti-cancer, has been widely reported and made it a vital anchor for the development of new therapeutic agents (213).

Parallel to these results in NCIB-3610, SMY strain evidenced deregulation on siderophores biosynthesis and thiamine cofactor biosynthesis routes. The first metabolic route is related to catecholate-type siderophores production, mainly petrobactin and bacillibactin, as these are the principal compounds produced by *Bacillus* species of such family of molecules (163, 214). Results suggest a repression in the expression of genes *yxkB* (Fig. 4-2, Table 4-2, codifying for iron(3+)-hydroxamate-binding protein) and *dhbB* (supplementary material Table S-2), codifying for isochorismatase), both of them implied in iron transport, either through membrane transporters or bacillibactin biosynthesis respectively. This coherently overlaps with results from biochemical characterization of this inducible antagonism (Chapter 3), were a reduced production of siderophores is observed in the presence of TTC for strain *B. subtilis* NCIB-3610. These results altogether strongly evidence that siderophores production in *B. subtilis* cells is downregulated in TTC amended media and thus, this class of compounds are not responsible for the inducible antagonism observed.

In the other hand, thiamine cofactor (vitamin B1) biosynthesis is closely related to pyrimidines as half of its structure is formed by these nucleotides derivatives (215). It is also indispensable for the activity of the carbohydrate and branched-chain amino acid metabolic enzymes in its active form thiamin diphosphate (ThDP) (215, 216). Concretely, downregulation of genes *thisS* and *thisG* in *B. subtilis* SMY, both central in thiamine cofactor biosynthesis, implies a deviation of nitrogen metabolism into forming more nucleotides and thus, distancing its fate of forming thiamine and other cofactors, possibly causing a downstream repression of carbohydrate forming enzymes and amino acids like valine,

leucine and isoleucine (branched chain). This aligns with the downregulation of gene *lich* (Fig. 4-3, Table 4-3), whose product is a presumed phospho-beta-glucosidase involved in alternative carbon sources utilization (217) which reportedly has NAD and metal binding sites for becoming active (138). It is known that pentose phosphate pathway, which feeds itself from carbohydrate metabolism in the cells, is responsible for supplying ribose for PRPP synthesis, a key intermediate in L-histidine, pyrimidines and purines biosynthesis (Fig. 4-4, 4-5, 4-6). Thus, these results in sum suggest a sufficient pool of carbohydrates in the cells for the synthesis of ribose intermediates, repressing the expression of genes from alternative carbon sources utilization involved in its synthesis, possibly by carbon catabolite repression (217). In the same line, an apparent higher use of salvage pathways to produce key ribose-containing intermediates for purines, pyrimidines and L-histidine synthesis might be taking place. Besides, the increased production of these nitrogen derives products without the need in the cells for increasing carbohydrate production, indicates a need for utilizing excess nitrogen, conceivably coming from excess reduction product TPF open ring (Fig. 2-1, Chapter 2).

NAD^+/NADH balance in the cells is fundamental for the energy metabolism, it and its phosphorylated products being central molecules in cells functioning and hydride acceptors and donors in a variety of cellular redox reactions (218). Among NAD precursor are nitrogen derived compounds including aspartate and tryptophan (219). *Bacillus* cells growing in TTC amended media could see their redox metabolism altered, due to the pressure posed by the reduction of the tetrazolium ring into TPF, hence altering the intracellular NAD^+/NADH pool, since redox dies reduction, as the ones taking place inside the cells from TTC presence, has been observed to be done by respiratory chain dehydrogenases which use NADH as electron donor (104). This could explain the significant over-expression of genes related to DNA-repair and DNA-damage machinery in *B. subtilis* NCIB-3610, as is *mutS*. The product of this gene, is protein MutS is involved in the repair of mismatches in DNA, specifically activated during oxidative stress (138). This result could justify results from higher nucleic acids content (Table 4-1) in cells growing in TTC amended media, supporting the upregulation in nucleotides overproduction in order to form more nucleic acids in the face of oxidative stress conditions.

Other relevant downregulated genes in *B. subtilis* NCIB-3610 are related to membrane stability and biofilm formation, with *epsA*, first gene of the operon responsible for exopolysaccharide biosynthetic route being downregulated in *Bacillus* cells growing on TTC amended media as well as *sqhC* (Fig. 4-3, Table 4-3), responsible for producing sporulenol synthase, a key enzyme in hopanoids metabolism. These two processes denote a somehow impaired ability to secrete exopolysaccharide and form biofilms, in cells under this

condition, along with plasma membrane alterations, since hopanoids are considered functional analogues of cholesterol in bacterial membranes, playing a central role in membrane order and fluidity, through interaction with glycolipids in outer membranes to form a highly ordered bilayer in a manner analogous to the interaction of sterols with sphingolipids in eukaryotic plasma membranes (220). Interestingly, Sáenz *et al* (221) demonstrated that a hopanoid-deficient mutant of the gram negative *Methylobacterium extorquens*, had higher antibiotic sensitivity, introducing a link between membrane order and an energy-dependent, membrane-associated function in prokaryotes, ligated to an impaired drug-efflux mechanism. This could signify an impaired capacity of *B. subtilis* cells growing under TTC presence to detoxify themselves from sub-inhibitory concentrations of the substance and could explain as well the results of higher nucleic acid content in extractions from cells growing in TTC amended media (Table 4-1), possibly presenting a leakage of overproduced nitrogenous bases, nucleic acids and nitrogen metabolism intermediates across perturbed membranes.

Several other genes, associated to sporulation and stationary phase general regulation and to characterized antimicrobials production (Fig. 4-3, Table 4-3) are non-DE in *B. subtilis* NCIB-3610 growing on TTC amended media, coherently meeting biochemical characterization results that tested the inducible antagonism capacity of knockout genes from this strain, in some of these same genes (Chapter 3). Non-DE could indicate that entering stationary phase and sporulation is not switched off or altered when the expression of the inducible antagonism phenotype takes place, as genes from this pathway, especially *spo0A* and others downstream, have a central role in sporulation (160). Interestingly, some of these genes encode components of the DNA replication machinery and govern chemotaxis, among which are transcriptional regulators as *abrB*, which controls the transition between vegetative growth and the onset of stationary phase and sporulation.

In the overall results, is interesting to note that inducible antagonism in *B. subtilis* NCIB-3610 is higher than in SMY strain, meaning that larger *R. solanacearum* AW1 inhibition zones were observed for the first strain as producer of inducible compounds, suggesting a larger involvement of upregulated genes from *B. subtilis* NCIB-3610 in the production of inducible compounds and possibly, of DE genes from transcriptomic analysis for SMY being more relevant to the basic biological processes which are being altered in the cells when dealing with intracellular TTC reduction and accumulation of TPF. Besides, specially for SMY strains, several hypothetical proteins, which account for open reading frames (ORF) in *B. subtilis* genome that have been identified as possible proteins but no biological substance has been isolated and attributed to that particular genomic sequence, are downregulated

in the presence of TTC, denoting that there is still an abundant biological universe to explore coming from the cellular processes unchained by this observed phenomenon of inducible antagonism.

4.5 Conclusion

An upregulation of L-histidine, purine and pyrimidine nitrogenous bases biosynthetic pathways is taking place in *B. subtilis* cells growing under TTC presence, altering the general nitrogen and other amino acids metabolism, suggesting a concentration of intermediates and end products from these routes in the cytoplasm and negatively affecting the expression of other associated pathways as are thiamine cofactor, pentose phosphate routes and affecting other important biological processes as siderophores production, DNA-repair and membrane fluidity and stability.

CHAPTER 5

5. Metabolomics

Abstract

Metabolomics is a powerful tool to systematically and simultaneously analyse the composition and features of the chemical space of a determined active extract. Therefore, in order to determine which compounds were differentially produced during the inducible antagonism assay with *B. subtilis* NCIB-3610, an active extract was subjected to metabolomic analysis. Extractions from plates where *B. subtilis* NCIB-3610 was growing under non-TTC presence and from fresh culture medium plates acted as negative controls for constructing the background metabolic composition of this strain. Data obtained from UPLC-MS detection of metabolites was subjected to bioinformatic treatment through GNPS platform, Cytoscape spectral network analysis and final curation and annotation of the metabolic networks using available literature and online chemical databases. Result indicates that 95 specific precursor ions are more abundant or unique for the active extract. The more abundant compounds, cluster in network analysis among a group of 82 nodes, while the uniquely produced ones are individual, most of them non-clustered nodes. Other nodes were found to correspond to identified natural products from *Bacillus* as are surfactins, fengycins and siderophores. All of them were equally produced by *Bacillus* cells, under inducible antagonism conditions with TTC presence and in negative controls, growing without TTC. Data mining in chemical databases, of unique and over-expressed compounds using their molecular mass values and analyzing potential hits, suggests that these unique or over produced molecules in TTC presence are potentially related to products of the nitrogen metabolism as aminoacids, ribonucleotides, dipeptides and polipeptides, or contain functional groups related to nitrogenous compounds or its biosynthetic pathways intermediates as are imidazoles, pyrrols, carboxamides. This result indicates a possible induction of nitrogen metabolism biosynthetic pathways which produce nitrogenated compounds. The induction may be caused by intracellular accumulation of TPF, the product of reduced TTC inside the cells.

5.1 Introduction

Amid the search for new drugs and active compounds coming from natural, including microbial, sources it is recognized that diversity within biologically relevant chemical space (the space occupied by all the chemical compounds produced under a determined

circumstance) is more important than other attributes (9), as could be the natural concentrations or the amount produced of certain substance. In the quest for characterizing and identifying the chemical output of a precise biological sample, the term ‘metabolic fingerprint’ was first coined to illustrate all the individual metabolites contained in it (36), but later on it was replaced by ‘metabolite profiling’ or ‘metabolomics’ which absolutely requires the identification of each class of metabolites and its levels (222), thus creating more complex data sets.

Almost the entire set of data for metabolomic analysis is obtained using chromatography and mass spectrometry (MS) as the main technologies available, although nuclear magnetic resonance (NMR) has also been widely employed for analyzing metabolite concentration and fluxes, beside MS (61). Both metabolite analyzers, although more powerful every passing day still have limitations in their capacity to resolve very structurally close metabolic species (61). In addition, for instance MS techniques are well-suited for high-throughput characterization of NPs, but there is a pressing need for an infrastructure to enable sharing and curation of data (70), to correctly characterize the large amount of information retrieved from the biological sample.

Thus, in order to be able to obtain the greatest amount of information from these large data sets, metabolomics analysis are most frequently performed through molecular networks, these being visual displays of the chemical space present in tandem mass spectrometry (MS/MS) experiments. This visualization approach can detect sets of spectra from related molecules, deriving in the term spectral networks, even when the spectra themselves are not matched to any known compounds available in public databases or online libraries (73). This becomes highly valuable given the fact that comprehensive software and proper computational infra-structure are not readily available nowadays and only low-throughput sharing of either raw or annotated spectra is feasible, leaving potentially useful information in MS/MS spectra behind and unexploited (70).

Available NP databases nowadays among non-free access and public ones, include Dictionary of Natural Products (223) and similar dereplication assistants which aid in the identification of known compounds, as well as other MS databases like MassBank (224) and MZcloud (225), which host MS/MS spectra but limit their availability for comparing against metabolomics data. A more complete and free-access, community sharing option, is presented by the platform Global Natural Products Social Molecular Networking (GNPS; <http://gnps.ucsd.edu>), which consists of data-driven platform for the storage, analysis, and knowledge dissemination of MS/MS spectra. The visualization of molecular networks in GNPS represents each MS/MS spectrum as a node, and spectrum-to-spectrum relatedness

as edges (connections) between nodes (70), allowing a visual comprehension by clusters of chemically related compounds and thus, aiding for a correct final interpretation of data.

The main objective of this chapter was to perform a metabolomic analysis of *B. subtilis* NCIB-3610 growing under TTC presence, in order to identify the compounds that were differentially produced in the inhibition zones and to characterize the chemical outcome of *B. subtilis* cells during the production of the inducible antagonism in TTC amended media.

5.2 Methodology

5.2.1 Microorganisms and culture media

B. subtilis NCIB-3610, belonging to BGSC collection (Table 3-1), was stored in 0.5X TSB plus 20% glycerol at -80 °C. It was streaked on LB agar and incubated for 24h at 37 °C before any experimental use. *R. solanacearum* AW1 (Table 3-2), employed for antagonism tests, was stored in BG medium plus 20% glycerol and activated in BG agar (118) at 30 °C for 48 - 72 h before any experimental use. Culture media employed for antagonism tests from *B. subtilis* NCIB-3610, active extracts and control extract against *R. solanacearum* AW1 was always BGT (+TTC) and BG (-TTC) (118).

5.2.2 Inducible compounds extraction

B. subtilis NCIB-3610 antagonism test were performed in BGTA following the agar plug method (described in section 3.2.4.1). Briefly it consists of a modified version of a previously described method (126), where an inoculum of *R. solanacearum* AW1 of 1×10^6 CFU/mL was plated onto BGTA plates for inducible activity production and onto BGA plates for negative controls. On top of the plated strains a 0.5 cm (diameter), plug containing the antagonistic strain grown in LB, was placed in the center or the outer part of the plate, placing a total of 3 discs per plate. After 48 h of incubation under environmental conditions or RT (22 ± 1 °C), the presence and size of inhibition zones were registered and cut with a sterile razor, completing up to 20 g of agar containing inducible zones. Four volumes (80 mL) of 100% methanol were added to the total amount of agar containing inhibition zones, followed by sonication at 20% amplitude in water bath for 20 min and a final extraction was performed under agitation at 150 rpm and dark conditions, for 4 h. Afterwards, centrifugation at 5000 rpm for 15 min was done to remove agar pieces and methanol was evaporated under vacuum on a rotary evaporator (Buchi, CH) at 45 °C. The residue was suspended on 2 mL of 50% methanol, centrifuged for 10 min at 14000 rpm and transferred into a sterile amber glass vial. Control extracts were obtained in the same fashion but extracting from *B. subtilis*

NCIB-3610 grown on BGA plates with no TTC presence and no *R. solanacearum* inoculation (non-induced control). Media control extract (negative control) was obtained extracting directly from 20 g of BGTA. Activity evaluation of each extract followed prior to metabolomic analysis.

5.2.3 Antagonism tests

All extracts were subjected to activity evaluation following agar well diffusion method, described in section 3.2.4.2 (226), with *R. solanacearum* AW1 inoculated both by plating and submerged method. Briefly, 100 μL of an inoculum of 1×10^6 CFU/mL of *R. solanacearum* AW1 was plated onto BGA and BGTA plates. Wells of 0.5 mm diameter were punched with a sterile pasteur pipette following the application of 100 μL of each extract; incubation was done for 48 h at RT (22 ± 1 °C) followed by measurement of inhibition zones of the pathogen. For the submerged method the same inoculum of *R. solanacearum* AW1 was added to sterilized BG or BGT agar before solidifying, at 40 ± 2 °C, mixed well for 30 s and poured into sterile plates. The same methodology was followed for other target bacteria employed in susceptibility test to potentially active compounds. Individual inoculums containing 1×10^6 CFU/mL of strains of *E. coli*, *Staphylococcus* sp., *S. enterica* and *Xanthomonas* sp. from (Table 3-3, chapter 3) were added by submerged fashion to sterile BG and BGT agar before solidifying. Wells of 0.5 mm diameter were punched with a sterile pasteur pipette following the application of 100 μL of each extract or a determined volume of a 1M compound stock solution in sterile distilled water, followed by incubation at 30°C for 24h, after which inhibition zones were measured.

5.2.4 Metabolomic data acquirement

Two replicates of each extract, the one containing inducible substances (active) and each control (non-induced *Bacillus* and control media or negative control), were subjected to UHPLC/MS analysis. Two additional negative control were included in the analysis, these being 50% methanol and a 50 mg/L of the inducer TTC dissolved in methanol. The equipment for acquiring metabolomic data consisted of an UHPLC system (Dionex UltiMate 3000, ThermoFisher, USA) coupled to a Thermo Scientific Q-Exactive Quadrupole-Orbitrap mass spectrometer with a Heated Electrospray Ionization (HESI) source. Sample was injected (0.5 mL) into a C18 column (50 mm x 2.1 mm, 2.2 μm particle size, Thermo Scientific AcclaimTM RSLC) at 0.4 mL/min flow rate and 30 °C. Separation was carried by a gradient of solvent A (water + 0.1% TFA) and solvent B (methanol + 0.1% TFA), starting at 10% B for 0-1.5 min, then increasing from 10%-100% from 1.5-11.5 min, then at 100% B from 11.5-14.5 min, lowering from 100%-10% from 14.5-15 and ending at 10% B from 15-18 min. Peak

detection was done at 214 nm on a universal diode detector, followed by injection into coupled MS equipment. MS runs were done in a positive ion mode, with a scan range of 150-2000 m/z. Full scan parameters were: resolution of 70,000 full width at half-maximum (FWHM), automatic gain control (AGC) target of 3×10^6 ions and a maximum ion injected time (IT) of 100 ms. The injection capillary temperature was 300 °C, sweep gas was N₂ and spray voltage was 3.5 kV. MS/MS parameters were: resolution of 17,500 FWHM, AGC target of 1×10^5 ions, maximum IT of 50 ms, quadrupole isolation window of 4.0 m/z, normalized collision energy (NCE) of 30%. Tandem MS was acquired using the data-dependent Top5 method considering precursor ion abundance. Data obtained from UHPLC and MS was visualized using Xcalibur™ software.

5.2.5 Bioinformatic data treatment

Data files were obtained from the UHPLC-MS unit on a .raw extension and were converted to .mzXML extension using MSconvert (ProteoWizard). Once this procedure was followed, files were uploaded to the Mass Spectrometry Interactive Virtual Environment (MassIVE) data repository for further analysis through Global Natural Products Social Molecular Networking (GNPS) web platform (70). Once the files were uploaded, a network analysis was done using the following parameters: data was filtered by removing all MS/MS peaks within +/- 17 Da of the precursor m/z. MS/MS spectra were window filtered by choosing only the top 6 peaks in the +/- 50Da window throughout the spectrum. The data was then clustered with MS-Cluster with a parent mass tolerance of 2.0 Da and a MS/MS fragment ion tolerance of 0.5 Da to create consensus spectra. Further, consensus spectra that contained less than 5 spectra were discarded. A network was then created where edges were filtered to have a cosine score above 0.75 and more than 6 matched peaks. Further edges between two nodes were kept in the network if and only if each of the nodes appeared in each other's respective top 10 most similar nodes. The spectra in the network were then searched against GNPS' spectral libraries. The library spectra were filtered in the same manner as the input data. All matches kept between network spectra and library spectra were required to have a score above 0.7 and at least 6 matched peaks. Analog search was enabled against the library with a maximum mass shift of 100.0 Da.

5.2.6 Spectral network curation and annotation

Complementary data analysis was performed using Cytoscape 3.5 (72). For this, complete datasets for the GNPS network analysis were downloaded and uploaded onto Cytoscape platform. Network was generated using precursor ion mass as the node value and m/z difference (deltaMZ parameter) and cosine as the edge values. Group discrimination was

enabled by assigning a color for each treatment or group, later clearing nodes from negative control groups. Self-loops, corresponding to non-clustering precursor ions were also displayed. Finally, the generated network was manually curated by filtering nodes which only included files from the two replicates for each treatment. Manual annotation followed, identifying BGC for *B. subtilis* NCIB-3610 by AntiSmash (supplementary material S-4) and then identifying clusters in the network which displayed precursor ions with the same MS value (m/z value) as the predicted compound (BGC). Once identified, their MS/MS were analyzed and a match with a literature reported compound was called when one of the precursor ions from the cluster shared the same molecular weight (m/z) ± 0.5 Da and six or more peaks of its MS/MS spectra with the literature reported compound (supplementary material Table S-4).

5.2.7 Data mining

A final step was carried for important sub-networks or specific nodes, denoting a unique presence or a higher abundance on the active extracts. The m/z value of these nodes was extracted manually or using Cytoscape exportation tools into a spreadsheet Microsoft Excel file. These unknown m/z values were used as a query on molecular weight search on Chemspider (227) and PubChem (228) databases using a source code (supplementary material Fig. S-14). Tolerance for calling a match was 0.01 Da of the original compound molecular weight. The first compound to appear in the list of hits in the database was selected as a potential chemical nature for that particular molecule.

5.3 Results

5.3.1 Activity is retained in the extract obtained from inducible inhibition zones

Antagonistic activity of all extracts was evaluated by well diffusion methodology, using *R. solanacearum* AW1 as the target strain. Activity was retained in crude extracts coming from inducible inhibition zones produced by *B. subtilis* NCIB-3610, but not from control extracts coming from *Bacillus* cells growing in non-TTC amended media or from control media alone (Table 5-1; supplementary material Fig. S-15).

The quantity of active extracts applied (100 μ L) produces inhibition zones of smaller size (5.0 ± 0.1) than the original inhibition zones produced by *B. subtilis* NCIB-3610 cells growing under TTC presence, which are of 7.7 ± 0.2 or 15.3 ± 0.7 , in antagonism trials with submerged and surface plated inoculation of *R. solanacearum* AW1, respectively. Although,

activity observed is sufficient to proceed with a metabolomic analysis and determine the compounds that were differentially produced in the inducible antagonism assay.

Table 5-1. Antagonistic activity against *R. solanacearum* AW1 from active and control extracts used in metabolomic analysis

TREATMENT	INHIBITION ZONE (mm)	
	Submerged trial	Surface plated trial
<i>B. subtilis</i> NCIB-3610	7.7±0.2	15.3 ±0.7
Extract from <i>B. subtilis</i> NCIB-3610 inhibition zones	5.0 ± 0.1	12.5 ± 2.5
Extract from non-induced <i>B. subtilis</i> NCIB-3610	0.0 ± 0.0	0.0 ± 0.0
Extract from BGTA medium	0.0 ± 0.0	0.0 ± 0.0

Intervals represent standard errors of the mean (n=3).

+I denotes 50 mg/L TTC amendment in the medium -I denotes TTC absence in the medium.

Submerged or surface plated trial mean the way *R. solanacearum* AW1 (target strain) was added to the antagonism trial

5.3.2 Spectral networking metabolomic analysis for *B. subtilis* NCIB-3610 in GNPS platform evidences a complex network with 54 library hits and compounds only present in the active extract

Results from GNPS spectral networking analysis of metabolomic data (<https://gnps.ucsd.edu/ProteoSAFe/status.jsp?task=3a62050b552d4281ab438b649c70bd3e>), summarize UPLC-MS information obtained from two time-independently obtained active extracts and controls. Given that molecular networks are visual displays of the chemical space present in MS experiments, the statistics of a specific analysis evidence the complexity, purity and other variables such as interrelatedness of compounds and chemical diversity, from the dataset obtained.

In this particular networking analysis, statistics (Table 5-2) evidence that a great number of nodes (2513) is obtained from all extracts, denoting a complex mixture when compared with other studies (75), specifically in the number of nodes. Besides, only 54 clusternodes were identified when comparing MS/MS spectra against NPs libraries, thus the importance of doing further network annotation using other tools, as BGC prediction using AntiSmash (supplementary material Table S3).

GNPS can be used for molecular networking (70, 229), which is a spectral correlation and visualization approach that detects and clusters sets of spectra from related molecules even when the spectra themselves are not matched to any known compounds. The results

obtained for this particular network evidence that only 1.274 spectra were identified against NPs libraries on GNPS, this being less than 3% of the total spectra in consideration (43.940). Thus, the molecular networking element of the analysis becomes highly important since grouping nodes by chemical structure similar (clustering) based on their MS/MS data, facilitates annotation of the network, by assumption that neighbor molecules (nodes) fragment in similar ways reflected in their MS/MS patterns, according to the cosine value employed in the analysis (0.75, methods 5.2.5). The number of unidentified neighbor spectra for this analysis was of 1.287, being accordingly annotated based on the neighbor node that presented the match in the NPs libraries. This molecular network analysis allowed the identification of known compounds inside the chemical space of this metabolomic analysis to raise to 19.6%, adding the 7.421 spectra belonging to identified components which denote spectral families of compounds, represented as well by clusters of nodes interconnected by edges, based on their MS/MS spectra similar and annotated as specific chemical families. These statistics apply to the original networking analysis, before manual annotation using AntiSmash and Cytoscape whole network visualization.

Table 5-2. GNPS Spectral networking analysis summary

PARAMETER	VALUE
Number of nodes	2.513
Number of pairs	1.693
Number of ID'd clusternodes	54
Number of ID'd clusternodes not in components	25
Number of connected components identified	16
Number of clusternodes in identified components	262
Number of spectra in consideration	43.940
Number of spectra in network	21.546
Number of ID'd spectra	1.274
Number of ID'd spectra not in components	118
Number of unidentified neighbor spectra	1.287
Number of spectra in identified components	7.421

Nodes: a specific precursor ion with a m/z value associated for which one or more spectra have been identified by MS

Clusternodes: group of nodes connected by edges based on a calculated value (cosine) according to their structural similarity (MS/MS spectra similarity)

Pairs: pairs of nodes

Components: spectral families of compounds (nodes and clusters interconnected), based on their MS/MS spectra similarity

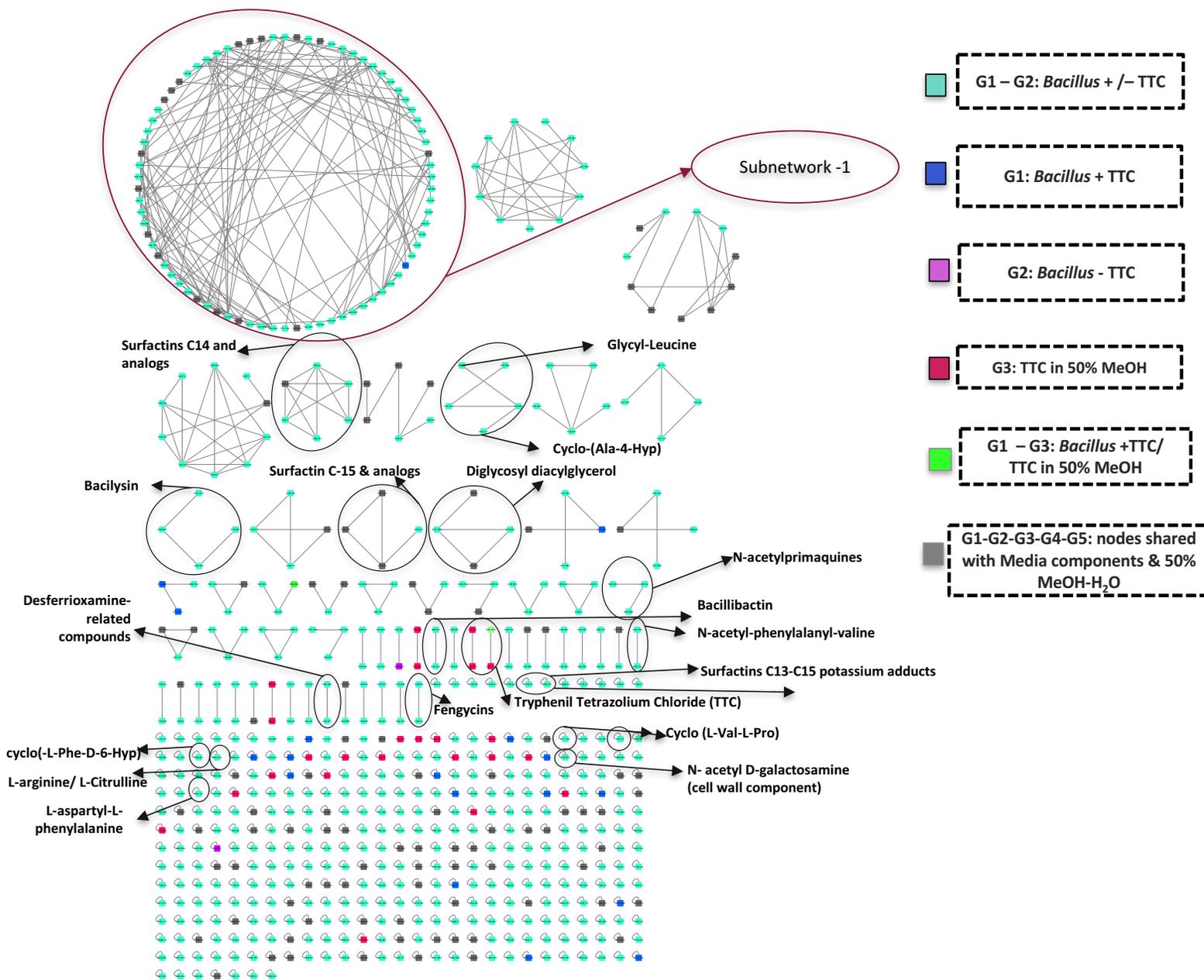
5.3.3 The active extract presents unique and more abundant compounds than The non-induced control extract

Following extraction, metabolomic data acquisition and GNPS spectral networking of crude extracts of inducible inhibition zones and controls, a final spectral network was obtained (Fig. 5-1). Manual curation and annotation followed, marking compounds identified both by GNPS NPs libraries and by AntiSmash prediction, with later manual curation (supplementary material Table S-4). The network only displays grey nodes (containing spectra found in control extracts, from BGTA medium or 50% methanol) that evidenced a highly abundant number of spectra in the active extract, outnumbering the maximum two spectra found in control extracts for that specific precursor ion.

When specifically regarding network clusters and components, formed by the nodes structural relatedness, is interesting to note that 29 multinode clusters (containing more than 3 nodes) are found in the network. Six of them are annotated, representing already characterized NPs and most of them composed by cyan nodes, which include spectra from both active and non-induced control extracts. Interestingly and coherently, these clusters represent compounds reported to be naturally produced by *Bacillus* cells, as surfactins and bacilysin. It can be suggested for these compounds, that they are not induced, neither repressed in TTC presence, but that still can play a role in the inducible antagonism, although are not the directly responsible for the inducible antagonism phenomenon observed. This result correlates with what has been observed and discussed in previous chapters (3 and 4), where either by biochemical or molecular experimentations, the same conclusion is reached. Traditional and largely characterized NPs produced by *Bacillus* can no be associated as the compounds responsible of the inducible inhibition zones produced by *Bacillus* sp. cells in TTC presence.

A total of 31 pair clusters (containing two nodes) are found in the network, among which a small cluster of two pairs (four nodes) is found, corresponding to the inducer compound TTC, including a node with the exact inducer compound molecular mass ($334.1 + [H]^+ = 335.125$). These nodes (red), detected in a 50 mg/L TTC solution in 50% methanol, are not related or clustered to unique nodes from the active extract (blue nodes) or nodes from compounds found overexpressed in the active but shared with non-induced control (cyan nodes). Besides this cluster, other chemical families are able to be recognized inside these pairs, as are other NPs already characterized in *Bacillus*: fengycins and siderophores bacilibactin and desferrioxamine-related compounds (supplementary material Table S-4).

Figure 5-1. Curated and annotated spectral network for *B. subtilis* NCIB-3610 crude extracts (active and controls)



Other identified compounds were among the non-clustered nodes, which have no identified structural similarity to other compounds in the chemical space and thus, are not clustered or grouped in components of spectral families. Among these are most of the unique nodes (blue), detected only in the active extract, none of them identified as known compounds,

thus representing challenging data to further analyse. Besides these results, other identified compounds are surfactin C-13 (1076) and surfactin C-15 (1081) potassium adducts, single aminoacids, dipeptides and cyclic dipeptides, as well as cell wall components like N-acetyl D-galactosamine and diglycosyl diacylglycerol.

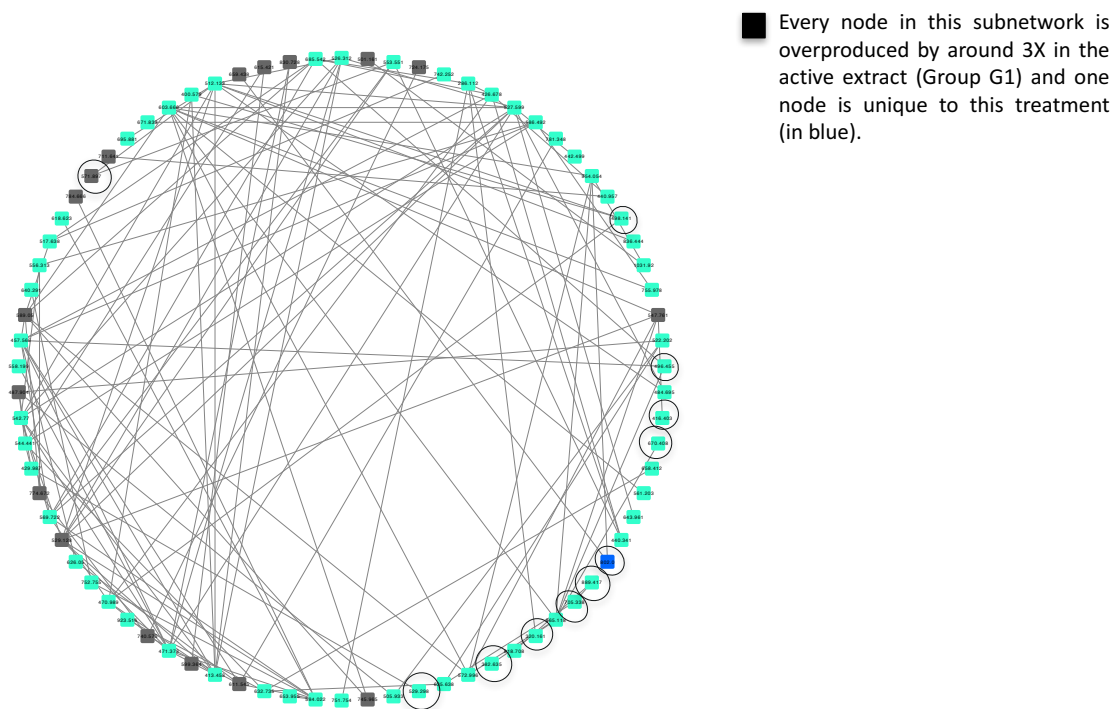
Among other interesting chemical families found in the network as multinode clusters are the N-acetylprimaquines cluster and the Glycyl-Leucine and Cyclo-(Ala-4-Hyp) cluster, which denotes compounds from the nitrogen metabolism being overexpressed in the active extract (information supported in the GNPS spectral networking analysis report: <https://gnps.ucsd.edu/ProteoSAFe/status.jsp?task=3a62050b552d4281ab438b649c70bd3e>), either in the dipeptides and cyclic depeptides families (two times more abundant in the active extract) or in the primaquines or 8-aminoquinolones synthetic derivatives (three times more abundant in the active extract). The finding of these compounds inside the metabolomic network for *B. subtilis* NCIB-3610 induced bioactivity is further discussed.

5.3.4 Spectral networking analysis presents a subnetwork with interrelated unidentified compounds significantly more abundant in the active extracts

Selected subnetwork-1 (Fig. 5-2), evidences an interesting behavior being the only large cluster that does not present homology to any predicted compounds. Besides, the particularity of this network is that all 82 nodes are structurally related, since molecular networking analysis connected them all in a component or spectral family. The nodes or compounds which form this subnetwork, even though shared between active and non-induced control extracts, are more abundant in the active extract, rising the value of this selected cluster.

Information for all nodes from this subnetwork has been withdrawn from GNPS spectral networking report and processed (Table 5-3, supplementary material Table S-5). For all the nodes, detailed information on the number of spectra for the active extract and for the non-induced control (supplementary material Table S-5) was taken as a basis for calculating an abundance ratio, later selecting only 11 nodes which were minimum 3-fold more abundant in the active extract than in the non-induced control extract (Table 5-3). Of special attention is compound presenting an m/z value of 802.000, since it is also the only unique node from the cluster (blue node in Fig. 5-2), meaning it was found exclusively in the active extract.

Figure 5-2. Subnetwork-1 of non-annotated and more abundant compounds in from spectral network analysis



The selected nodes (Table 5-3), which were unique for the active extracts or above three times more abundant in it, were all subjected to data mining in the two public chemical databases which have the more abundant selection of the chemical space (230) (Pubmed and Chempider) using the source code (supplementary material Fig. S-14). The nodes which returned hits in the databases presenting the same molecular weight (MW) values ± 0.01 Da were carefully analyzed and a potential match compound was selected (method 5.2.7), for which its structure, name and molecular formula was recorded (Table 5-4).

Besides the more abundant precursor ions, a total of 17 unique nodes (including the one from subtenwork-1) were found for the active extract (blue nodes), representing molecular entities present exclusively in the two replicates of active extracts (Table 5-3). These nodes were also subjected to data mining using the source code (supplementary material Fig. S-14) and exclusively the ones presenting matches in chemical databases for the molecular

weight (MW) values ± 0.01 Da were analyzed and their main functional groups or chemical classification identified (Table 5-4).

Table 5-3. Selected nodes for data mining from spectral networking analysis of *B. subtilis* NCIB-3610 extracts

PRECURSOR MASS (m/z value) or [M+H]⁺	NUMBER OF SPECTRA FOR ACTIVE EXTRACT*	NUMBER OF SPECTRA FOR NON-INDUCED EXTRACT*	OVEREXPRESSION RATIO (ABUNDANCE IN ACTIVE EXTRACT)
195.092	5	0	5.0
248.149	5	0	5.0
253.019	5	0	5.0
275.151	6	0	6.0
312.107	5	0	5.0
320.161	7	2	3.5
337.152	17	0	17.0
379.664	5	0	5.0
382.635	6	2	3.0
385.403	6	0	6.0
394.947	5	0	5.0
416.403	10	3	3.3
496.455	12	4	3.0
498.141	18	6	3.0
529.298	5	1	5.0
571.897	29	8	3.6
573.369	5	0	5.0
581.510	5	0	5.0
614.881	7	0	7.0
615.525	6	0	6.0
670.408	10	2	5.0
676.192	7	0	7.0
705.338	9	3	3.0
802.000	9	0	9.0
889.417	9	2	4.5
956.418	8	0	8.0
979.159	5	0	5.0
995.998	5	0	5.0

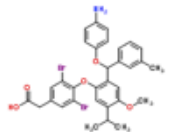
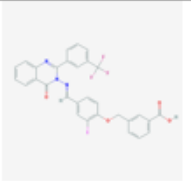
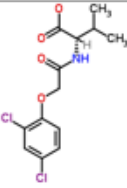
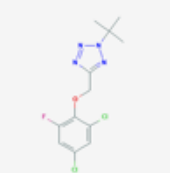
All selected nodes were detected in two time-independently obtained active extracts

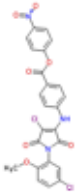
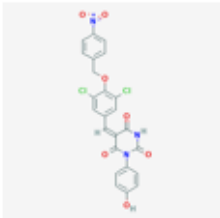
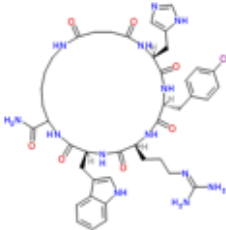
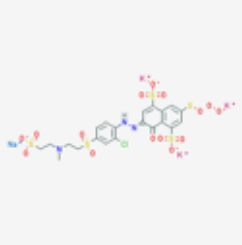
[M+H]⁺ means that molecular mass value of each compound is [M+H]⁺-1.

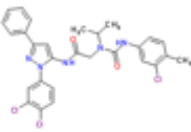
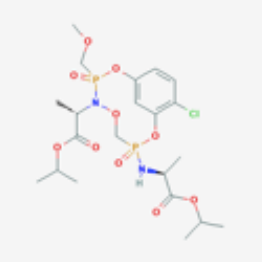
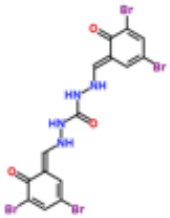
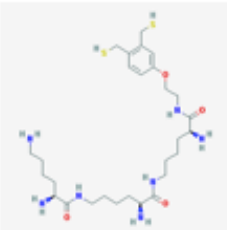
Number of spectra for each metabolite were obtained for each condition from GNPS network analysis

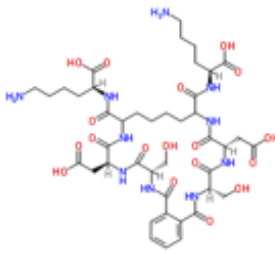
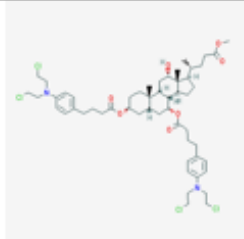
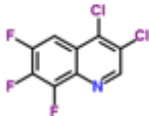
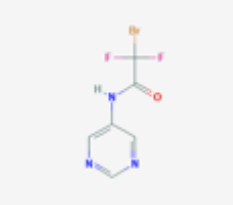
When looking specifically into the functional groups that data mining displays as a match for the selected nodes (Table 5-4), it is not possible to determine which compounds are of synthetic or natural origin. Thus, in order to narrow the possible functional groups associated to the inducible antimicrobial activity, only the ones associated to a natural origin were selected by further data mining, using the chemical name of the compound or its main functional groups found in Chemspider. The database Dictionary of Natural products (DNP) was employed for this purpose: (<http://dnp.chemnetbase.com/faces/chemical/ChemicalSearch.xhtml>).

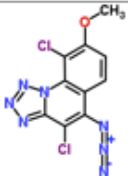
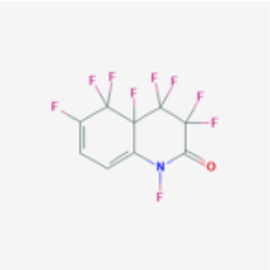
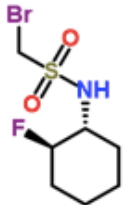
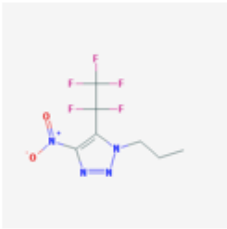
Table 5-4. Subnetwork-1 and unique precursor ions data mining in Chemspider and Pubchem

Node compound Molecular Mass	[M+H] ⁻¹	Hit compound molecular formula	Structure	IUPAC Name	Hit compound molecular Mass	Selected chemical family/functional groups
ChemSpider Hits						
670,408	669,408	C32H31Br2NO		(4-[2-((4-Aminophenoxy)[3-methylphenyl)methyl]-5-isopropyl-4-methoxyphenoxy]-3,5-dibromophenyl)acetic acid	669,400	Aminophenoxy - dibromophenyl
PubChem Hits						
		C30H19F3IN3O4		3-[[2-iodo-4-[[4-oxo-2-[3-(trifluoromethyl)phenyl]quinazolin-3-yl]iminomethyl]phenoxy)methyl]benzoic acid	669,399	Quinazoline - Iminomethyl
ChemSpider Hits						
320,161	319,161	C13H14Cl2NO		(2S)-2-[[[(2,4-Dichlorophenoxy)acetyl]amino]-3-methylbutanoate	319,161	Acetylamino - Methylbutanoate
PubChem Hits						
		C12H13Cl2FN4O		2-tert-butyl-5-[[2,4-dichloro-6-fluorophenoxy)methyl]tetrazole	319,161	Tetrazole

		ChemSpider Hits			
			4-Nitrophenyl 4-[[4-chloro-1-(5-chloro-2-methoxyphenyl)-2,5-dioxo-2,5-dihydro-1H-pyrrol-3-yl]amino]benzoate	528.298	Pyrrol - Amionbenzoate
529,298	528,298				
		PubChem Hits			
			(5E)-5-[[[3,5-dichloro-4-[(4-nitrophenyl)methoxy]phenyl]methylidene]-1-(4-hydroxyphenyl)-1,3-diazinane-2,4,6-trione	528.298 g/mol	Phenylmetilidene-Diazine - Trione
		ChemSpider Hits			
			(3S,6S,9R,12S)-9-(4-Chlorobenzyl)-6-{3-[[diaminomethylene]amino]propyl}-12-{1H-imidazol-5-ylmethyl}-3-(1H-indol-3-ylmethyl)-2,5,8,11,14,17-hexaoxo-1,4,7,10,13,18-hexaazacyclotricosane-23-carboxamide	888.414	Imidazol Carboxamide
889,417	888,417				
		PubChem Hits			
			tripotassium;sodium;3-[[[2-chloro-4-[2-[methyl(2-sulfonatoethyl)amino]ethylsulfonyl]phenyl]hydrazinylidene]-7-oxidoperoxysulfanyl-4-oxonaphthalene-1,5-disulfonate	888.416 g/mol	Hidrazinylidene

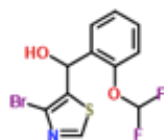
		ChemSpider Hits			
			<p>N2-((3-Chloro-4-methylphenyl)carbamoyl)-N-[1-(3,4-dichlorophenyl)-3-phenyl-1H-pyrazol-5-yl]-N2-isopropylglycinamide</p>	570.897	Glycinamide
571,897	570,897	PubChem Hits			
			<p>propan-2-yl (2S)-2-[[[10-chloro-3-(methoxymethyl)-3,7-dioxo-4-((2S)-1-oxo-1-propan-2-yloxypropan-2-yl]-2,5,8-trioxo-4-aza-3,5,7-triazolo[4,5-f]trideca-1(13),9,11-trien-7-yl]amino]propanoate</p>	570.897	Aminopropanoate
		ChemSpider Hits			
			<p>N'',N'''-Bis[(E)-(3,5-dibromo-6-oxo-2,4-cyclohexadien-1-ylidene)methyl]carbonohydrazide</p>	613.881	Carbonohydrazide
614,881	613,881	PubChem Hits			
			<p>(2S)-2,6-diamino-N-([(5S)-5-amino-6-([(5S)-5-amino-6-[2-[3,4-bis(sulfanylmethyl)phenoxy]ethylamino]-6-oxohexyl]amino)-6-oxohexyl]hexanamide</p>	613.881 g/mol	Hexanamide

		ChemSpider Hits			
			(2S,2'S)-2,2'-[[(3S,6S,17S,20S)-6,17-Bis(carboxymethyl)-3,20-bis(hydroxymethyl)-1,4,7,16,19,22-hexaoxo-1,2,3,4,5,6,7,8,9,10,11,12,13,14,15,16,17,18,19,20,21,22-docosahydro-2,5,8,15,18,21-benzohexaazacyclotetracosine-9,14-diy]]bis(carbonylimino)]bis(6-aminohexanoic acid)	994.998	Aminohexanoic acid
995,998	994,998				
		PubChem Hits			
			3alpha,7alpha-Bis[[4-[4-[bis(2-chloroethyl)amino]phenyl]butyryl]oxy]-12alpha-hydroxy-5beta-cholan-24-oic acid methyl ester	994.998	Aminophenyl
		C53H76Cl4N2O7			
		ChemSpider Hits			
			3,4-Dichloro-6,7,8-trifluoroquinoline	252.020	Fluoroquinolona
253,019	252,019				
		PubChem Hits			
			2-Bromo-2,2-difluoro-N-pyrimidin-5-ylacetamide	252.019 g/mo	Pyrimidinylacetamide
		C6H4BrF2N3O			

		ChemSpider Hits			
					
		C10H6Cl2N7O	5-Azido-4,9-dichloro-8-methoxytetrazolo[1,5-a]quinoline	311,106	Quinoline
		PubChem Hits			
312,107	311,107				
		C9H2F9NO	,3,3,4,4,4a,5,5,6-Nonafluoroquinolin-2-one	311.107	Fluoroquinoline
		ChemSpider Hits			
					
		C7H13BrFNO2S	1-Bromo-N-[(1R,2R)-2-fluorocyclohexyl]methanesulfonamide	271.151	Sulfonamide
275,151	274,151				
		C7H7F5N4O2	4-nitro-5-(1,1,2,2,2-pentafluoroethyl)-1-propyl-1H-1,2,4-triazole	274.151 g/mol	Triazole

ChemSpider Hits

C11H8BrF2NO2S



(4-Bromo-1,3-thiazol-2-yl)[4-(difluoromethoxy)phenyl]methanol

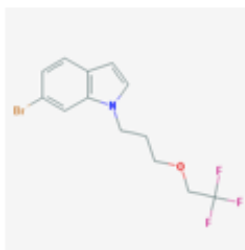
336,152

Thiazol

337,152

336,152

PubChem Hits

[C13H13BrF3NO](#)

6-Bromo-1-[3-(2,2,2-trifluoroethoxy)propyl]indole

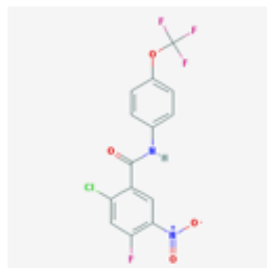
336.152 g/mol

Indole

PubChem Hits

379,664

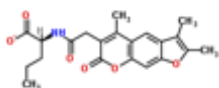
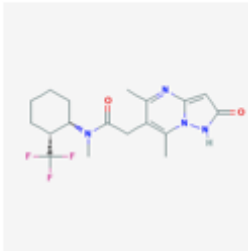
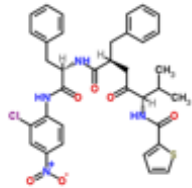
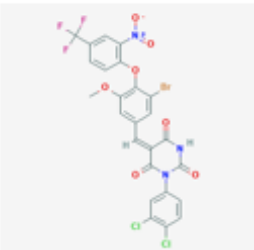
378,664

[C14H7ClF4N2O4](#)

2-chloro-4-fluoro-5-nitro-N-[4-(trifluoromethoxy)phenyl]benzamide

378.664

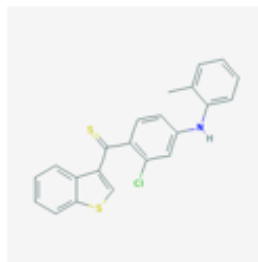
Benzamide

		ChemSpider Hits			
			(2S)-2-([(2,3,5-Trimethyl-7-oxo-7H-furo[3,2-g]chromen-6-yl)acetyl]amino)pentanoate	384.403	Aminopentanoate
385,403	384,403	PubChem Hits			
			2-[5,7-dimethyl-2-oxo-1H-pyrazolo[1,5-a]pyrimidin-6-yl]-N-methyl-N-[(1S,2R)-2-(trifluoromethyl)cyclohexyl]acetamide	384.403	Acetamide - Pyrimidine
		ChemSpider Hits			
			α -([(2R,5S)-2-Benzyl-6-methyl-4-oxo-5-[[2-(2-chloro-4-nitrophenyl)amino]heptanoyl]-N-phenylalaninamide	675.193	L-phenylalaninamide
676,192	675,192	PubChem Hits			
			(5E)-5-[[3-bromo-5-methoxy-4-[2-nitro-4-(trifluoromethyl)phenoxy]phenyl]methylidene]-1-(3,4-dichlorophenyl)-1,3-diazinane-2,4,6-trione	675.192	Trione

394,947

393,947

PubChem Hits

[C22H16ClNS2](#)

1-benzothiophen-3-yl-[2-chloro-4-(2-methylanilino)phenyl]methanethione

393.947

Methanethione

ChemSpider Hits

CSH8BrNS



4-Bromobutyl thiocyanate

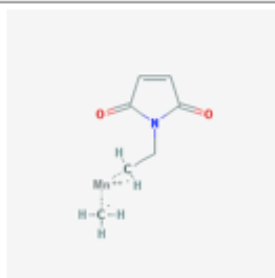
194.093

Thiocyanate

195,092

194,092

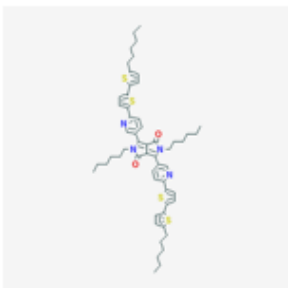
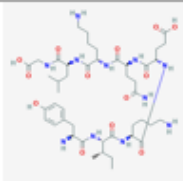
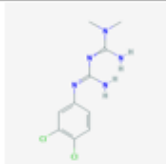
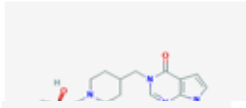
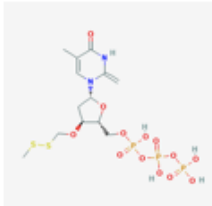
PubChem Hits

[C7H9MnNO2](#)

carbanide;1-ethylpyrrole-2,5-dione;manganese(2+)

194.092

Carmamide

956,418	955,418	PubChem Hits			
	C56H66N4O2S4		2,5-dihexyl-1,4-bis[6-[5-(5-hexylthiophen-2-yl)thiophen-2-yl]pyridin-3-yl]pyrrolo[3,4-c]pyrrole-3,6-dione	955.41 g/mol	Pyrrol
979,159	978,159	PubChem Hits			
	C45H75N11O13		L-tyrosyl-L-isoleucyl-L-lysyl-L-alpha-glutamyl-L-glutamyl-L-lysyl-L-leucyl-glycine	978.159	Octapeptide
248,149	247,149	PubChem Hits			
	C10H13Cl2N5		2-[N'-(3,4-dichlorophenyl)carbamidoyl]-1,1-dimethylguanidine	274.149	Dimethylguanidine
581,510	580,510	PubChem Hits			
			7-(3,4-dichlorophenyl)-3-[[1-[(3R,4R)-4-hydroxy-3-phenylpiperidine-4-		
573,369	572,369	PubChem Hits			
	C13H23N2O13P3S2		[hydroxy-[[[(2R,3S,5R)-3-[(methylidisulfanyl)methoxy]-5-(5-methyl-2-methylidene-4-oxopyrimidin-1-yl)oxolan-2-yl]methoxy]phosphoryl]phosphono hydrogen phosphate	572,369	Oxopyrimidine

5.3.5 The inducible antagonistic compounds potentially include selected functional groups associated to intermediates or products of the nitrogen metabolism

A list of semisynthetic and naturally produced compounds has been established based on a combined analysis of the functional groups obtained from data mining in Pubchem and Chempider, with a further refinement of their natural origin in DNP (Table 5-5). Several other compounds found as potentially involved in the inducible antagonism were included, as L-histidine, AICAR and orotic acid, which are intermediates of nitrogen metabolism pathways found upregulated in *Bacillus* cells during the production of this phenomenon of inducible antagonistic activity. The rest of compounds included in the list, were found to be part of common on these two conditions: found through metabolomic analysis as well as being products, derivatives or intermediates of the biosynthetic pathways of aminoacids, purines, pyrimidines.

These list of potential compounds (Table 5-5) includes a broad chemical classification and the CAS number of the substances, in order to conform a natural and semisynthetic battery of products which can be tested for their antibiotic *in vitro* potential against *R. solanacearum* and other target pathogens of the inducible antagonism.

5.3.6 Selected potential compounds from Table 5-5 present activity only against pathogens sensitive to the inducible antagonistic compounds

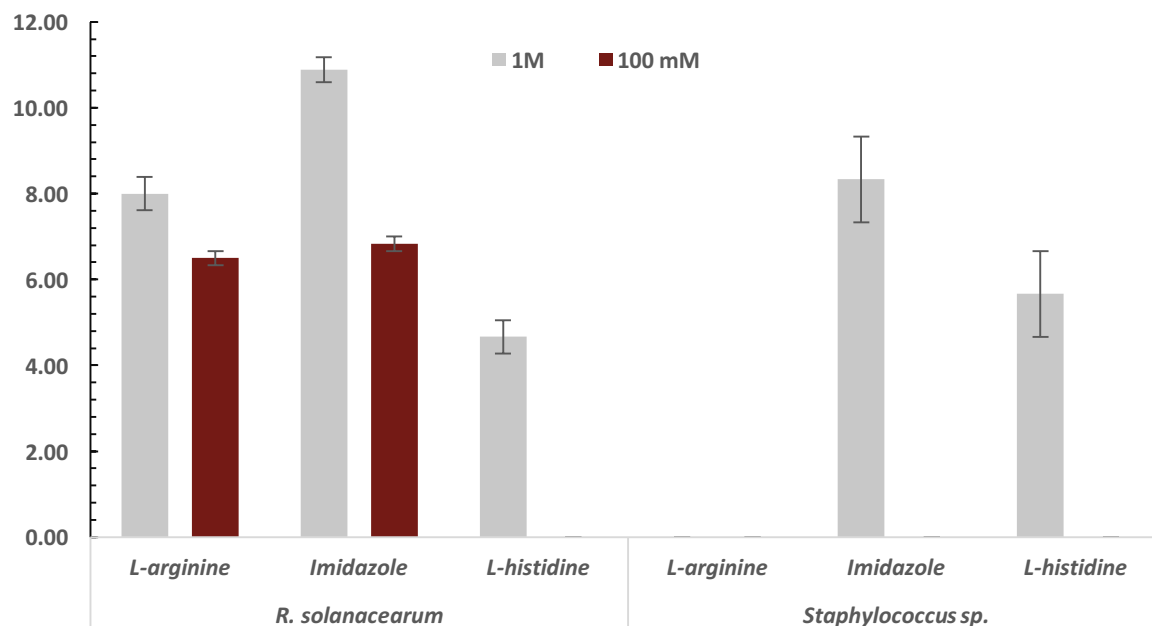
Selected metabolites from Table 5-5, specifically Imidazole, L-Arginine and L-Histidine were tested in concentrations of 100 μ m, 100 mM and 1 M against the pathogens *R. solanacearum*, *Staphylococcus* sp., *E. coli*, *Xanthomonas* sp. and *S. enterica*.

Results are illustrated in Fig. 5-3, where it can be observed that inhibition zones of *R. solanacearum* growth were produced by the three compounds: Imidazole, L-Arginine and L-Histidine at concentrations of 1 M and only by Imidazole and L-Arginine at concentrations of 100 mM. *Staphylococcus* sp. cells were sensitive as well to two of the tested compounds, Imidazole and L-Histidine, only at concentrations of 1 M (Fig. 3-5). This results contrast with the lack of activity of these compounds against the pathogens *X. campestris*, *S. enterica* and *E. coli*, connecting this results with the sensitivity of tested pathogens to the inducible antimicrobial compounds produced by *Bacillus* sp. The inducible compounds were active only against *R. solanacearum*, *Staphylococcus* sp. and *E. coli*.

Table 5-5. List of metabolites to which the inducible antagonistic compounds are chemically related

NAMES	CHEMICAL CLASSIFICATION	CAS N°
2-amino 5-guanidinovaleric acid L-arginine	Aminoacid	74-79-3
Aicar 5'-phosphoribosyl-5-aminoimidazole-4-carboxamide	Adenosine analog	2627-69-2
Quinazoline	Aromatic heterocycle	253-82-7
Pyrrol Azole 1-H pyrrol	Aromatic heterocycle	109-97-7
L-Histidine (S)-2-Amino-3-(4-imidazolyl) propionic acid	Aminoacid	71-00-1
L-aspartyl-L-phenylalanine Glycyl-Leucine Gly-Leu GLcyl-L-Leucine	Dipeptide	13433-09-5 869-19-2
L-aspartyl-L-phenylalanine	Dipeptide	13433-09-5
cyclo(L-Phe-trans-4-hydroxy-L-Pro)	Piperazinedione/ Diketopiperazines	118477-06-8
Orotic acid	Heterocyclic compound	50887-69-9
Imidazole	Aromatic heterocycle	288-32-4
Glycinamide	Amide derivative	598-41-4
L-Phenylalaninamide	Amide derivative	5241-58-7
2-Aminobenzoate	Rare aminoacid	118-92-3
Indol 2,3-Benzopyrrole	Aromatic heterocycle	120-72-9
Pyrimidine 1,3-Diazine	Aromatic heterocycle	289-95-2
1,1-Dimethylguanidine	Amidines and ureas	6145-42-2
Uracil 2,4(1H,3H)-pyrimidinedione	Pyrimidine derivative	66-22-8

Figure 5-3. Metabolites obtained as candidate compounds from metabolomic data mining evidence antibiotic activity against *R. solanacearum* and *Staphylococcus* sp.



5.1 Discussion

Comparative metabolomic analysis of *B. subtilis* NCIB-3610 active and control extracts, obtained from inducible and non-inducible conditions, rendered a substantially large collection of compounds. It has been properly clustered and visualized, through molecular networking analysis as well curated and annotated so that only consistent nodes (compounds), obtained in two time-independent replicates of the extracts were included and identified in the network (Fig 5-1).

An interesting finding, which not only provides evidence of the validity of the method employed, to detect and identify NPs from *Bacillus* in complex mixtures, is the presence of already identified metabolites from *B. subtilis* as are surfactins, fengycins, bacilysin, and bacillibactin in the network. Equally interesting is the finding of them in equal proportions, in terms of numbers of scans found for each precursor ion associated to the spectral families of these compounds, in active and control extracts. This result strongly correlates with previous conclusions, reported in other chapters of this research, on which is stated that traditional NPs from *B. subtilis*, largely studied and identified, may not be the direct responsables of the inducible antagonism. Experimentation from different techniques as are the inducible antagonism produced by knockout mutants in central routes for the

production of the mentioned compounds and differential gene expression, as well as metabolomic analysis of the chemical space of this strain, connect in this particular results. Although

The study by Watrous *et al* (229), features a metabolomic analysis for the same model strain *B. subtilis* NCIB-3610, although obtained from cells growing in nutrient agar (NA). Data is collected using nanoDESI as the MS technique and the study contains findings which correlate with the present study. For instance, the detection of surfactins C-14 and C-15 among the main compounds of the library, as well as diglycosyl diglycerides, like diglycosyl diacylglycerol. The finding of these compounds in two independent studies, although deciphering the chemical space of *B. subtilis* NCIB-3610 under very distinct growth and development circumstances, as well as using two different MS techniques, denotes a validity of the metabolomics and molecular networking approach for rendering an accurate view of the parvome or set of secreted natural products produced by *B. subtilis* cells.

Data visualization using molecular networks allows one to discover molecules that are still unclassified but may be biologically relevant especially when comparing samples from two states (229). This is the particular case for subnetwork-1 (Fig 5-2) in this study, which allows the identification inside the network (Fig. 5-1) of overproduced compounds in the active extract which were not identified in NPs libraries. These spectral correlation permitted the reduction of relevant molecules involved in the inducible antagonism, and their selection for further data mining. Although the network statistics (Table 5-2) denote a complex set of compounds and given that robust and intelligible molecular networks can be cataloged by the number of nodes and edges (231), it was possible in the present experimentation to identify outstanding compounds due to a high cosine score value (0.75) employed which admitted the clustering of similar products. As other studies have demonstrated, cosine value parameter is an important statistic, which should be above 0.7 in order to provide a good network quality and should be maximized (75, 231). On the same line, self-loop nodes, representing isolated MS2 spectra, should be minimized. The finding of 371 self-loop nodes in the present network denotes the complexity of the extract and the need to further purify through collection of fractions from purification columns, in order to provide a better resolution for the chemical space of this phenomenon.

Despite the importance of the study and the applied potential for biotechnology and medicine of the diverse chemistries present in natural products (NP), a large portion of it remains untapped because NPs databases are not searchable with raw data and the NPs community has no way to share data other than in published papers (70). Although mass spectrometry (MS) techniques are well-suited to high-throughput characterization of NP,

there is a pressing need for an infrastructure to enable sharing and curation of data. Thus, the strategy followed in this research to assess the chemical nature of selected substances in subnetwork-1 (Fig. 5-2, Table 5-3) and in unique nodes for the active extract (blue nodes, Fig. 5-1, Table 5-3) was to search within the available public chemical databases, using intrinsic properties of the compounds, as their exact molecular weight and main functional groups. The main findings from this data mining exercise are potential metabolites or naturally produced compounds to which each selected precursor ion can be related (supplementary material Table S-6, Table 5-4), although a match can not be called until comparing their MS/MS spectra. But this information is hardly available using only intrinsic properties of the molecules and as said before, is not still an raw spectral data in libraries not linked to the spectral networking platform.

The chemical space of the inducible antagonism phenomenon contains single aminoacids, dipeptides and cyclic depeptides found in small clusters and as self-loop nodes as are (Fig. 5-1): L-aspartyl-L-Phenylalanine, N-acetyl-phenylalanyl-valine, cyclo(L-Phe-trans-4-hydroxy-L-Pro), L-arginine, Cyclo-L-Val-Pro, Glycyl-Leucine and Cyclo-(Ala-4-Hyp). The presence of this compounds in the network, most of them slightly more abundant in the active extract, denotes the presence of compounds which are final product or derivatives of the aminoacids metabolism. This result implies the upregulation of the nitrogen metabolism in TTC exposed cells. This result couples as well with the data mining results (Table 5-4) for the more abundant and unique compounds for the active extract present in the network.

Although synthetic, nubiotics or non-natural oligoucletides with nuclease-resistant backbones (232) have gained an important place among potential novel drug candidates, since they are nucleoside analogs that can be recognized as physiological molecules and be incorporated into DNA and RNA, consequently inhibiting cellular division and viral replication (233). In this sense, some nucleoside analogs are actually used as therapeutic agents in inhibition of cancer cell growth, inhibition of viral replication or immunosuppression. There is a high upregulation of the nitrogen metabolism in *Bacillus* cells during the production of this phenomenon of inducible antimicrobial activity in the presence of TTC, observed through transcriptomics (chapter 4). There is as well, a more abundant production of aminoacids and related products observable in the chemical space, through metabolomics. Besides, TTC is a synthetic nitrogenous compound which once reduced to TPF inside the cells is accumulated (146). Parallel to this observations, the artificial synthesis of non-natural nucleosides derivatives has been done, in a more environmentally friendly alternative to chemical synthesis, through enzymatic synthesis using nucleoside phosphorylases, as well as nucleoside 2'-deoxyribosyltransferases (NDTs)

(233). These are multimeric enzymes, which can be employed in the enzymatic synthesis of nucleosides by mediating the transfer of glycosyl residues to acceptor bases (234). The main microbial source of NDTs for nucleoside enzymatic synthesis are different species of *Lactobacillus*, as well as extremophiles among which other species of Firmicutes are reported to be good producers of NDTs, as the psychrophilic *Bacillus psychrosaccharolyticus* (233, 235). These findings suggest that *Bacillus* sp. strains used in this study could be a NDT source and be transforming their nucleotides into semi-synthetic derivatives using these enzymes, in the presence of a toxic and excess of nitrogen environment as is intracellular accumulation of TPF.

In this same line are the compounds identified in a small cluster in the network as the N-acetylprimaquines cluster. These compound has been proved to be produce by microorganisms *via* a biotransformation of a sythetic antibiotic and antimalarial drug primaquine. The specific case is for a strain of *Streptomyces rimosus* which was recognized, during metabolic studies with microorganisms, as the author of converted primaquine to the previously reported N-acetyl derivative (236). In another study, an N-acetylated metabolite and a methylene-linked dimeric product, both of which had been previously reported, were produced by *Streptomyces roseochromogenus* (ATCC 13400) processing a dose of primaquine. Besides a novel sulfur-containing microbial metabolite was identified as well as a product of the metabolizing of this synthetic compound (237). A similar situation could be occurring with TPF: a biotransformation of this open tetrazoles ring into nitrogenous derivatives with antimicrobial activity.

Antismash analysis evidences 31 total compounds produced, of which only 6 are detected by MS, thus representing an expression of aproximately 20% of biosynthetic potential under these culture conditions (supplementary material Table S-3). These correalties with the largely reported activation of only a reduced number of BGC in bacteria under normal culture conditions (170).

The above reported findings allow to suggest that a possible induction of nitrogen metabolism biosynthetic pathways which produce nitrogenated compounds and derivatives is taking place during this inducible antagonism phenomenon. The induction may be caused by intracellular accumulation of TPF, the product of reduced TTC inside the cells and the secreted metabolites, inhibit the growth of certain sensitive bacteria.

5.2 Conclusion

Compounds found to be uniquely produced or more abundant in the active extracts obtained from *B. subtilis* NCIB-3610 growing under TTC containing media potentially belong to chemical families from the nitrogen metabolism as amino acids, modified amino acids, dipeptides, cyclic dipeptides or derivatives of purines and pyrimidines with functional groups as imidazoles, carboxamides, amidines and indols, according to metabolomic analysis, with certain of them as Imidazole, L-Arginine and L-Histidine being active against the main sensitive pathogen, *R. solanacearum*. These results suggest that the identified compounds could be implied in the observed inducible antimicrobial activity against *R. solanacearum* and other target strains.

6. Concluding remarks and suggestions

The findings of this research present a model for the induced production of antibiotic substances from Aerobic Endospore Forming Bacterial cells in the presence of the synthetic chemical compound TTC. The model has been validated in a broad number of species from the order Bacillales and a TTC dose-dependant production of the inducible compounds was identified, besides detecting that the inducible antibiotic substances did not belong to the traditional classes of natural products already described in *Bacillus* sp. as are lipopeptides, poliketides, siderophores and certain bacteriocins. The phenomenon was studied at the molecular and chemical composition levels, finding that nitrogen metabolism is significantly altered due to TTC reduction into TPF by AEFB cells or by the metabolizing of TPF accumulated intracellularly. From this stage of biochemical characterization, a further experimental step could shed some light on the amount of TPF being accumulated and metabolized inside AEFB cells:

- The observation of active *Bacillus* sp. cells growing in the presence of TTC by electron microscopy (SEM), would allow time measurements of the dimension of formazan crystals being formed inside the cells. Thus, this would allow a measurement of their kinetics during all stages of a fermentation.

From the molecular analysis through transcriptomic techniques, and the construction of a differential gene expression profile for *Bacillus* sp. growing in both conditions, with and without the inducer, three highly upregulated metabolic pathways were found. These were L-Hisidine, purines and pyrimidines biosynthetic, salvage and interconversion processes, indicating an accumulation of intermediates of these pathways, which was further investigated through metabolomics. Although, following the actions suggested below, would further validate the gene-expression profiles under this induced bioactivity conditions:

- By selecting specific biosynthetic genes of the nitrogen metabolism implied biosynthetic pathways, as for instance the ones responsible for producing the intermediates AICAR (*purH*) and Imidazole-glycerol-3-P (*hisH* and *hisF*), a qPCR analysis could be performed in the presence and absence of TTC in *B. cereus* EACB-1047 and *B. pumilus* EACB-0009 native strains. This assay would highly validate the findings since these two strains present a high induced bioactivity.

Following transcriptomic and gene-expression analysis, spectral networking analysis using UHPLC-MS obtained data from active and control extracts, of this induced antagonistic activity in *Bacillus* sp. cells, evidenced that a group of interrelated metabolites were uniquely present or more abundant in the active extract than in controls. These metabolites, unidentified by the natural products libraries from GNPS platform, were further explored through data mining using their molecular mass. Analysis of the first hits and validation in the Dictionary of Natural Products indicates that these metabolites are either nitrogen metabolism intermediates, derivatives as are aminoacids, dipeptides, nitrogenous bases, or have within their structure, functional groups from these metabolic pathways as are imidazoles, carboxamides, amidines, indoles. Some of these compounds were tested against the main sensitive pathogens to the inducible antibiotics from *Bacillus* sp., finding that Imidazole, L-Arginine and L-Hisidine were active.

Despite the interesting findings, further work here would greatly clarify the chemical nature of these inducible antibiotic substances. Some experimental activities that should be pursued are described below:

- The extraction protocol of the inducible antimicrobial substances from inhibition zones should be optimized in order to be able to further purify the extract by HPLC, avoiding to the maximum the loss of bioactivity.
- When optimized, the active extract must be submitted to a bio-assay guided fractioning. This could increase the resolution of the metabolomic analysis and can be reached by changing the extraction solvent for a mixture of polar and non-polar ones, as for instance acetonitrile:water:trifluoroacetic acid (79.95:20:0.05), which is largely employed for proteins, aminoacid and nitrogenous compounds.
- A softer concentration technique for liable compounds, as lyophilisation, should be implemented as well for the obtention of stonger active extracts, and compare results against vacuum drying.
- Performing a metabolomic analysis of active extracts obtained from *B. cereus* EA-CB1047 native strains and comparing results against the ones obtained for *B. subtilis* NCIB-3610, would allow for further refinement of common and important clusters of metabolites.

Finally, besides a clear elucidation of the chemical nature of the inducible antibiotic substances, there is an important step towards the future application of these induced antimicrobial metabolites in real agricultural or clinical solutions. This is about the optimization of the production of the inducible antimicrobial compounds in liquid fermentations of AEFB.

7. Supplementary material

- **Table S-1.** Initial Screening of AEFB strains collection

STRAINS	MOLECULAR ID BY 16S rDNA	<i>Serratia marcescens</i>		<i>Ralstonia solanacearum</i>		
		BGTA (+TTC) INHIBITION ZONE (mm)		BGTA (+TTC) INHIBITION ZONE (mm)		BGA (-TTC) INHIBITION ZONE (mm)
EA-CB1451		+		15,9 ± 0,4		10,9 ± 0,9
EA-CB1452		+		12,9 ± 1,7		11,3 ± 0,8
EA-CB1468		+		11,6 ± 2,2		11,0 ± 0,5
EA-CB1469		+		9,9 ± 0,5		12,0 ± 2,0
EA-CB1478		+		13,0 ± 0,1		10,3 ± 0,8
EA-CB1479		+		12,0 ± 1,8		11,3 ± 0,3
EA-CB1483		+		10,2 ± 0,8		10,9 ± 0,1
EA-CB0486		7,5 ± 0,3		12,2 ± 0,9		10,8 ± 0,8
EA-CB0846		6,7 ± 0,4		9,6 ± 0,3		11,5 ± 0,9
EA-CB0018		6,5 ± 0,3		12,2 ± 1,0		9,6 ± 0,7
EA-CB1023		6,5 ± 0,3		11,3 ± 0,9		10,1 ± 0,7
EA-CB0843		6,2 ± 0,3		10,8 ± 0,7		10,1 ± 0,6
EA-CB1149		5,8 ± 0,6		11,8 ± 1,1		11,0 ± 0,7
EA-CB0847		5,5 ± 0,3		11,4 ± 0,5		10,6 ± 0,7
EA-CB0959		5,5 ± 0,3		11,7 ± 0,7		10,6 ± 0,8
EA-CB1329		5,5 ± 1,2		13,3 ± 0,1		10,8 ± 0,5
EA-CB1018		5,3 ± 0,2		6,9 ± 0,9		5,5 ± 1,8
EA-CB0489		5,0 ± 0,3		11,2 ± 0,7		10,4 ± 0,5
EA-CB0960		5,0 ± 0,3		13,9 ± 1,5		11,1 ± 0,7

EA-CB1268		4,8 ± 0,2	11,9 ± 0,1	10,8 ± 0,8
EA-CB0123		4,8 ± 0,2	10,7 ± 0,8	13,3 ± 1,8
EA-CB0155		4,6 ± 0,0	12,4 ± 0,8	8,5 ± 0,0
EA-CB0622		4,5 ± 0,1	12,2 ± 0,2	10,0 ± 1,5
EA-CB0162		4,5 ± 0,2	11,9 ± 0,5	8,5 ± 0,0
EA-CB0158		4,2 ± 0,2	11,6 ± 0,9	9,0 ± 0,0
EA-CB0585		4,0 ± 0,1	12,8 ± 0,5	11,5 ± 2,0
EA-CB0652		4,0 ± 0,1	11,9 ± 0,6	8,8 ± 1,8
EA-CB0224		3,9 ± 0,1	13,1 ± 0,4	9,0 ± 1,5
EA-CB0087		3,9 ± 0,1	10,4 ± 1,0	11,0 ± 1,5
EA-CB0695		3,9 ± 0,1	12,4 ± 0,5	10,3 ± 1,3
EA-CB0176		3,8 ± 0,2	11,9 ± 0,5	9,1 ± 1,6
EA-CB0166		3,8 ± 0,1	12,7 ± 0,4	9,1 ± 0,1
EA-CB0303		3,6 ± 0,1	12,2 ± 0,9	9,0 ± 0,0
EA-CB0650		3,6 ± 0,1	11,8 ± 0,4	7,5 ± 0,0
EA-CB0318		3,6 ± 0,2	12,3 ± 1,0	9,5 ± 0,0
EA-CB0644		3,6 ± 0,0	11,2 ± 0,6	9,1 ± 1,4
EA-CB0651		3,5 ± 0,1	13,7 ± 0,6	10,5 ± 0,0
EA-CB0559		3,4 ± 0,1	12,2 ± 0,8	10,0 ± 0,0
EA-CB0595		3,1 ± 0,1	12,7 ± 0,2	10,5 ± 1,0
EA-CB1432		3,1 ± 0,2	12,5 ± 0,3	10,4 ± 1,4
EA-CB1439		2,9 ± 0,2	11,8 ± 0,4	9,8 ± 1,3
EA-CB1446		2,9 ± 0,1	11,6 ± 0,4	9,1 ± 1,9
EA-CB1419		2,8 ± 0,2	ND	ND
EA-CB1406		2,6 ± 0,1	11,0 ± 1,0	9,0 ± 2,0
EA-CB1433		2,5 ± 0,0	11,9 ± 1,2	10,1 ± 1,1
EA-CB1420		2,5 ± 0,1	11,7 ± 0,8	8,8 ± 1,8
EA-CB1434		2,2 ± 0,2	12,1 ± 0,5	9,5 ± 1,5
EA-CB0575	<i>B. subtilis</i>	0,0 ± 0,0	10,5 ± 0,1	0,0 ± 0,0
EA-CB0015	<i>B. subtilis</i>	0,0 ± 0,0	5,6 ± 0,4	0,0 ± 0,0

EA-CB0083		0,0 ± 0,0		ND		0,0 ± 0,0		
EA-CB0086		0,0 ± 0,0	12,6 ± 1,6			ND		
EA-CB0131		0,0 ± 0,0		ND		0,0 ± 0,0		
EA-CB0586	<i>B. subtilis</i>	0,0 ± 0,0	8,2 ± 2,2			0,0 ± 0,0		
EA-CB0743		0,0 ± 0,0		ND		0,0 ± 0,0		
EA-CB0792		0,0 ± 0,0		ND		0,0 ± 0,0		
EA-CB0799		0,0 ± 0,0		ND		0,0 ± 0,0		
EA-CB0827		0,0 ± 0,0		ND		0,0 ± 0,0		
EA-CB0840		0,0 ± 0,0		ND		0,0 ± 0,0		
EA-CB0844		0,0 ± 0,0		ND		0,0 ± 0,0		
EA-CB0845		0,0 ± 0,0		ND		0,0 ± 0,0		
EA-CB0849		0,0 ± 0,0		ND		0,0 ± 0,0		
EA-CB0862		0,0 ± 0,0		ND		0,0 ± 0,0		
EA-CB0863		0,0 ± 0,0		ND		0,0 ± 0,0		
EA-CB0874		0,0 ± 0,0		ND		0,0 ± 0,0		
EA-CB0882		0,0 ± 0,0		ND		0,0 ± 0,0		
EA-CB0883		0,0 ± 0,0		ND		0,0 ± 0,0		
EA-CB0888		0,0 ± 0,0		ND		0,0 ± 0,0		
EA-CB0898		0,0 ± 0,0		ND		0,0 ± 0,0		
EA-CB0904		0,0 ± 0,0		ND		0,0 ± 0,0		
EA-CB0912		0,0 ± 0,0		ND		ND		
EA-CB0913		0,0 ± 0,0		ND		0,0 ± 0,0		
EA-CB0921		0,0 ± 0,0		ND		0,0 ± 0,0		
EA-CB0933		0,0 ± 0,0		ND		0,0 ± 0,0		
EA-CB0934	'operational group <i>B. amyloliquefaciens</i> '	0,0 ± 0,0	11,0 ± 0,5			11,3 ± 1,1		
EA-CB0937		0,0 ± 0,0		ND		0,0 ± 0,0		
EA-CB0946		0,0 ± 0,0		ND		0,0 ± 0,0		
EA-CB0975		0,0 ± 0,0		ND		0,0 ± 0,0		
EA-CB0993		0,0 ± 0,0		ND		0,0 ± 0,0		

EA-CB1005		0,0 ± 0,0		ND		ND		
EA-CB1008		0,0 ± 0,0		ND		0,0 ± 0,0		
EA-CB1009		0,0 ± 0,0		ND		0,0 ± 0,0		
EA-CB1047	<i>B. cereus</i>	0,0 ± 0,0	11,6 ± 0,9			0,0 ± 0,0		
EA-CB1057		0,0 ± 0,0		ND		9,8 ± 1,3		
EA-CB1066		0,0 ± 0,0		ND		0,0 ± 0,0		
EA-CB1121		0,0 ± 0,0		ND		0,0 ± 0,0		
EA-CB1131		0,0 ± 0,0		ND		0,0 ± 0,0		
EA-CB1146		0,0 ± 0,0		ND		0,0 ± 0,0		
EA-CB1165		0,0 ± 0,0		ND		11,0 ± 0,0		
EA-CB1216		0,0 ± 0,0		ND		0,0 ± 0,0		
EA-CB1217		0,0 ± 0,0		ND		0,0 ± 0,0		
EA-CB1230		0,0 ± 0,0		ND		0,0 ± 0,0		
EA-CB1241		0,0 ± 0,0		ND		0,0 ± 0,0		
EA-CB1273		0,0 ± 0,0		ND		10,0 ± 1,0		
EA-CB1280		0,0 ± 0,0		ND		9,5 ± 0,5		
EA-CB1287		0,0 ± 0,0		ND		0,0 ± 0,0		
EA-CB1315		0,0 ± 0,0		ND		0,0 ± 0,0		
EA-CB1384	<i>B. pumilus</i>	0,0 ± 0,0	11,2 ± 1,4			11,6 ± 2,4		
EA-CB1418	'operational group <i>B. amyloliquefaciens</i> '	0,0 ± 0,0	11,4 ± 0,8			9,8 ± 2,3		
EA-CB1421	'operational group <i>B. amyloliquefaciens</i> '	0,0 ± 0,0	10,8 ± 0,1			9,8 ± 1,7		
EA-CB1423		0,0 ± 0,0		ND		ND		
EA-CB1425	'operational group <i>B. amyloliquefaciens</i> '	0,0 ± 0,0	13,7 ± 0,9			8,5 ± 0,0		
EA-CB1436		0,0 ± 0,0		ND		ND		
EA-CB1440	'operational group <i>B. amyloliquefaciens</i> '	0,0 ± 0,0	12,8 ± 0,5			9,5 ± 1,5		
EA-CB1449	'operational group <i>B. amyloliquefaciens</i> '	0,0 ± 0,0	13,9 ± 0,2			7,5 ± 0,0		

EA-CB1450		0,0 ± 0,0		ND		0,0 ± 0,0
EA-CB1461		0,0 ± 0,0	>25			ND
EA-CB1463		0,0 ± 0,0	20,2 ±			ND
EA-CB1465		0,0 ± 0,0	>25			0,0 ± 0,0
EA-CB1466		0,0 ± 0,0	16,5 ±	0,3		ND
EA-CB1467		0,0 ± 0,0	14,7 ±	0,2		ND
EA-CB1470		0,0 ± 0,0	0,0 ±	0,0		ND
EA-CB1471		0,0 ± 0,0	18,0 ±	1,0		ND
EA-CB1472		0,0 ± 0,0	>25			ND
EA-CB1473		0,0 ± 0,0	>25			0,0 ± 0,0
EA-CB1475		0,0 ± 0,0	>25			ND
EA-CB1476		0,0 ± 0,0	18,9 ±	2,1		ND
EA-CB1480		0,0 ± 0,0	13,1 ±	0,1		ND
EA-CB1481		0,0 ± 0,0	15,3 ±	0,9		ND
EA-CB1482		0,0 ± 0,0	14,5 ±	1,0		ND
EA-CB1484		0,0 ± 0,0	>25			ND
EA-CB1485		0,0 ± 0,0	18,9 ±	2,3		ND
EA-CB1486	<i>B. subtilis</i>	0,0 ± 0,0	12,6 ±	1,0		0,0 ± 0,0
EA-CB1487		0,0 ± 0,0	11,4 ±	0,0		ND
EA-CB1490		0,0 ± 0,0	18,2 ±	0,0		ND
EA-CB1491		0,0 ± 0,0	15,0 ±	0,2		ND
<i>B. subtilis</i> UA321		0,0 ± 0,0	12,0 ±	1,0		0,0 ± 0,0
<i>B. subtilis</i> QST713		2,1 ± 0,1	12,2 ±	0,3		11,0 ± 1,2
Evaluated Strains		1496	74			104
Antagonists		47	73			58
% of antagonists		3,1	98,6			55,8
Inhibition Zone average(mm)		4,2 ± 0,2 a	12,4 ± 0,3			10,0 ± 0,2 b

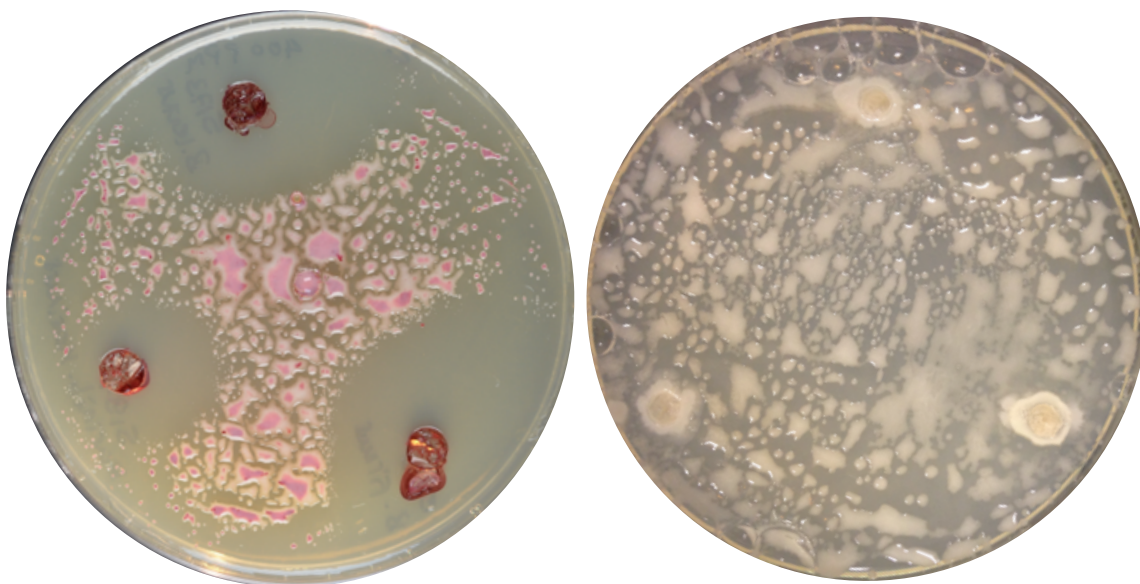
Key

47 strains tested against *S. marcescens* and *R. solanacearum*

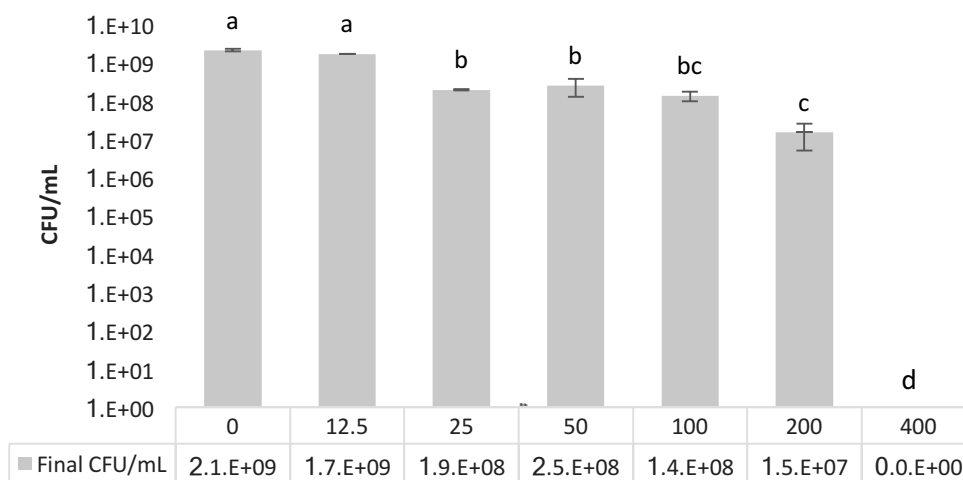
8 strains antagonists only in TTC presence

7 strains antagonists both in the presence and absence of TTC

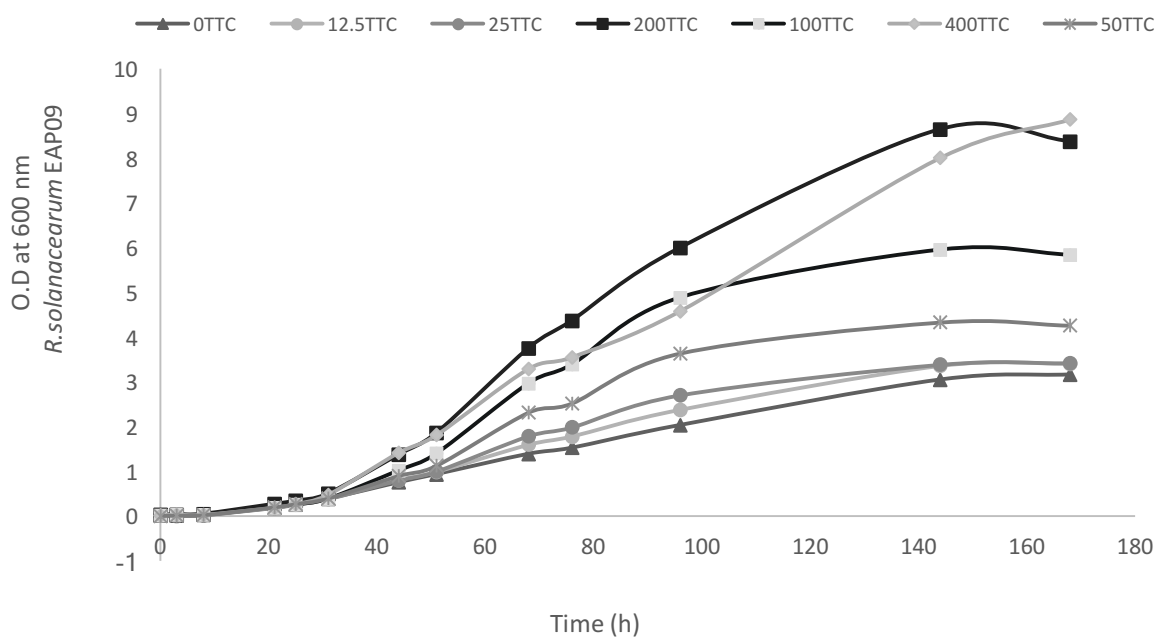
- **Figure S-1:** Inhibition zones of *R. solanacearum* AW1 produced *B. cereus* EA-CB1047 in the presence of inducer compound (50 ppm) and non- induced control, in the absence of TTC.



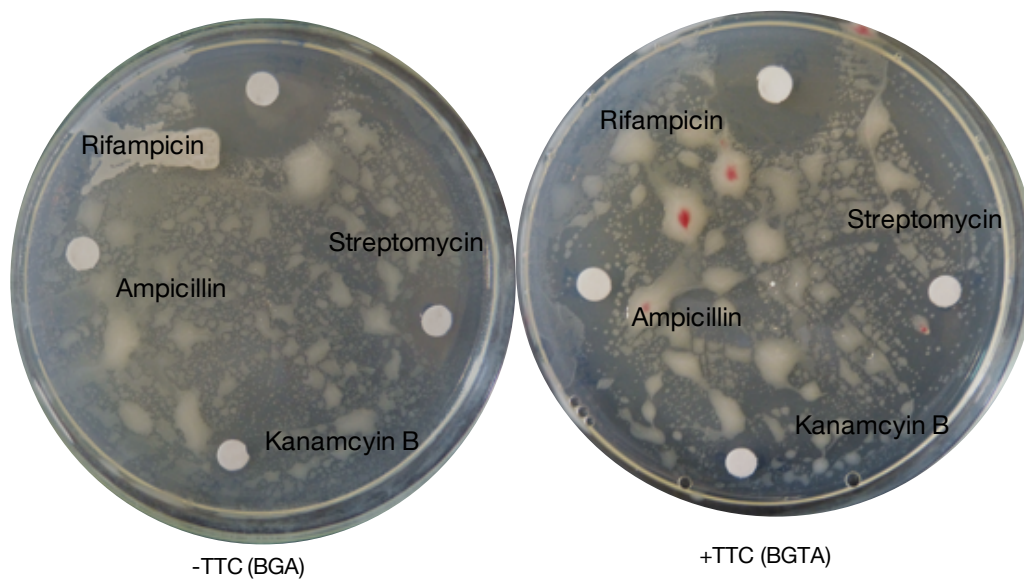
- **Figure S-2:** *B. cereus* EA-CB1047 viability after 68 h of fermentation in the presence of different TTC concentrations



• **Figure S-3:** *R. solanacearum* EAP09 growth curves in the presence of TTC



• **Figure S-4:** antibiotics sensitivity of *R. solanacearum* EAP09 in TTC presence and absence



- **Figure S-5:** inhibition zone produced by *B. cereus* EA-CB1047 and *B. pumilus* EA-CB0009 against *R. solanacearum* EAP09 with TTC only added locally

B. cereus EA-CB1047 inhibition zones with TTC locally added (in well)

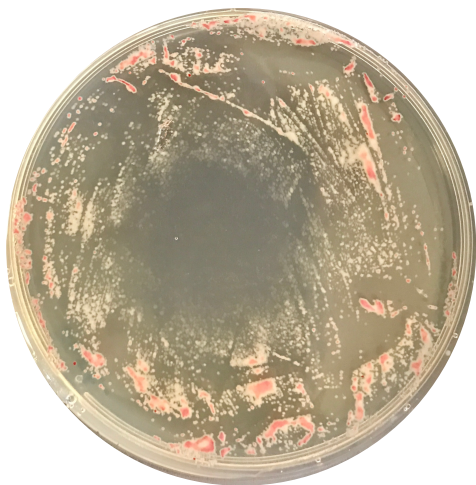


B. subtilis EA-CB0009 inhibition zones with TTC locally added (in well)

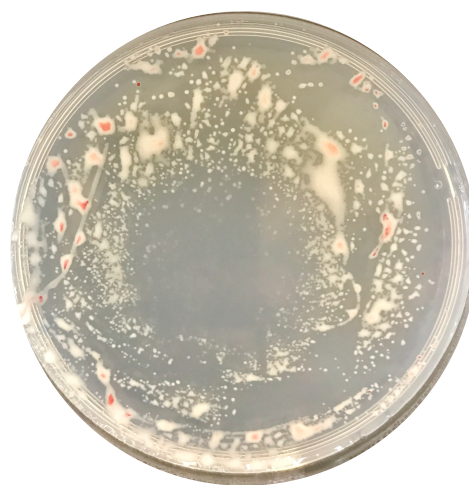


- **Figure S-6:** Inhibition zones produced by *B. cereus* 1047 growing over membranes for 48h, before plating *R. solanacearum* AW1

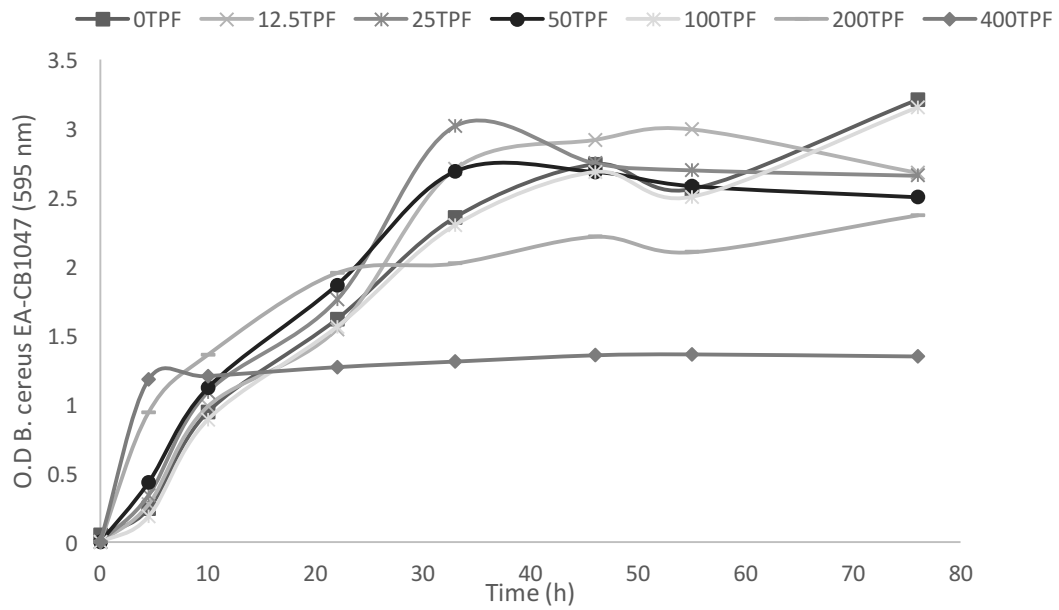
B. cereus EA-CB1047 diffused inducible compounds (after 48h of incubation over a nylon-polyamide membrane)



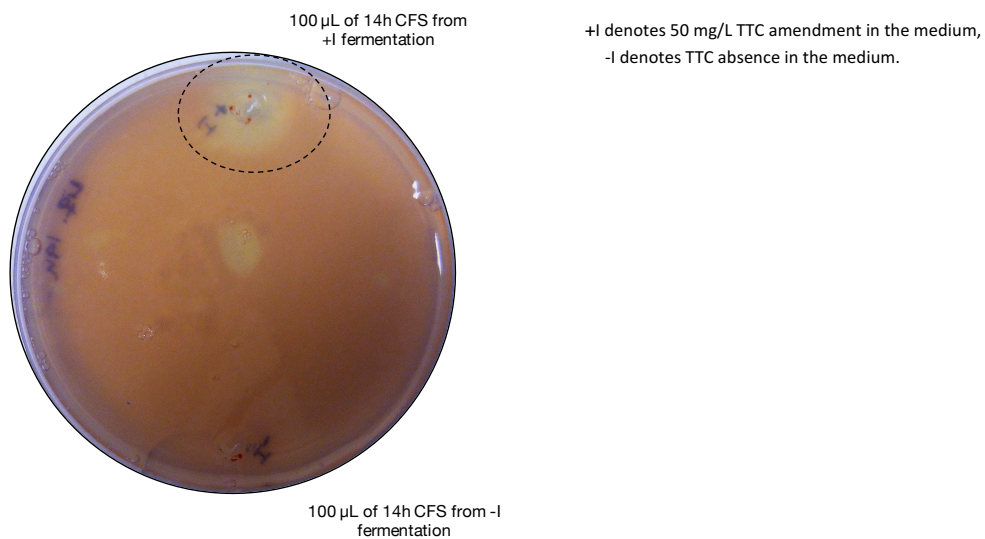
B. cereus EA-CB1047 diffused inducible compounds (after 48h of incubation over a nylon-polyamide membrane) + reconstitution of BG medium nutrients



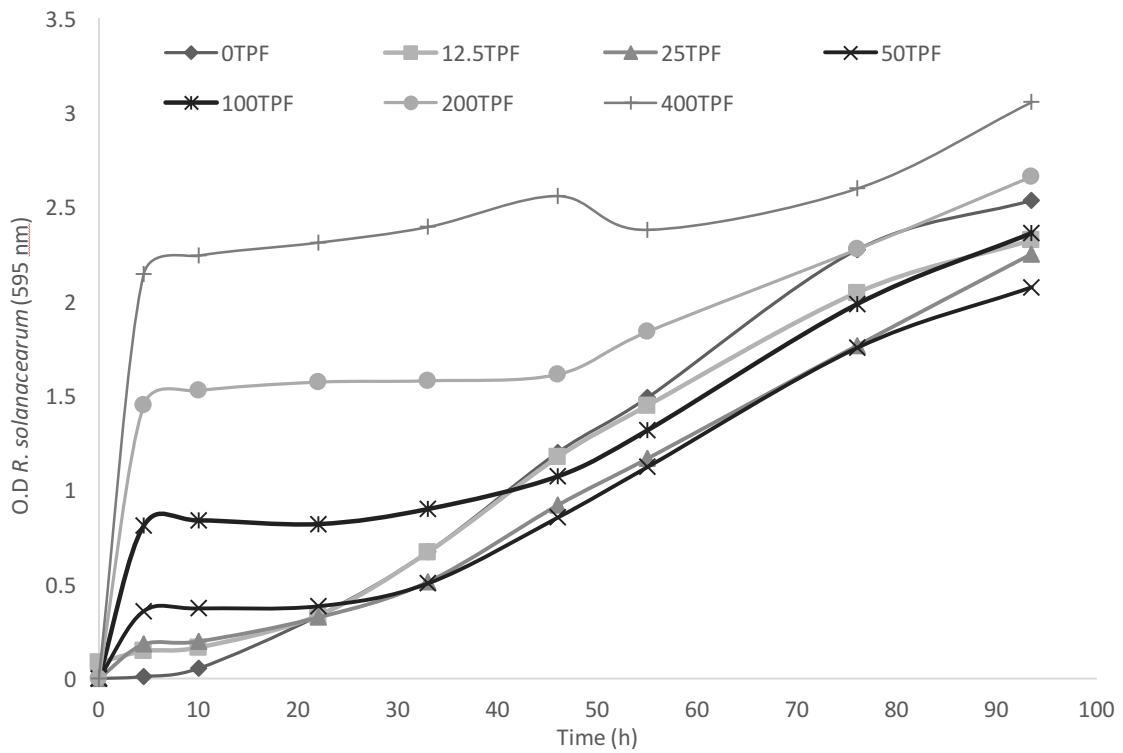
- **Figure S-7: Biomass behavior of *B. cereus* in the presence of TPF**



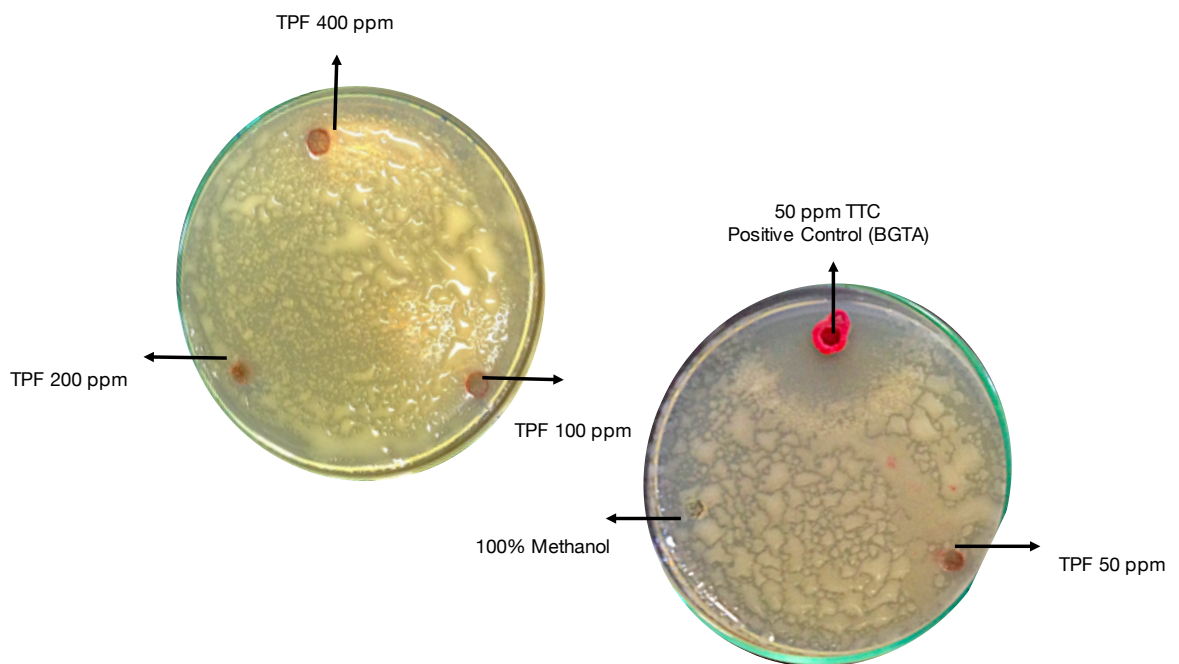
- **Figure S-8: Inhibition zones from *B. cereus* EA-CB1047 CFS at 14 h of monoculture fermentation in TTC presence**



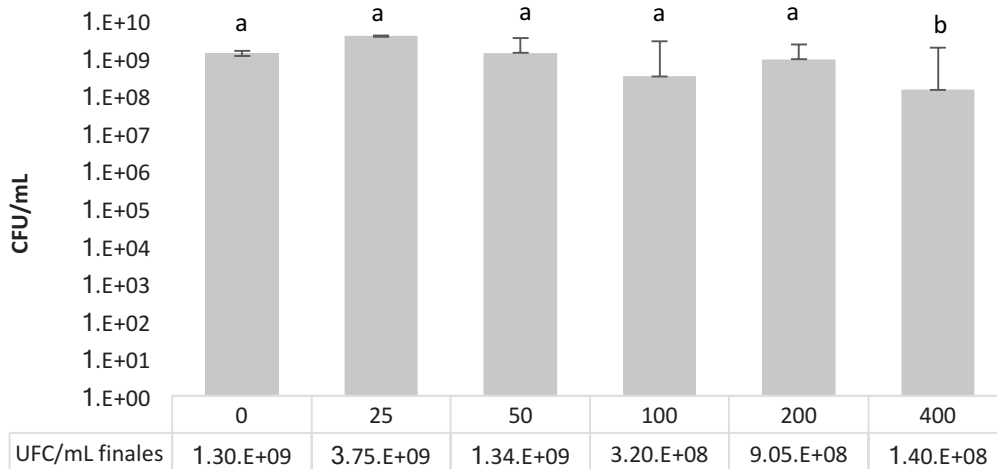
• **Figure S-9:** *R. solanacearum* EAP09 growth curves in TPF presence



• **Figure S-10:** Extracellular TPF does not produce inhibition zones against *R. solanacearum*



- **Figure S-11:** *B. cereus* EACB-1047 viability after 68h of fermentation in the presence of different TPF concentrations



- **Figure S-12:** statistical analysis for Chapter 3 figures and tables

Table 3-4

```

multcompLetters(P11,
compare="<",
threshold=0.05,
Letters=letters,
reversed = FALSE)
B. cereus EA-CB 1047 "abc"
B. coagulans ZK5189 "abcdef"
B. simplex ZK5093 "cdef"
B. lentus ZK5173 "cdef"
P. Pasadenensis EA-CB0840 "f"

```

```

B. pumilus EA-CB 0009 "a"
B. altitudinis EA-CB1450 "abcd"
B. subtilis EA-CB0015 "cdef"
B. firmus ZK5172 "cdef"
B. licheniformis ATCC14580 "abcdef"
B. amyloliquefaciens EA-CB0959 "b"
B. subtilis NCIB 3610 "cdef"
B. megaterium EA-CB0185 "e"
Aeribacillus palidus ZK5191 "abcdef"
B. thuringiensis ZK5165 "abcdef"
B. subtilis SMY "cdef"
Marinibacillus marinus ZK5187 "def"

```

Table 3-5

Fit: aov(formula = TTC..1 ~ OTRASPP, data = datos)

\$OTRASPP	diff	lwr	upr	p adj
Control Positivo B. cereus 1047-Burkholderia sp.	11.55	3.033256	20.0667441	0.0066953
Delftia tsuruhatensis G1-Burkholderia sp.	0.25	-8.266744	8.7667441	0.9999983
Herbaspirillum seropedicae G6-Burkholderia sp.	-9.30	-19.134289	0.5342890	0.0677641
Pseudomona putida 95-Burkholderia sp.	2.10	-6.416744	10.6167441	0.9563401
Serratia marcescens G2-Burkholderia sp.	2.55	-7.284289	12.3842890	0.9465796
Delftia tsuruhatensis G1-Control Positivo B. cereus 1047	-11.30	-18.253892	-4.3461076	0.0015621
Herbaspirillum seropedicae G6-Control Positivo B. cereus 1047	-20.85	-29.366744	-12.3332559	0.0000327
Pseudomona putida 95-Control Positivo B. cereus 1047	-9.45	-16.403892	-2.4961076	0.0065920
Serratia marcescens G2-Control Positivo B. cereus 1047	-9.00	-17.516744	-0.4832559	0.0362934
Herbaspirillum seropedicae G6-Delftia tsuruhatensis G1	-9.55	-18.066744	-1.0332559	0.0251600
Pseudomona putida 95-Delftia tsuruhatensis G1	1.85	-5.103892	8.8038924	0.9408906
Serratia marcescens G2-Delftia tsuruhatensis G1	2.30	-6.216744	10.8167441	0.9373268
Pseudomona putida 95-Herbaspirillum seropedicae G6	11.40	2.883256	19.9167441	0.0073851
Serratia marcescens G2-Herbaspirillum seropedicae G6	11.85	2.015711	21.6842890	0.0156533
Serratia marcescens G2-Pseudomona putida 95	0.45	-8.066744	8.9667441	0.9999681

Figure 3-2

B. cereus EA-CB1047

Tukey multiple comparisons of means
95% family-wise confidence level

Fit: aov(formula = HALO ~ TZC, data = datos)

\$TZC	diff	lwr	upr	p adj
cien-cero	28.666667	24.842367	32.4909663	0.0000000
cincuenta-cero	25.333333	21.509034	29.1576330	0.0000000
Cuatrocientos-cero	7.666667	3.842367	11.4909663	0.0002346
Doscientos-cero	9.666667	5.842367	13.4909663	0.0000236
veinticinco-cero	21.333333	17.509034	25.1576330	0.0000000
cincuenta-cien	-3.333333	-7.157633	0.4909663	0.1018216
Cuatrocientos-cien	-21.000000	-24.824300	-17.1757004	0.0000000
Doscientos-cien	-19.000000	-22.824300	-15.1757004	0.0000000
veinticinco-cien	-7.333333	-11.157633	-3.5090337	0.0003562
Cuatrocientos-cincuenta	-17.666667	-21.490966	-13.8423670	0.0000000
Doscientos-cincuenta	-15.666667	-19.490966	-11.8423670	0.0000001
veinticinco-cincuenta	-4.000000	-7.824300	-0.1757004	0.0385813
Doscientos-Cuatrocientos	2.000000	-1.824300	5.8242996	0.5241982
veinticinco-Cuatrocientos	13.666667	9.842367	17.4909663	0.0000006
veinticinco-Doscientos	11.666667	7.842367	15.4909663	0.0000032

B. pumilus EA-CB0009

```
> lukeymSD(x=modelo2, ordered = FALSE, conf.level = 0.95)
```

```
Tukey multiple comparisons of means
 95% family-wise confidence level
```

```
Fit: aov(formula = HALO ~ TZC, data = datos)
```

```
$TZC
```

	diff	lwr	upr	p adj
cien-cero	23.3750000	20.0419178	26.70808223	0.0000000
cincuenta-cero	22.6666667	19.0665264	26.26680695	0.0000000
Cuatrocientos-cero	19.6250000	16.2919178	22.95808223	0.0000000
Doscientos-cero	23.6250000	20.2919178	26.95808223	0.0000000
Veinticinco-cero	20.1250000	16.7919178	23.45808223	0.0000000
cincuenta-cien	-0.7083333	-4.3084736	2.89180695	0.9871214
Cuatrocientos-cien	-3.7500000	-7.0830822	-0.41691777	0.0226579
Doscientos-cien	0.2500000	-3.0830822	3.58308223	0.9998689
Veinticinco-cien	-3.2500000	-6.5830822	0.08308223	0.0583045
Cuatrocientos-cincuenta	-3.0416667	-6.6418069	0.55847361	0.1259572
Doscientos-cincuenta	0.9583333	-2.6418069	4.55847361	0.9529838
Veinticinco-cincuenta	-2.5416667	-6.1418069	1.05847361	0.2631989
Doscientos-Cuatrocientos	4.0000000	0.6669178	7.33308223	0.0139370
Veinticinco-Cuatrocientos	0.5000000	-2.8330822	3.83308223	0.9962834
Veinticinco-Doscientos	-3.5000000	-6.8330822	-0.16691777	0.0365532

B. subtilis EA-CB0015

```
Tukey multiple comparisons of means
 95% family-wise confidence level
```

```
Fit: aov(formula = HALO ~ TZC, data = datos)
```

```
$TZC
```

	diff	lwr	upr	p adj
cien-cero	9.500	7.4721715	11.5278285	0.0000000
cincuenta-cero	10.500	8.4721715	12.5278285	0.0000000
Cuatrocientos-cero	11.750	9.7221715	13.7778285	0.0000000
Veinticinco-cero	8.625	6.5971715	10.6528285	0.0000000
cincuenta-cien	1.000	-1.0278285	3.0278285	0.5643620
Cuatrocientos-cien	2.250	0.2221715	4.2778285	0.0263776
Veinticinco-cien	-0.875	-2.9028285	1.1528285	0.6764788
Cuatrocientos-cincuenta	1.250	-0.7778285	3.2778285	0.3568874
Veinticinco-cincuenta	-1.875	-3.9028285	0.1528285	0.0766666
Veinticinco-Cuatrocientos	-3.125	-5.1528285	-1.0971715	0.0020127

B. amyloliquefaciens EA-CB0959

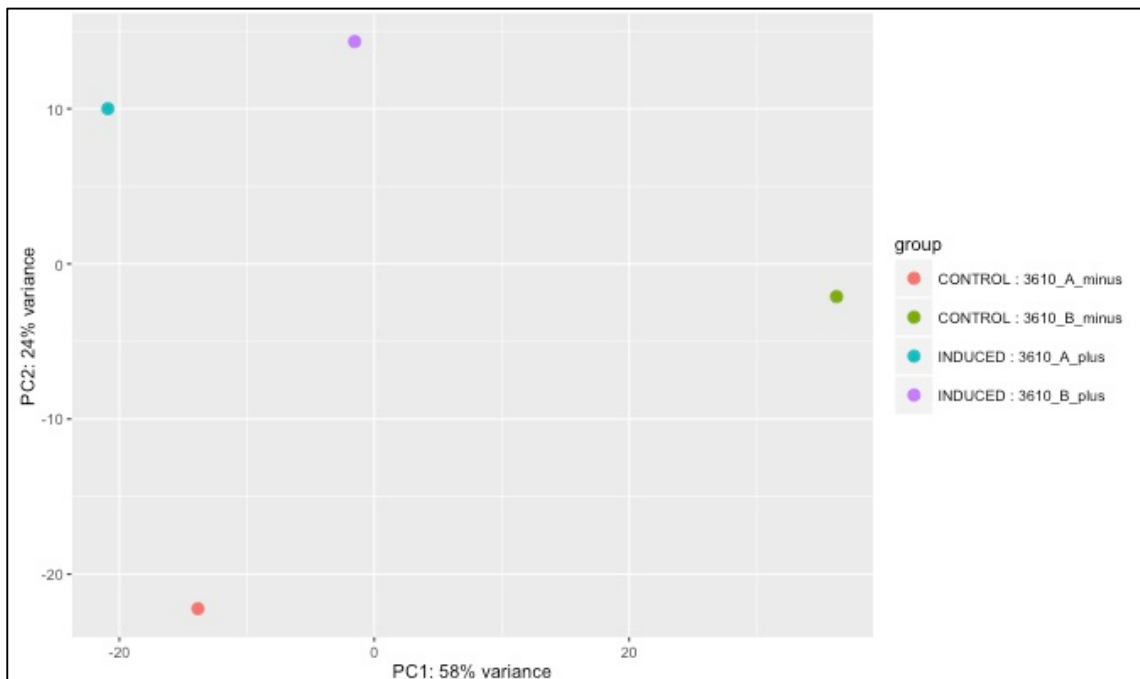
Tukey multiple comparisons of means
 95% family-wise confidence level
 factor levels have been ordered

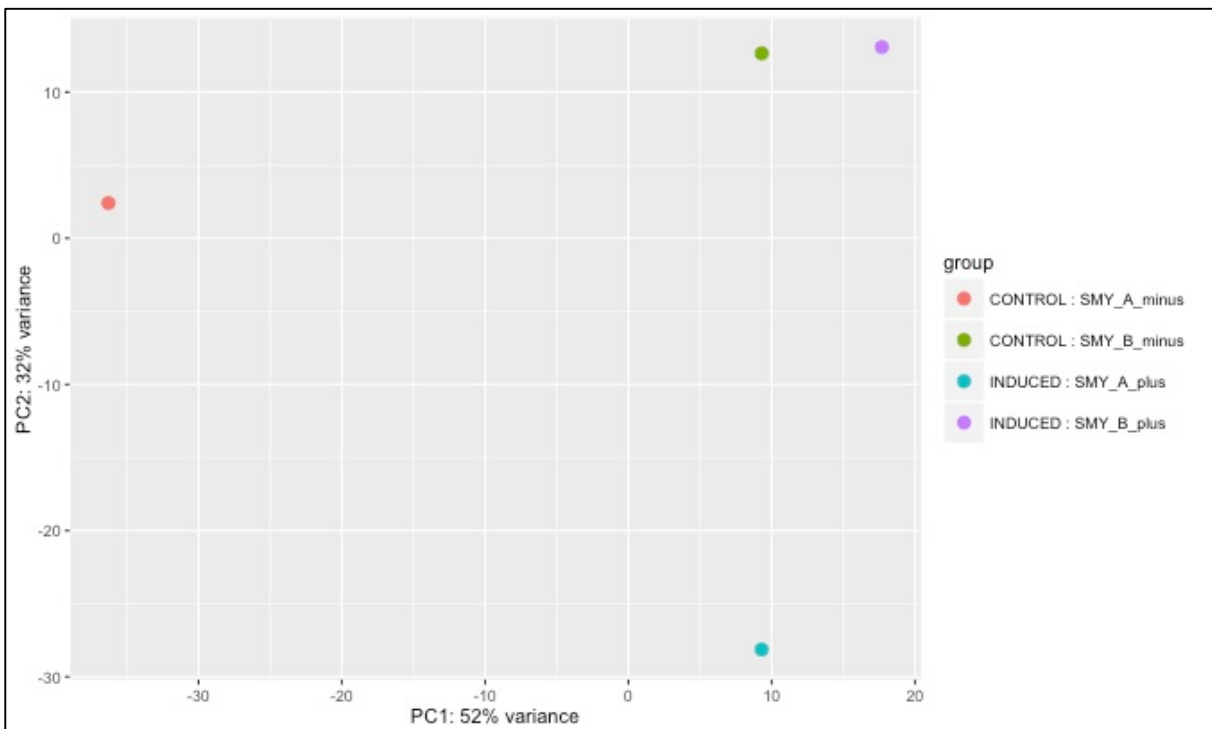
Fit: aov(formula = HAL0 ~ TZC, data = datos)

\$TZC

	diff	lwr	upr	p adj
cero-Cuatrocientos	4.50	1.3992359	7.600764	0.0034266
cien-Cuatrocientos	4.75	1.6492359	7.850764	0.0021247
cincuenta-Cuatrocientos	7.50	4.3992359	10.600764	0.0000171
Veinticinco-Cuatrocientos	8.75	5.6492359	11.850764	0.0000026
cien-cero	0.25	-2.8507641	3.350764	0.9990488
cincuenta-cero	3.00	-0.1007641	6.100764	0.0602118
Veinticinco-cero	4.25	1.1492359	7.350764	0.0055449
cincuenta-cien	2.75	-0.3507641	5.850764	0.0944731
Veinticinco-cien	4.00	0.8992359	7.100764	0.0089889
Veinticinco-cincuenta	1.25	-1.8507641	4.350764	0.7266138

- **Figure S-13:** RNA-seq data statistical analysis





- **Table S-2:** RNA-seq DE analysis. Expression ratios for all DE genes in each methodology for each strain

<i>B. subtilis</i> 3610				
Gene	Biological Function	DE-seq	Tuxedo	EDGE-pro
BS3610_RS19690	ATP phosphoribosyltransferase regulatory subunit	-	5,50707	0
BS3610_RS12360	hypothetical protein	-	-4,09383	0
BS3610_RS21795	transporter	-4,490505116	0	-4,467074622
BS3610_RS11850	hypothetical protein	-4,759460796	0	0
BS3610_RS12365	hypothetical protein	-3,932743489	-4,09383	0
BS3610_RS11810	SPBc2 prophage-derived HNH homing endonuclease YosQ	0	0	-4,16985419
BS3610_RS12395	hypothetical protein	-	-4,09383	0
BS3610_RS12060	hypothetical protein	-5,34704145	0	0
BS3610_RS12390	hypothetical protein	-	-4,09383	0
BS3610_RS12375	hypothetical protein	-	-4,09383	0
BS3610_RS19665	<i>hisA</i> : 1-(5-phosphoribosyl)-5-[(5-phosphoribosylamino)methylideneamino] imidazole-4-carboxamide isomerase	4,945763474	6,06561	0
BS3610_RS12430	hypothetical protein	-	-5,04497	0
BS3610_RS12370	hypothetical protein	-4,38486334	-4,09383	-4,314375812
BS3610_RS12435	phage portal protein	-	-5,04497	0
BS3610_RS19660	imidazole glycerol phosphate synthase subunit HisH	4,48539529	6,06561	4,372750487
BS3610_RS12410	hypothetical protein	-	-5,04497	0
BS3610_RS12350	hypothetical protein	-	-4,09383	0
BS3610_RS12415	hypothetical protein	-	-5,04497	0
BS3610_RS24045	hypothetical protein	-5,364275472	-5,04497	0

BS3610_RS12355	hypothetical protein	-	-4,09383	0
BS3610_RS24005	ribonucleotide-diphosphate reductase	0	0	-4,254304351
BS3610_RS12450	SPBc2 prophage-derived recombinase-like protein YomM	-	-5,04497	0
BS3610_RS19680	histidinol dehydrogenase	4,849383112	5,50707	4,676397657
BS3610_RS19685	ATP phosphoribosyltransferase	4,702523988	5,50707	4,53381139
BS3610_RS11990	hypothetical protein	-4,559446425	0	-4,482910651
BS3610_RS12420	hypothetical protein	-	-5,04497	0
BS3610_RS11800	thioredoxin	-4,969376393	0	0
BS3610_RS12385	hypothetical protein	-	-4,09383	0
BS3610_RS12445	hypothetical protein	-	-5,04497	0
BS3610_RS12380	hypothetical protein	-	-4,09383	0
BS3610_RS12425	hypothetical protein	-	-5,04497	0
BS3610_RS12500	hypothetical protein	-3,849931142	0	-3,805814788
BS3610_RS15915	L-aspartate oxidase	0	0	-4,581510017
BS3610_RS18470	sugar ABC transporter substrate-binding protein	-3,849931142	0	0
BS3610_RS12505	hypothetical protein	0	0	-3,929609046
BS3610_RS04330	major myo-inositol transporter <i>IoIT</i>	-4,237730549	0	-4,267924935
BS3610_RS19670	imidazole glycerol phosphate synthase subunit HisH	4,735586803	5,50707	4,646752752
BS3610_RS12400	hypothetical protein	-	-4,09383	0
BS3610_RS19655	histidine biosynthesis bifunctional protein HisIE	4,152334435	6,06561	4,784088256
BS3610_RS12345	hypothetical protein	-	-4,09383	0
BS3610_RS19675	imidazoleglycerol-phosphate dehydratase	4,405223657	5,50707	4,239612219
BS3610_RS12405	hypothetical protein	-3,956726263	0	-3,905595272
BS3610_RS11985	hypothetical protein	-4,367248768	0	-4,2527513
BS3610_RS12440	hypothetical protein	-	-5,04497	0

B. subtilis SMY

Gene	Biological Function	DE-seq	Tuxedo	EDGE
SMY_RS17470	2,3-dihydroxybenzoate-2,3-dehydrogenase	-3,551665937	0	0
SMY_RS17990	serine protease	4,091449313	0	3,963728677
SMY_RS04115	membrane protein	-3,705965104	0	-3,684443746
SMY_RS11270	hypothetical protein	0	0	-4,39994528
SMY_RS11740	hypothetical protein	-4,314491816	0	0
SMY_RS17455	Isochorismatase <i>dhbB</i>	-4,590768178	0	-4,45538829
SMY_RS23055	DNA repair protein	0	-2,407679054	0
SMY_RS11640	hypothetical protein	0	-4,37195	0
SMY_RS11660	hypothetical protein	0	-4,37195	0
SMY_RS00780	50S ribosomal protein L14	-3,96183139	0	0
SMY_RS22045	MFS transporter	5,46261842	0	5,26519812
SMY_RS11665	hypothetical protein	0	-4,37195	0
SMY_RS19065	cytochrome P450	-4,066116904	0	0
SMY_RS11700	hypothetical protein	-4,066116904	-4,37195	-4,147472547
SMY_RS11725	hypothetical protein	0	-4,37195	0
SMY_RS20485	1-pyrroline-5-carboxylate dehydrogenase	-3,609269112	0	0
SMY_RS11650	hypothetical protein	0	-4,37195	0
SMY_RS17460	enterobactin synthase subunit E	0	0	-3,827248887
SMY_RS11070	deoxyuridine 5'-triphosphate nucleotidohydrolase <i>yncF</i>	0	-7,442172194	0
SMY_RS07945	hypothetical protein	-3,968947495	0	-3,90853085
SMY_RS11645	hypothetical protein	-4,322187374	-4,37195	0
SMY_RS21230	hypothetical protein	-3,860448289	0	-3,847718902
SMY_RS11695	hypothetical protein	-4,008773239	-4,37195	-3,961518285

SMY_RS14165	Holin <i>xhB</i>	0	8,066175319	0
SMY_RS11795	hypothetical protein	0	0	-4,588414953
SMY_RS05740	3-oxoacyl-ACP synthase	-4,868673866	0	-4,697672046
SMY_RS17465	isochorismate synthase	-3,890821806	0	-3,792912408
SMY_RS11260	hypothetical protein	-4,723542569	0	-4,592988487
SMY_RS11630	hypothetical protein	0	-4,37195	0
SMY_RS11635	hypothetical protein	0	-4,37195	0
SMY_RS11085	HNH endonuclease	-4,557644323	0	-4,388921183
SMY_RS00790	50S ribosomal protein L5	-4,206328078	0	-4,03864531
SMY_RS11710	hypothetical protein	0	-4,37195	0
SMY_RS11715	hypothetical protein	0	-4,37195	0
SMY_RS11675	hypothetical protein	0	-4,37195	0
SMY_RS06050	cell wall-associated protease	-3,542105376	0	0
SMY_RS00775	30S ribosomal protein S17	-3,99720487	0	0
SMY_RS00810	50S ribosomal protein L18	-4,159036203	0	0
SMY_RS11670	hypothetical protein	0	-4,37195	0
SMY_RS11655	hypothetical protein	-3,940840424	-4,37195	-3,823905616
SMY_RS11730	hypothetical protein	0	-4,37195	0
SMY_RS21200	hypothetical protein	0	0	-3,715163464
SMY_RS00670	50S ribosomal protein L10	-4,048434484	0	0
SMY_RS00805	50S ribosomal protein L6	-4,301090808	0	-4,116855839
SMY_RS00800	30S ribosomal protein S8	-4,00568365	0	0
SMY_RS21435	iron(3+)-hydroxamate-binding protein <i>yxkB</i>	-4,294769945	-5,13856	-4,173251344
SMY_RS07940	flavodoxin	-4,470127127	0	-4,149235035
SMY_RS11735	recombinase	0	-4,37195	0

SMY_RS11790	hypothetical protein	-4,222256739	0	-4,06363315
SMY_RS11685	hypothetical protein	0	-4,37195	0
SMY_RS11800	N-acetylmuramoyl-L-alanine amidase <i>lytC</i>	-3,763585868	0	0
SMY_RS11690	hypothetical protein	-3,763585868	-4,37195	-4,153821494
SMY_RS11680	hypothetical protein	0	-4,37195	0

- **Figure S-14:** Source code for data mining in chemical databases using precursor mass as entry

```
In [40]: from chemspipy import ChemSpider
        from IPython.display import display, Image

        cs = ChemSpider('c306881c-e280-46f8-b91b-559df2b75182')

        masses = []
        with open("precursor_masses.txt") as mass_file:
            for line in mass_file:
                masses.append(float(line))

        #def tol_setting(mass):
        #    tol = 0.01
        #    mass_results = cs.simple_search_by_mass(mass, tol)
        #    while len(mass_results) > 5:
        #        tol *= 0.95
        #        mass_results = cs.simple_search_by_mass(mass, tol)
        #    return tol

        for mass, numcomp in zip(masses, range(len(masses))):
            #tol = tol_setting(mass)
            tol = 0.001
            mass_results = cs.simple_search_by_mass(mass, tol)
            print("Busqueda del compuesto " + str(numcomp + 1) + " de " + str(len(masses)))
            print("Busqueda de una masa de " + str(mass) + " con una tolerancia de " + str(tol))

            for compound, counter in zip(mass_results[0:5], range(len(mass_results[0:5]))):
                print("Resultado " + str(counter + 1))
                imagefilename = str(compound.csid) + ".png"
                with open(imagefilename, "wb") as outimage:
                    outimage.write(compound.image)
                print("Compuesto: " + str(compound.csid))
                print("Formula molecular: " + compound.molecular_formula)
                print("Peso molecular: " + str(compound.molecular_weight))
                print("SMILES: " + compound.smiles)
                print("Nombre comun: " + compound.common_name)
                print(compound.image_url)
                display(Image(imagefilename))

                print("\n")
            print("\n\n\n")
```

- **Figure S-15: Activity of extracts against *R. solanacearum* AW1**



- **Table S-3: AntiSmash analysis results for *B. subtilis* NCIB-3610**

INPUT ACCESSION NUMBER	INPUT NAME	GENE CLUSTER TYPE	MOST SIMILAR KNOWN CLUSTER
NZ_CM000488.1	NZ_CM000488.1 <i>Bacillus subtilis</i> subsp. <i>subtilis</i> str. NCIB 3610 chromosome, whole genome shotgun sequence	sactipeptide-head_to_tail	Sporulation_killing_factor_skfA_biosynthetic_gene_cluster (100% of genes show similarity)
NZ_CM000488.1	NZ_CM000488.1 <i>Bacillus subtilis</i> subsp. <i>subtilis</i> str. NCIB 3610 chromosome, whole genome shotgun sequence	nrps	Surfactin_biosynthetic_gene_cluster (82% of genes show similarity)
NZ_CM000488.1	NZ_CM000488.1 <i>Bacillus subtilis</i> subsp. <i>subtilis</i> str. NCIB 3610 chromosome, whole genome shotgun sequence	cf_putative	
NZ_CM000488.1	NZ_CM000488.1 <i>Bacillus subtilis</i> subsp. <i>subtilis</i> str. NCIB 3610 chromosome, whole genome shotgun sequence	cf_putative	
NZ_CM000488.1	NZ_CM000488.1 <i>Bacillus subtilis</i> subsp. <i>subtilis</i> str. NCIB 3610 chromosome,	cf_putative	

	whole genome shotgun sequence		
NZ_CM000488.1	NZ_CM000488.1 Bacillus subtilis subsp. subtilis str. NCIB 3610 chromosome, whole genome shotgun sequence	cf_putative	
NZ_CM000488.1	NZ_CM000488.1 Bacillus subtilis subsp. subtilis str. NCIB 3610 chromosome, whole genome shotgun sequence	cf_fatty_acid	
NZ_CM000488.1	NZ_CM000488.1 Bacillus subtilis subsp. subtilis str. NCIB 3610 chromosome, whole genome shotgun sequence	cf_putative	
NZ_CM000488.1	NZ_CM000488.1 Bacillus subtilis subsp. subtilis str. NCIB 3610 chromosome, whole genome shotgun sequence	cf_putative	Zwittermycin_A_biosynthetic_gene_cluster (14% of genes show similarity)
NZ_CM000488.1	NZ_CM000488.1 Bacillus subtilis subsp. subtilis str. NCIB 3610 chromosome, whole genome shotgun sequence	terpene	
NZ_CM000488.1	NZ_CM000488.1 Bacillus subtilis subsp. subtilis str. NCIB 3610 chromosome, whole genome shotgun sequence	cf_fatty_acid	Citrulline_biosynthetic_gene_cluster (27% of genes show similarity)
NZ_CM000488.1	NZ_CM000488.1 Bacillus subtilis subsp. subtilis str. NCIB 3610 chromosome, whole genome shotgun sequence	cf_putative	
NZ_CM000488.1	NZ_CM000488.1 Bacillus subtilis subsp. subtilis str. NCIB 3610 chromosome, whole genome shotgun sequence	nrps-transatpks-otherks	Bacillaene_biosynthetic_gene_cluster (100% of genes show similarity)
NZ_CM000488.1	NZ_CM000488.1 Bacillus subtilis subsp. subtilis str. NCIB 3610 chromosome, whole genome shotgun sequence	nrps	Fengycin_biosynthetic_gene_cluster (100% of genes show similarity)
NZ_CM000488.1	NZ_CM000488.1 Bacillus subtilis subsp. subtilis str. NCIB 3610 chromosome, whole genome shotgun sequence	terpene	

NZ_CM000488.1	NZ_CM000488.1 <i>Bacillus subtilis</i> subsp. <i>subtilis</i> str. NCIB 3610 chromosome, whole genome shotgun sequence	glycocin	Sublancin_168_biosynthetic_gene_cluster (66% of genes show similarity)
NZ_CM000488.1	NZ_CM000488.1 <i>Bacillus subtilis</i> subsp. <i>subtilis</i> str. NCIB 3610 chromosome, whole genome shotgun sequence	t3pks	
NZ_CM000488.1	NZ_CM000488.1 <i>Bacillus subtilis</i> subsp. <i>subtilis</i> str. NCIB 3610 chromosome, whole genome shotgun sequence	cf_putative	
NZ_CM000488.1	NZ_CM000488.1 <i>Bacillus subtilis</i> subsp. <i>subtilis</i> str. NCIB 3610 chromosome, whole genome shotgun sequence	cf_putative	
NZ_CM000488.1	NZ_CM000488.1 <i>Bacillus subtilis</i> subsp. <i>subtilis</i> str. NCIB 3610 chromosome, whole genome shotgun sequence	cf_putative	
NZ_CM000488.1	NZ_CM000488.1 <i>Bacillus subtilis</i> subsp. <i>subtilis</i> str. NCIB 3610 chromosome, whole genome shotgun sequence	cf_saccharide	
NZ_CM000488.1	NZ_CM000488.1 <i>Bacillus subtilis</i> subsp. <i>subtilis</i> str. NCIB 3610 chromosome, whole genome shotgun sequence	nrps	Bacillibactin_biosynthetic_gene_cluster (92% of genes show similarity)
NZ_CM000488.1	NZ_CM000488.1 <i>Bacillus subtilis</i> subsp. <i>subtilis</i> str. NCIB 3610 chromosome, whole genome shotgun sequence	cf_putative	
NZ_CM000488.1	NZ_CM000488.1 <i>Bacillus subtilis</i> subsp. <i>subtilis</i> str. NCIB 3610 chromosome, whole genome shotgun sequence	cf_saccharide	
NZ_CM000488.1	NZ_CM000488.1 <i>Bacillus subtilis</i> subsp. <i>subtilis</i> str. NCIB 3610 chromosome, whole genome shotgun sequence	other	
NZ_CM000488.1	NZ_CM000488.1 <i>Bacillus subtilis</i> subsp. <i>subtilis</i> str. NCIB 3610 chromosome,	cf_saccharide	Teichuronic_acid_biosynthetic_gene_cluster (100% of genes show similarity)

	whole genome shotgun sequence		
NZ_CM000488.1	NZ_CM000488.1 Bacillus subtilis subsp. subtilis str. NCIB 3610 chromosome, whole genome shotgun sequence	cf_putative	
NZ_CM000488.1	NZ_CM000488.1 Bacillus subtilis subsp. subtilis str. NCIB 3610 chromosome, whole genome shotgun sequence	sactipeptide-head_to_tail	
NZ_CM000488.1	NZ_CM000488.1 Bacillus subtilis subsp. subtilis str. NCIB 3610 chromosome, whole genome shotgun sequence	cf_saccharide	Subtilisin_A_biosynthetic_gene_cluster (87% of genes show similarity)
NZ_CM000488.1	NZ_CM000488.1 Bacillus subtilis subsp. subtilis str. NCIB 3610 chromosome, whole genome shotgun sequence	cf_putative	Bacilysin_biosynthetic_gene_cluster (100% of genes show similarity)
NZ_CM000488.1	NZ_CM000488.1 Bacillus subtilis subsp. subtilis str. NCIB 3610 chromosome, whole genome shotgun sequence	cf_putative	Bacillomycin_biosynthetic_gene_cluster (40% of genes show similarity)

- **Table S-4:** supports of manual annotation for network (Fig. 5-1). Data from GNPS library hits, from *in silico* BGC prediction by Antismash and reference MS/MS from available literature

<i>in silico</i> BGC ANALYSIS - ANTISMASH								
Gene Cluster Type	Most similar known cluster	m/z+1 [M+H] ⁺ values - Literature	Sources	Similar m/z+1 [M+H] ⁺ values - Network	library ID	Reported MS2 - Peaks	Networks MS2 - Peaks	Shared Peaks
nrps (lipopetide)	Surfactin BGC (82% of genes show similarity)	1031.75	Al-Ajlani et al, 2007.	1030.64	Surfactins C13-C15	Identified by GNPS		30
		1059.72	Microbial Cell	1058.82		Identified by GNPS	26	
		1075, 83	Factories 2007	1076.64		Identified by GNPS	25	
		1081.3	Chen et al, 2008. Let. Applied Mic.	1081.03		Identified by GNPS	24	
		1036.34	from <i>B. subtilis</i>	1036.69		Identified by GNPS	28	

		Sigma-Aldrich						
cf_fatty acid (alpha-aminoacid)	Citrulline BGC (27% of genes show similarity)	176.2	L-Citrulline PubChem	175.339	Arginine 2-amino-5-thylideneamino) pentanoic acid	61.1	60.06	
						70.1	70.07	
						72.7	72.08	
						116.2	116.07	
						130.2	130.09	
						147.2	147.01	
						159.1	159.1	
						176.2	176.06	
nrps (lipopeptide)	Fengycin BGC (100% of genes show similarity)	1462.70	Villegas-Escobar et al, 2012. J Nat Prod	1462.54	No Library ID	1064.57	1063.51	
						950.49	949.45	
						458.26	457.24	
						330.16	330.17	
						250.15	249.16	
						226.12	226.12	
						198.12	198.12	
						115.08	115.09	
						1344.78	1343.16	
						1064.5	1063.5	
						950.49	949.44	
561.3	561.27							
475.22	474.27							
1477.60	1478.59	412.30	412.22	11				
226.12	226.12							
198.12	198.12							
169.13	169.12							
115.08	115.09							
102.05	102.06							
nrps (Psiderophore)	Bacillibactin biosynthetic gene cluster (92% of genes show similarity)	883.2	Lee et al, 2011. Plos ONE	883.79	No Library ID	883.42	883.42	
						587.0	588.30	
						313.19	313.1	
		883	Miethke et al, 2006.	883.79		295.1	295.14	7
		293.1	292.13					
		249.1	250.12					
191.6	192.16							
cf_saccharide	Teichuronic acid BGC (100% of genes show similarity)				Identified by GNPS	6		

	N-acetylgalactosaminic acid	221,089	Chemspider	276.07	N-acetyl-D-Galactosamine		
	Glucuronic acid	194,139	Chemspider	-			
						271.19	271.1
		270,285	Pubchem			225.17	225.1
cf_saccharide (dipeptide antibiotic)	Bacilysin_BGC (100% of genes show similarity)			270.96	No Library ID	200.11	200
						182.16	182.1
			Özcengiz & Ogulur, 2015. New Biotechnology			165.1	165.1
		270				136.08	136

6

- **Table S-5:** Subnetwork-1 nodes, precursor ions m/z values and abundance ratio for the active extract

PRECURSOR MASS	NUMBER OF SPECTRA FOR ACTIVE EXTRACT	NUMBER OF SPECTRA FOR NON-INDUCED EXTRACT	ABUNDANCE RATIO
558.199	35	20	1,750
571.897	29	8	3,625
611.545	69	35	1,971
781.348	19	10	1,900
382.635	6	2	3,000
865.118	8	5	1,600
489.264	9	5	1,800
429.987	39	22	1,773
487.904	36	14	2,571
501.161	24	19	1,263
584.022	76	37	2,054
659.438	26	13	2,000
784.666	30	14	2,143
724.175	23	8	2,875
818.708	7	5	1,400
889.417	9	2	4,500

440.341	9	5	1,800
553.551	23	11	2,091
572.996	6	7	0,857
514.386	11	5	2,200
836.444	17	7	2,429
529.298	5	1	5,000
653.955	73	37	1,973
505.933	5	2	2,500
522.202	15	6	2,500
640.291	32	18	1,778
752.755	42	19	2,211
618.623	31	20	1,550
745.965	5	2	2,500
286.112	21	16	1,313
320.161	7	2	3,500
923.516	49	24	2,042
643.961	9	5	1,800
670.408	10	2	5,000
484.695	11	9	1,222
705.338	9	3	3,000
695.881	28	14	2,000
635.638	6	4	1,500
1069.9	32	17	1,882
498.141	18	6	3,000
442.499	19	10	1,900
751.754	4	2	2,000
599.364	57	23	2,478
711.641	28	15	1,867
561.203	9	6	1,500
685.542	25	15	1,667
589.05	33	20	1,650
586.492	20	14	1,429
755.978	16	7	2,286
529.128	41	26	1,577
527.599	21	8	2,625
457.565	34	17	2,000
626.05	42	23	1,826
512.133	26	12	2,167

526.312	24	11	2,182
413.453	66	35	1,886
426.678	21	11	1,909
470.989	45	23	1,957
440.957	18	10	1,800
556.313	32	15	2,133
774.672	39	15	2,600
496.455	12	4	3,000
400.579	26	15	1,733
954.054	19	11	1,727
1031.92	17	12	1,417
387.346	16	11	1,455
569.722	41	24	1,708
544.441	37	13	2,846
615.421	26	9	2,889
830.728	25	22	1,136
671.833	27	18	1,500
416.403	10	3	3,333
547.761	15	8	1,875
471.373	54	29	1,862
603.666	27	17	1,588
632.735	70	30	2,333
658.412	10	4	2,500
542.77	36	30	1,200
802.0	9	0	9,000
742.252	22	8	2,750
517.638	32	17	1,882
740.575	53	26	2,038

REFERENCES

1. Fleming A (1980) Classics in infectious diseases: on the antibacterial action of cultures of a penicillium, with special reference to their use in the isolation of *B. influenzae* by Alexander Fleming, Reprinted from the British Journal of Experimental Pathology 10:226-236, 1929. *Rev Infect Dis* 2(1):129-139.
2. Davies J & Davies D (2010) Origins and evolution of antibiotic resistance. *Microbiol Mol Biol Rev* 74(3):417-433.
3. Allen HK, *et al.* (2010) Call of the wild: antibiotic resistance genes in natural environments. *Nat Rev Microbiol* 8(4):251-259.
4. Abraham EP & Chain E (1988) An enzyme from bacteria able to destroy penicillin. 1940. *Rev Infect Dis* 10(4):677-678.
5. World Health Organization WHO (2014) Antimicrobial Resistance Global Report on Surveillance. (World Health Organization WHO, Geneva, Switzerland).
6. Genilloud O (2014) The re-emerging role of microbial natural products in antibiotic discovery. *Antonie van Leeuwenhoek* 106(1):173-188.
7. Rodríguez-Rojas A, Rodríguez-Beltrán J, Couce A, & Blázquez J (2013) Antibiotics and antibiotic resistance: a bitter fight against evolution. *Int J Med Microbiol* 303(6-7):293-297.
8. Tommasi R, Brown DG, Walkup GK, Manchester JI, & Miller AA (2015) ESKAPEing the labyrinth of antibacterial discovery. *Nat Rev Drug Discov* 14(8):529-542.
9. Harvey AL, Edrada-Ebel R, & Quinn RJ (2015) The re-emergence of natural products for drug discovery in the genomics era. *Nat Rev Drug Discov* 14(2):111-129.
10. Kieny M-P (2014) Current WHO model for development/preservation of new antibiotics. (World Health Organization., Geneva).
11. Wright GD (2017) Opportunities for natural products in 21(st) century antibiotic discovery. *Nat Prod Rep* 34(7):694-701.
12. Laxminarayan R & Powers JH (2011) Antibacterial R&D incentives. *Nat Rev Drug Discov* 10(10):727-728.
13. Hancock RE & Strohl WR (2001) Antimicrobials in the 21 st century. Editorial Overview. *Current Opinion in Microbiology* 4:491-492.
14. Stockwell VO & Duffy V (2012) Use of antibiotics in plant agriculture. *Rev. sci. tech. Off. int. Epiz.* 31(1):199-210.
15. Goodman R (1959) The influence of antibiotics on plants and plant disease control. *Antibiotics: Their Chemistry and Non-Medical Uses*, ed Goldberg H (van Nostrand, Princeton), pp 322-448.
16. US Geological Survey USGS (2006) Pesticides in the Nation's Streams and Ground Water, 1992-2001—What findings may mean to human health, aquatic life, and fish-eating wildlife (USGS, Washington D.C.).
17. McManus PS, Stockwell VO, Sundin GW, & Jones AL (2002) Antibiotic use in plant agriculture. *Annu Rev Phytopathol* 40:443-465.
18. Sherburne JJ, *et al.* (2016) Occurrence of Triclocarban and Triclosan in an Agro-ecosystem Following Application of Biosolids. *Environmental Science & Technology* 50(24):13206-13214.
19. Wu Z (2017) Balancing food security and AMR: A review of economic literature on antimicrobial use in food animal production. in *China Agricultural Economic Review*, pp 14-31.
20. Van Boeckel TP, *et al.* (2015) Global trends in antimicrobial use in food animals. *Proc Natl Acad Sci U S A* 112(18):5649-5654.
21. World Health Organization: WHO (2014) WHO's first global report on antibiotic resistance reveals serious, worldwide threat to public health.
22. Food and Drug Administration (2017) *Summary report on Antimicrobials Sold or Distributed for Use in Food-Producing Animals* (FDA Center for Veterinary Medicine).

23. Health W & Organization (2017) *Prioritization of pathogens to guide discovery, research and development of new antibiotics for drug-resistant bacterial infections, including tuberculosis*. (Geneva:).
24. Sorensen AC, Lawrence RS, & Davis MF (2014) Interplay between policy and science regarding low-dose antimicrobial use in livestock. *Front Microbiol* 5:86.
25. European Commission (2011) Action plan against the rising threats from antimicrobial resistance: communication from the Commission to the European Parliament and the Council. ed Consumers DHa (Brussels).
26. Laxminarayan R, T. Van Boeckel and A. Teillant (2015) *The Economic Costs of Withdrawing Antimicrobial Growth Promoters from the Livestock Sector* (OECD Publishing).
27. USDA (2014) *Antimicrobial Resistance Action Plan*.
28. World Health Organization (2017) Antibacterial Agents in Clinical Development: a n analysis of the antibacterial clinical development pipeline, including tuberculosis. (Geneva, Switzerland).
29. Kealey C, Creaven CA, Murphy CD, & Brady CB (2017) New approaches to antibiotic discovery. *Biotechnol Lett* 39(6):805-817.
30. Grabley S & Thiericke R (1999) Bioactive agents from natural sources: trends in discovery and application. *Adv Biochem Eng Biotechnol* 64:101-154.
31. Ling LL, *et al.* (2015) A new antibiotic kills pathogens without detectable resistance. *Nature* 517(7535):455-459.
32. Gavrish E, *et al.* (2014) Lassomycin, a ribosomally synthesized cyclic peptide, kills *mycobacterium tuberculosis* by targeting the ATP-dependent protease ClpC1P1P2. *Chem Biol* 21(4):509-518.
33. Zipperer A, *et al.* (2016) Human commensals producing a novel antibiotic impair pathogen colonization. *Nature* 535(7613):511-516.
34. Gullo V, McAlpine J, Lam K, Baker D, & Petersen F (2006) Drug discovery from natural products. *Journal of Industrial Microbiology and Biotechnology* 33(7):523-531.
35. Pelaez F (2006) The historical delivery of antibiotics from microbial natural products-can history repeat? *Biochem Pharmacol*, (England), Vol 71, pp 981-990.
36. Harvey A (2000) Strategies for discovering drugs from previously unexplored natural products. *Drug Discov Today* 5(7):294-300.
37. Shoda M (2000) Bacterial control of plant diseases. *Journal of bioscience and bioengineering* 89 (6):515-521.
38. Le Goff G & *al e* (2013) Isolation and Characterization of Unusual Hydrazides from *Streptomyces* sp. Impact of the Cultivation Support and Extraction Procedure. *J. Nat. Prod.* 76:142-149.
39. Chopra I, Hesse L, & O'Neill AJ (2002) Exploiting current understanding of antibiotic action for discovery of new drugs. *J Appl Microbiol* 92 Suppl:4S-15S.
40. Cragg GM, Newman DJ, & Snader KM (1997) Natural products in drug discovery and development. *J Nat Prod* 60(1):52-60.
41. Brown ED & Wright GD (2016) Antibacterial drug discovery in the resistance era. *Nature* 529(7586):336-343.
42. Lewis K (2017) New approaches to antimicrobial discovery. *Biochem Pharmacol* 134:87-98.
43. Reen FJ, Romano S, Dobson AD, & O'Gara F (2015) The Sound of Silence: Activating Silent Biosynthetic Gene Clusters in Marine Microorganisms. *Mar Drugs* 13(8):4754-4783.
44. Bode HB, Bethe B, Höfs R, & Zeeck A (2002) Big effects from small changes: possible ways to explore nature's chemical diversity. *Chembiochem* 3(7):619-627.
45. Overmann J, Abt B, & Sikorski J (2017) Present and Future of Culturing Bacteria. *Annu Rev Microbiol* 71:711-730.
46. Danczak RE, *et al.* (2017) Members of the Candidate Phyla Radiation are functionally differentiated by carbon- and nitrogen-cycling capabilities. *Microbiome* 5(1):112.
47. Brown CT, *et al.* (2015) Unusual biology across a group comprising more than 15% of domain Bacteria. *Nature* 523(7559):208-211.

48. Kaerberlein T, Lewis K, & Epstein SS (2002) Isolating "uncultivable" microorganisms in pure culture in a simulated natural environment. *Science* 296(5570):1127-1129.
49. Nichols D, *et al.* (2010) Use of ichip for high-throughput in situ cultivation of "uncultivable" microbial species. *Appl Environ Microbiol* 76(8):2445-2450.
50. Wilson MC, *et al.* (2014) An environmental bacterial taxon with a large and distinct metabolic repertoire. *Nature* 506(7486):58-62.
51. Wu C, Kim HK, van Wezel GP, & Choi YH (2015) Metabolomics in the natural products field—a gateway to novel antibiotics. *Drug Discov Today Technol* 13:11-17.
52. Traxler MF, Watrous JD, Alexandrov T, Dorrestein PC, & Kolter R (2013) Interspecies interactions stimulate diversification of the *Streptomyces coelicolor* secreted metabolome. *MBio* 4(4).
53. Schroeckh V, *et al.* (2009) Intimate bacterial-fungal interaction triggers biosynthesis of archetypal polyketides in *Aspergillus nidulans*. *Proc Natl Acad Sci U S A* 106(34):14558-14563.
54. Seyedsayamdost MR (2014) High-throughput platform for the discovery of elicitors of silent bacterial gene clusters. *Proc Natl Acad Sci U S A* 111(20):7266-7271.
55. Traxler MF & Kolter R (2015) Natural products in soil microbe interactions and evolution. *Nat Prod Rep* 32(7):956-970.
56. Challis GL (2008) Mining microbial genomes for new natural products and biosynthetic pathways. *Microbiology* 154(Pt 6):1555-1569.
57. Debono M, *et al.* (1987) A21978C, a complex of new acidic peptide antibiotics: isolation, chemistry, and mass spectral structure elucidation. *J Antibiot (Tokyo)* 40(6):761-777.
58. Johnson A (2007) Drug evaluation: OPT-80, a narrow-spectrum macrocyclic antibiotic. *Curr Opin Investig Drugs. Curr Opin Investig Drugs* 8 168–173.
59. McClerren A & *et al* (Discovery and in vitro biosynthesis of haloduracin, a two-component lantibiotic. *Proc. Natl Acad. Sci. USA* 103 17243–17248
60. Schlotterbeck G, Ross A, Dieterle F, & Senn H (2006) Metabolic profiling technologies for biomarker discovery in biomedicine and drug development. *Pharmacogenomics* 7(7):1055-1075.
61. Harrigan G (2002) Metabolic profiling: pathways in drug discovery. *Drug Discov Today* 7(6):351-352.
62. Hufsky F, Scheubert K, & Böcker S (2014) New kids on the block: novel informatics methods for natural product discovery. *Nat Prod Rep* 31(6):807-817.
63. Hubert J, *et al.* (2014) Identification of natural metabolites in mixture: a pattern recognition strategy based on (13)C NMR. *Anal Chem* 86(6):2955-2962.
64. Ebada SS, Edrada RA, Lin W, & Proksch P (2008) Methods for isolation, purification and structural elucidation of bioactive secondary metabolites from marine invertebrates. *Nat Protoc* 3(12):1820-1831.
65. Tawfike AF, Viegelmann C, & Edrada-Ebel R (2013) Metabolomics and dereplication strategies in natural products. *Methods Mol Biol* 1055:227-244.
66. Barding GA, Orr DJ, Sathnur SM, & Larive CK (2013) VIZR—an automated chemometric technique for metabolic profiling. *Anal Bioanal Chem* 405(26):8409-8417.
67. Ibrahim A, *et al.* (2012) Dereplicating nonribosomal peptides using an informatic search algorithm for natural products (iSNAP) discovery. *Proc Natl Acad Sci U S A* 109(47):19196-19201.
68. Scheltema RA, Jankevics A, Jansen RC, Swertz MA, & Breitling R (2011) PeakML/mzMatch: a file format, Java library, R library, and tool-chain for mass spectrometry data analysis. *Anal Chem* 83(7):2786-2793.
69. Pluskal T, Castillo S, Villar-Briones A, & Oresic M (2010) MZmine 2: modular framework for processing, visualizing, and analyzing mass spectrometry-based molecular profile data. *BMC Bioinformatics* 11:395.
70. Wang M, *et al.* (2016) Sharing and community curation of mass spectrometry data with Global Natural Products Social Molecular Networking. *Nat Biotechnol* 34(8):828-837.

71. Tautenhahn R, Patti GJ, Rinehart D, & Siuzdak G (2012) XCMS Online: a web-based platform to process untargeted metabolomic data. *Anal Chem* 84(11):5035-5039.
72. Shannon P, *et al.* (2003) Cytoscape: a software environment for integrated models of biomolecular interaction networks. *Genome Res* 13(11):2498-2504.
73. Hur M, *et al.* (2013) A global approach to analysis and interpretation of metabolic data for plant natural product discovery. *Nat Prod Rep* 30(4):565-583.
74. Appleton DR, Buss AD, & Butler MS (2007) A simple method for high-throughput extract prefractionation for biological screening. *Chimia* 61(6):327-331.
75. Olivon F, *et al.* (2017) Bioactive Natural Products Prioritization Using Massive Multi-informational Molecular Networks. *Acs Chemical Biology* 12(10):2644-2651.
76. Ceballos I (2009) Selección de bacterias aeróbicas formadoras de endospora. MSc. thesis Univerisdad Nacional de Colombia, Medellín, Colombia.
77. Ceballos I, *et al.* (2012) Cultivable bacteria populations associated with leaves of banana and plantain plants and their antagonistic activity against *Mycosphaerella fijiensis*. *Microb Ecol* 64(3):641-653.
78. Posada LF, *et al.* (2016) Bioprospecting of aerobic endospore-forming bacteria with biotechnological potential for growth promotion of banana plants. *Scientia Horticulturae* 212(Supplement C):81 - 90.
79. Villegas V (2012) Identificación y caracterización de extractos bacterianos biológicamente activos contra patógenos de *Musa* sp. Doctoral Thesis (Universidad Nacional de Colombia, Medellín, Colombia).
80. Demain AL (2014) Importance of microbial natural products and the need to revitalize their discovery. *J Ind Microbiol Biotechnol* 41(2):185-201.
81. Hamdache A, Lamarti A, Aleu J, & Collado IG (2011) Non-peptide metabolites from the genus *Bacillus*. *J Nat Prod* 74(4):893-899.
82. Ongena M & Jacques P (2008) *Bacillus* lipopeptides: versatile weapons for plant disease biocontrol. *Trends in microbiology* 16 (3):115--125.
83. Raaijmakers J, de Bruijn I, Nybro O, & Ongena M (2010) Natural functions of lipopeptides from *Bacillus* and *Pseudomonas*: more than surfactants and antibiotics. *FEMS Microbiology Reviews* 34:1037-1062.
84. Earl AM, Losick R, & Kolter R (2008) Ecology and genomics of *Bacillus subtilis*. *Trends Microbiol* 16(6):269-275.
85. Westers L, Westers H, & Quax WJ (2004) *Bacillus subtilis* as cell factory for pharmaceutical proteins: a biotechnological approach to optimize the host organism. *Biochim Biophys Acta* 1694(1-3):299-310.
86. Yuliar, Nion YA, & Toyota K (2015) Recent Trends in Control Methods for Bacterial Wilt Diseases Caused by *Ralstonia solanacearum*. *Microbes and Environments* 30(1):1-11.
87. Mansfield J, *et al.* (2012) Top 10 plant pathogenic bacteria in molecular plant pathology. *Mol Plant Pathol* 13(6):614-629.
88. Elphinstone JG (2005) Bacterial Wilt Disease and the *Ralstonia solanacearum* Species Complex. *The current bacterial wilt situation: A global view*, ed C. Allen PP, & A. C. Hayward. (APS Press, St. Paul, Minnesota), pp 9-28.
89. Fegan M & Prior P (2005) How complex is the *Ralstonia solanacearum* species complex. *Bacterial wilt disease and the Ralstonia solanacearum species complex* eds Allen C, Prior P, & Hayward AC (APS Press, Saint Paul USA,), pp 449-461.
90. Prior P, *et al.* (2016) Genomic and proteomic evidence supporting the division of the plant pathogen *Ralstonia solanacearum* into three species. *BMC Genomics* 17:90.
91. Peeters N, Guidot A, Vailleau F, & Valls M (2013) *Ralstonia solanacearum*, a widespread bacterial plant pathogen in the post-genomic era. *Mol Plant Pathol* 14(7):651-662.
92. Wang JF & Lin CH (2005) Integrated management of tomato bacterial wilt. ed AVRDC The world vegetable center (Bureau of Animal and Plant Quarantine and Health Inspection, Council of Agriculture, Republic of China., Taiwan).
93. FAO (2017) Food and Agriculture Organization: EST Commodities.
94. AUGURA Asociación de Bananeros de Colombia (2016) Coyuntura Bananera Año 2016.

95. OECD (2015) OECD Review in Agricultural Policies: Colombia 2015. (OECD Publishing).
96. AUGURA
(http://www.augura.com.co/index.php?option=com_content&view=article&id=63&Itemid=16) (Asociación de Bananeros de Colombia AUGURA). [Último acceso: 10 de Octubre de 2014].
97. Agronet (2014) Estadísticas del sector agropecuario. [En línea] Disponible online: <http://www.agronet.gov.co/agronetweb1/Inicio.aspx>.
98. Bornacelly H (2011) Status de la enfermedad del MOKO (*Ralstonia solanacearum*) en banano en colombia.
99. Hurtado R (2012) Boletín Técnico Cenibanano: Caracterización de síntomas de la enfermedad del Moko en Invernadero y Campo cuando se simulan labores que causen heridas en la plantas de banano y plátano. ed Cenibanano (Augura).
100. Castañeda DA & Espinosa JA (2005) Behavior and impact of the moko disease in the urabá region (Colombia), during the past 35 years and proposal of a risk index for the disease. *Rev.Fac.Nal.Agr.Medellín* 58 (1):(2587--2599).
101. Mattson AM, Jensen CO, & Dutcher RA (1947) Triphenyltetrazolium Chloride as a Dye for Vital Tissues. *Science* 106(2752):294-295.
102. Nineham AW (1954) The Chemistry of Formazans and Tetrazolium Salts (Research Laboratories, May & Baker Ltd., Dagenham, Essex, England).
103. Cui X, Vlahakis JZ, Crandall IE, & Szarek WA (2008) Anti-Plasmodium activity of tetrazolium salts. *Bioorg Med Chem* 16(4):1927-1947.
104. Berridge MV, Herst PM, & Tan AS (2005) Tetrazolium dyes as tools in cell biology: new insights into their cellular reduction. *Biotechnol Annu Rev* 11:127-152.
105. Bhosale JD, *et al.* (2013) Synthesis, characterization and biological activities of novel substituted formazans of 3,4-dimethyl-1H-pyrrole-2-carbohydrazide derivatives. *Journal of Pharmacy Research* 7(7):582-587.
106. Marshall NJ, Goodwin CJ, & Holt SJ (1995) A critical assessment of the use of microculture tetrazolium assays to measure cell growth and function. *Growth Regul* 5(2):69-84.
107. Scudiero DA, *et al.* (1988) Evaluation of a soluble tetrazolium/formazan assay for cell growth and drug sensitivity in culture using human and other tumor cell lines. *Cancer Res* 48(17):4827-4833.
108. von Peckman H & Runge P (1894) Oxydation der formazyilverbindungen I & II *Ber Dtsch Chem Gas* 27:323-324; 2920-2930.
109. Smith JJ & McFeters GA (1997) Mechanisms of INT (2-(4-iodophenyl)-3-(4-nitrophenyl)-5-phenyl tetrazolium chloride), and CTC (5-cyano-2,3-ditoly tetrazolium chloride) reduction in *Escherichia coli* K-12. *Journal of Microbiological Methods* 29(3):161-175.
110. Lakon G (1949) The Topographical Tetrazolium Method For Determining The Germinating Capacity Of Seeds. *Plant Physiol* 24(3):389-394.
111. Yang H, Acker J, Chen A, & McGann L (1998) *In situ* assessment of cell viability. *Cell Transplant* 7(5):443-451.
112. Duncan DR & Widholm JM (2004) Osmotic induced stimulation of the reduction of the viability dye 2,3,5-triphenyltetrazolium chloride by maize roots and callus cultures. *J Plant Physiol* 161(4):397-403.
113. Lederberg J (1948) Detection of Fermentative Variants with Tetrazolium. *J Bacteriol* 56(5):695.
114. Kelman A (1954) The relationship of pathogenicity of *Pseudomonas solanacearum* to colony appearance in a tetrazolium medium. *Phytopathology* 44(12):693-695.
115. Praveen-Kumar & Tarafdar JC (2003) 2,3,5-Triphenyltetrazolium chloride (TTC) as electron acceptor of culturable soil bacteria, fungi and actinomycetes. *Biology and Fertility of Soils* 38(3):186-189.
116. Tengerdy RP, Nagy JG, & Martin B (1967) Quantitative measurement of bacterial growth by the reduction of tetrazolium salts. *Appl Microbiol* 15(4):954-955.
117. Bochner BR (1989) Sleuthing out bacterial identities. *Nature* 339(6220):157-158.

118. Boucher CA, Barberis PA, Trigalet AP, & Demery DA (1985) Transposon mutagenesis of *Pseudomonas solanacearum* isolation of tn-5-induced avirulent mutants. *Journal of General Microbiology* 131(9):2449-2458.
119. Flavier AB, Clough SJ, Schell MA, & Denny TP (1997) Identification of 3-hydroxypalmitic acid methyl ester as a novel autoregulator controlling virulence in *Ralstonia solanacearum*. *Mol. Micro- biol.* 26 (2):251-259.
120. Shinohara M, Nakajima N, & Uehara Y (2007) Purification and characterization of a novel esterase (β -hydroxypalmitate methyl ester hydrolase) and prevention of the expression of virulence by *Ralstonia solanacearum*. *Journal of Applied Microbiology* 103(1):152-162.
121. Wicker E, *et al.* (2007) *Ralstonia solanacearum* strains from Martinique (French West Indies) exhibiting a new pathogenic potential. *Appl Environ Microbiol* 73(21):6790-6801.
122. Singh D, Yadav K, Chaudhary G, Singh Rana V, & Sharma RK (2016) Potential of *Bacillus amyloliquefaciens* for Biocontrol of Bacterial Wilt of Tomato Incited by *Ralstonia solanacearum*. *Journal of Plant Pathology & Microbiology* 7(1):1-6.
123. Wang X & Liang G (2014) Control efficacy of an endophytic *Bacillus amyloliquefaciens* strain BZ6-1 against peanut bacterial Wilt, *Ralstonia solanacearum*. *Biomed Res Int* 2014:465-435.
124. Clough SJ, Schell MA, & Denny TP (1994) Evidence for involvement of a volatile extracellular factor in *Pseudomonas solanacearum* virulence gene expression. *Molecular Plant-Microbe Interactions* 7(5):621-630.
125. Denny TPM, F. W.Brumbley, S. M. (1988) Characterization of *Pseudomonas solanacearum* Tn5 mutants deficient in extracellular polysaccharide. *Molecular Plant Microbe Interactions* 1(5):215-223.
126. Mora I, Cabrefiga J, & Montesinos E (2015) Cyclic Lipopeptide Biosynthetic Genes and Products, and Inhibitory Activity of Plant-Associated *Bacillus* against Phytopathogenic Bacteria. *PLoS One* 10(5):e0127738.
127. Fan B, Blom J, Klenk HP, & Borriss R (2017) *Bacillus amyloliquefaciens*, *Bacillus velezensis*, and *Bacillus siamensis* Form an 'Operational Group *B. amyloliquefaciens*' within the *B. subtilis* species complex. *Front Microbiol* 8:22.
128. Zhao H, *et al.* (2017) Biological activity of lipopeptides from *Bacillus*. *Appl Microbiol Biotechnol* 101(15):5951-5960.
129. Bais HP, Fall R, & Vivanco JM (2004) Biocontrol of *Bacillus subtilis* against infection of Arabidopsis roots by *Pseudomonas syringae* is facilitated by biofilm formation and surfactin production. *Plant Physiol* 134(1):307-319.
130. Stein T (2005) *Bacillus subtilis* antibiotics: structures, syntheses and specific functions. *Mol Microbiol* 56(4):845-857.
131. Marahiel MA (2009) Working outside the protein-synthesis rules: insights into non-ribosomal peptide synthesis. *J Pept Sci* 15(12):799-807.
132. Wang T, *et al.* (2015) Natural products from *Bacillus subtilis* with antimicrobial properties. *Chinese Journal of Chemical Engineering* 23(4):744 - 754.
133. Dimkić I, *et al.* (2017) The Profile and Antimicrobial Activity of *Bacillus* Lipopeptide Extracts of Five Potential Biocontrol Strains. *Front Microbiol* 8:925.
134. Etchegaray A, *et al.* (2008) Effect of a highly concentrated lipopeptide extract of *Bacillus subtilis* on fungal and bacterial cells. *Arch Microbiol* 190(6):611-622.
135. Byers JT, Lucas C, Salmond GP, & Welch M (2002) Nonenzymatic turnover of an *Erwinia carotovora* quorum-sensing signaling molecule. *J Bacteriol* 184(4):1163-1171.
136. Zhang HB, Wang LH, & Zhang LH (2002) Genetic control of quorum-sensing signal turnover in *agrobacterium tumefaciens*. *Proc. Natl. Acad. Sci.* 99 (7):4638-4643.
137. Alvarez B, Lopez MM, & Biosca EG (2008) Survival strategies and pathogenicity of *Ralstonia solanacearum* phylotype II subjected to prolonged starvation in environmental water microcosms. *Microbiology*, England), Vol 154, pp 3590-3598.
138. The UniProt Consortium (2017) UniProt: the universal protein knowledgebase. *Nucleic Acids Res* 45(D1):D158-D169.
139. Balouiri M, Sadiki M, & Ibsouda SK (2016) Methods for *in vitro* evaluating antimicrobial activity: A review. *Journal of Pharmaceutical Analysis* 6(2):71 - 79.

140. Bauer AW, Kirby WM, Sherris JC, & Turck M (1966) Antibiotic susceptibility testing by a standardized single disk method. *Am J Clin Pathol* 45(4):493-496.
141. Schwyn B & Neilands JB (1987) Universal chemical assay for the detection and determination of siderophores. *Anal Biochem* 160(1):47-56.
142. Team. RC (2014) R: A language and environment for statistical computing [Online access: <http://www.r-project.org/Vienna>, Austria].
143. Mathews CK, Van Holde KE, Appling D, & Anthony-Cahill SJ (2012) *Biochemistry* (Pearson, Canada) 4th Ed p 1368.
144. Cochrane SA & Vederas JC (2014) Lipopeptides from *Bacillus* and *Paenibacillus* spp.: A Gold Mine of Antibiotic Candidates. *Med Res Rev*.
145. Lovrekovich L & Klement Z (1960) Triphenyltetrazolium chloride tolerance of phytopathogenic bacteria. *Phytopathologische Zeitschrift* 39(2):129-133.
146. Weinberg ED (1953) Selective inhibition of microbial growth by the incorporation of triphenyl tetrazolium chloride in culture media. *J Bacteriol* 66(2):240-242.
147. Thom SM, Horobin RW, Seidler E, & Barer MR (1993) Factors affecting the selection and use of tetrazolium salts as cytochemical indicators of microbial viability and activity. *J Appl Bacteriol* 74(4):433-443.
148. Bertrand S, *et al.* (2013) Detection of metabolite induction in fungal co-cultures on solid media by high-throughput differential ultra-high pressure liquid chromatography-time-of-flight mass spectrometry fingerprinting. *J Chromatogr A* 1292:219-228.
149. Tyc O, *et al.* (2014) Impact of interspecific interactions on antimicrobial activity among soil bacteria. *Front Microbiol* 5:567.
150. Mukherjee S, Das P, & Sen R (2006) Towards commercial production of microbial surfactants. *Trends Biotechnol* 24(11):509-515.
151. Aleti G, Sessitsch A, & Brader G (2015) Genome mining: Prediction of lipopeptides and polyketides from *Bacillus* and related Firmicutes. *Comput Struct Biotechnol J* 13:192-203.
152. Fischbach MA & Walsh CT (2006) Assembly-line enzymology for polyketide and nonribosomal Peptide antibiotics: logic, machinery, and mechanisms. *Chem Rev* 106(8):3468-3496.
153. Jack RW, Tagg JR, & Ray B (1995) Bacteriocins of gram-positive bacteria. *Microbiol Rev* 59(2):171-200.
154. Oscáriz JC, Lasa I, & Pisabarro AG (1999) Detection and characterization of cerein 7, a new bacteriocin produced by *Bacillus cereus* with a broad spectrum of activity. *FEMS Microbiol Lett* 178(2):337-341.
155. Bizani D & Brandelli A (2002) Characterization of a bacteriocin produced by a newly isolated *Bacillus* sp. Strain 8 A. *J Appl Microbiol* 93(3):512-519.
156. Cherif A, *et al.* (2001) Thuricin 7: a novel bacteriocin produced by *Bacillus thuringiensis* BMG1.7, a new strain isolated from soil. *Lett Appl Microbiol* 32(4):243-247.
157. Gray EJ, *et al.* (2006) A novel bacteriocin, thuricin 17, produced by plant growth promoting rhizobacteria strain *Bacillus thuringiensis* NEB17: isolation and classification. *J Appl Microbiol* 100(3):545-554.
158. Ongena M, *et al.* (2007) Surfactin and fengycin lipopeptides of *Bacillus subtilis* as elicitors of induced systemic resistance in plants. *Environ Microbiol* 9(4):1084-1090.
159. Quisel JD, Burkholder WF, & Grossman AD (2001) In vivo effects of sporulation kinases on mutant Spo0A proteins in *Bacillus subtilis*. *J Bacteriol* 183(22):6573-6578.
160. Molle V, *et al.* (2003) The Spo0A regulon of *Bacillus subtilis*. *Mol Microbiol* 50(5):1683-1701.
161. Cimermancic P, *et al.* (2014) Insights into secondary metabolism from a global analysis of prokaryotic biosynthetic gene clusters. *Cell* 158(2):412-421.
162. Brochu A, *et al.* (1992) Modes of action and inhibitory activities of new siderophore-beta-lactam conjugates that use specific iron uptake pathways for entry into bacteria. *Antimicrob Agents Chemother* 36(10):2166-2175.
163. Khan A, Doshi HV, & Thakur MC (2016) *Bacillus* spp.: A Prolific Siderophore Producer. *Bacilli and Agrobiotechnology*, eds Islam MT, Rahman M, Pandey P, Jha CK, & Aeron A (Springer International Publishing, Cham), pp 309-323.

164. May JJ, Wendrich TM, & Marahiel MA (2001) The *dhb* operon of *Bacillus subtilis* encodes the biosynthetic template for the catecholic siderophore 2,3-dihydroxybenzoate-glycine-threonine trimeric ester bacillibactin. *J Biol Chem* 276(10):7209-7217.
165. Koppisch AT, *et al.* (2005) Petrobactin is the primary siderophore synthesized by *Bacillus anthracis* str. Sterne under conditions of iron starvation. *Biometals* 18(6):577-585.
166. Cantrell CL, Dayan FE, & Duke SO (2012) Natural products as sources for new pesticides. *J Nat Prod* 75(6):1231-1242.
167. Bentley SD, *et al.* (2002) Complete genome sequence of the model actinomycete *Streptomyces coelicolor* A3(2). *Nature*, (England), Vol 417, pp 141-147.
168. Keller NP, Turner G, & Bennett JW (2005) Fungal secondary metabolism-from biochemistry to genomics. *Nat Rev Microbiol* 3(12):937-947.
169. Nett M, Ikeda H, & Moore BS (2009) Genomic basis for natural product biosynthetic diversity in the actinomycetes. *Nat Prod Rep* 26(11):1362-1384.
170. Rutledge PJ & Challis GL (2015) Discovery of microbial natural products by activation of silent biosynthetic gene clusters. *Nat Rev Microbiol* 13(8):509-523.
171. Medema MH, *et al.* (2011) antiSMASH: rapid identification, annotation and analysis of secondary metabolite biosynthesis gene clusters in bacterial and fungal genome sequences. *Nucleic Acids Res* 39:W339-346.
172. Weber T (2014) In silico tools for the analysis of antibiotic biosynthetic pathways. *Int J Med Microbiol* 304(3-4):230-235.
173. Cheng G, *et al.* (2017) BGDMdocker: a Docker workflow for data mining and visualization of bacterial pan-genomes and biosynthetic gene clusters. *PeerJ* 5:e3948.
174. Wang Z, Gerstein M, & Snyder M (2009) RNA-Seq: a revolutionary tool for transcriptomics. *Nat Rev Genet* 10(1):57-63.
175. Institute NC (2018) Gene expression profile definition.
176. Magoc T, Wood D, & Salzberg SL (2013) EDGE-pro: Estimated Degree of Gene Expression in Prokaryotic Genomes. *Evol Bioinform Online* 9:127-136.
177. Blencke HM, *et al.* (2003) Transcriptional profiling of gene expression in response to glucose in *Bacillus subtilis*: regulation of the central metabolic pathways. *Metab Eng* 5(2):133-149.
178. Pavlidi N, *et al.* (2017) Transcriptomic responses of the olive fruit fly *Bactrocera oleae* and its symbiont *Candidatus Erwinia dacicola* to olive feeding. *Sci Rep* 7:42633.
179. Andrews P, Busch JL, de Joode T, Groenewegen A, & Alexandre H (2003) Sensory properties of virgin olive oil polyphenols: identification of deacetoxy-ligstroside aglycon as a key contributor to pungency. *J Agric Food Chem* 51(5):1415-1420.
180. Verbist B, *et al.* (2015) Using transcriptomics to guide lead optimization in drug discovery projects: Lessons learned from the QSTAR project. *Drug Discov Today* 20(5):505-513.
181. Iorio F, *et al.* (2010) Discovery of drug mode of action and drug repositioning from transcriptional responses. *Proc Natl Acad Sci U S A* 107(33):14621-14626.
182. Clark TA, Sugnet CW, & Ares M (2002) Genomewide analysis of mRNA processing in yeast using splicing-specific microarrays. *Science* 296(5569):907-910.
183. Royce TE, Rozowsky JS, & Gerstein MB (2007) Toward a universal microarray: prediction of gene expression through nearest-neighbor probe sequence identification. *Nucleic Acids Res* 35(15):e99.
184. Anders S, *et al.* (2013) Count-based differential expression analysis of RNA sequencing data using R and Bioconductor. *Nat Protoc* 8(9):1765-1786.
185. Trapnell C, *et al.* (2012) Differential gene and transcript expression analysis of RNA-seq experiments with TopHat and Cufflinks. *Nat Protoc* 7(3):562-578.
186. Geiss GK, *et al.* (2008) Direct multiplexed measurement of gene expression with color-coded probe pairs. *Nat Biotechnol* 26(3):317-325.
187. Turner S, Pryer KM, Miao VP, & Palmer JD (1999) Investigating deep phylogenetic relationships among cyanobacteria and plastids by small subunit rRNA sequence analysis. *J Eukaryot Microbiol* 46(4):327-338.
188. Anders S & Huber W (2010) Differential expression analysis for sequence count data. *Genome Biol* 11(10):R106.

189. McCarthy DJ & Smyth GK (2009) Testing significance relative to a fold-change threshold is a TREAT. *Bioinformatics* 25(6):765-771.
190. Lide DM, G.W.A. (1995) *Handbook of Data on Common Organic Compounds* (CRC Press, Inc., Boca Raton, FL.) 3rd. Ed p 212.
191. Fukushima T, *et al.* (2013) Gram-positive siderophore-shuttle with iron-exchange from Fe-siderophore to apo-siderophore by *Bacillus cereus* YxeB. *Proc Natl Acad Sci U S A* 110(34):13821-13826.
192. Mäder U, *et al.* (2002) Transcriptome and proteome analysis of *Bacillus subtilis* gene expression modulated by amino acid availability. *J Bacteriol* 184(15):4288-4295.
193. Mostertz J, Hochgräfe F, Jürgen B, Schweder T, & Hecker M (2008) The role of thioredoxin TrxA in *Bacillus subtilis*: a proteomics and transcriptomics approach. *Proteomics* 8(13):2676-2690.
194. Marinoni I, *et al.* (2008) Characterization of L-aspartate oxidase and quinolinate synthase from *Bacillus subtilis*. *FEBS J* 275(20):5090-5107.
195. Yoshida K, Yamamoto Y, Omae K, Yamamoto M, & Fujita Y (2002) Identification of two myo-inositol transporter genes of *Bacillus subtilis*. *J Bacteriol* 184(4):983-991.
196. Kanehisa M, Furumichi M, Tanabe M, Sato Y, & Morishima K (2017) KEGG: new perspectives on genomes, pathways, diseases and drugs. *Nucleic Acids Res* 45(D1):D353-D361.
197. Kirchner M & Schneider S (2017) Gene expression control by *Bacillus anthracis* purine riboswitches. *Rna* 23(5):762-769.
198. Berg GM & Jorgensen NOG (2006) Purine and pyrimidine metabolism by estuarine bacteria. *Aquatic Microbial Ecology* 42(3):215-226.
199. LaRue TA & Spencer JF (1968) The utilization of purines and pyrimidines by yeasts. *Can J Microbiol* 14(1):79-86.
200. Schultz AC, Nygaard P, & Saxild HH (2001) Functional analysis of 14 genes that constitute the purine catabolic pathway in *Bacillus subtilis* and evidence for a novel regulon controlled by the PucR transcription activator. *J Bacteriol* 183(11):3293-3302.
201. Vogels GD & Van der Drift C (1976) Degradation of purines and pyrimidines by microorganisms. *Bacteriol Rev* 40(2):403-468.
202. O'Donovan GA & Neuhard J (1970) Pyrimidine metabolism in microorganisms. *Bacteriol Rev* 34(3):278-343.
203. Berger F, Ramírez-Hernández MH, & Ziegler M (2004) The new life of a centenarian: signalling functions of NAD(P). *Trends Biochem Sci* 29(3):111-118.
204. Pollak N, Dölle C, & Ziegler M (2007) The power to reduce: pyridine nucleotides-small molecules with a multitude of functions. *Biochem J* 402(2):205-218.
205. Elhassan YS, Philp AA, & Lavery GG (2017) Targeting NAD⁺ in Metabolic Disease: New Insights Into an Old Molecule. *J Endocr Soc* 1(7):816-835.
206. Mathews CK, Van Holde KE, Appling D, & Anthony-Cahill SJ (2012) *Biochemistry*. (Pearson, Canada), 4th Ed, pp 820-861.
207. Reynolds ES, Lieberman I, & Kornberg A (1955) The metabolism of orotic acid in aerobic bacteria. *J Bacteriol* 69(3):250-255.
208. Bazurto JV, Heitman NJ, & Downs DM (2015) Aminoimidazole Carboxamide Ribotide Exerts Opposing Effects on Thiamine Synthesis in *Salmonella enterica*. *J Bacteriol* 197(17):2821-2830.
209. Kuramitsu HK, Udaka S, & Moyed HS (1964) Induction Of Inosine 5'-Phosphate Dehydrogenase And Xanthosine 5'-Phosphate Aminase By Ribosyl-4-Amino-5-Imidazolecarboxamide In Purine-Requiring Mutants of *Escherichia Coli* B. *J Biol Chem* 239:3425-3430.
210. Vincent MF, Marangos PJ, Gruber HE, & Van den Berghe G (1991) Inhibition by AICA riboside of gluconeogenesis in isolated rat hepatocytes. *Diabetes* 40(10):1259-1266.
211. Allen S, Zilles JL, & Downs DM (2002) Metabolic flux in both the purine mononucleotide and histidine biosynthetic pathways can influence synthesis of the hydroxymethyl pyrimidine moiety of thiamine in *Salmonella enterica*. *J Bacteriol* 184(22):6130-6137.

212. Andrade-Domínguez A, Salazar E, Vargas-Lagunas MeC, Kolter R, & Encarnación S (2014) Eco-evolutionary feedbacks drive species interactions. *ISME J* 8(5):1041-1054.
213. Shalmali N, Ali MR, & Bawa S (2018) Imidazole: An Essential Edifice for the Identification of New Lead Compounds and Drug Development. *Mini-Reviews in Medicinal Chemistry* 18(2):142-163.
214. Wilson MK, Abergel RJ, Raymond KN, Arceneaux JE, & Byers BR (2006) Siderophores of *Bacillus anthracis*, *Bacillus cereus*, and *Bacillus thuringiensis*. *Biochem Biophys Res Commun* 348(1):320-325.
215. Du Q, Wang H, & Xie J (2011) Thiamin (vitamin B1) biosynthesis and regulation: a rich source of antimicrobial drug targets? *Int J Biol Sci* 7(1):41-52.
216. Begley TP, *et al.* (1999) Thiamin biosynthesis in prokaryotes. *Arch Microbiol* 171(5):293-300.
217. Tobisch S, Glaser P, Krüger S, & Hecker M (1997) Identification and characterization of a new beta-glucoside utilization system in *Bacillus subtilis*. *J Bacteriol* 179(2):496-506.
218. Belenky P, Bogan KL, & Brenner C (2007) NAD⁺ metabolism in health and disease. *Trends Biochem Sci* 32(1):12-19.
219. Gazzaniga F, Stebbins R, Chang SZ, McPeck MA, & Brenner C (2009) Microbial NAD metabolism: lessons from comparative genomics. *Microbiol Mol Biol Rev* 73(3):529-541.
220. Ourisson G, Rohmer M, & Poralla K (1987) Prokaryotic hopanoids and other polyterpenoid sterol surrogates. *Annu Rev Microbiol* 41:301-333.
221. Sáenz JP, *et al.* (2015) Hopanoids as functional analogues of cholesterol in bacterial membranes. *Proc Natl Acad Sci U S A* 112(38):11971-11976.
222. Fiehn O (2001) Combining genomics, metabolome analysis, and biochemical modelling to understand metabolic networks. *Comp Funct Genomics* 2(3):155-168.
223. Dictionary of Natural Products. (<http://dnp.chemnetbase.com/>)
224. Horai H, *et al.* (2010) MassBank: a public repository for sharing mass spectral data for life sciences. *J Mass Spectrom* 45(7):703-714.
225. mzCloud: advanced mass spectral database. (<https://www.mzcloud.org/>)
226. Valgas C, Souza SMD, Smânia EFA, & Smânia Jr. A (2007) Screening methods to determine antibacterial activity of natural products. *Brazilian Journal of Microbiology* 38:369-380.
227. Pence HE & Williams A (2010) ChemSpider: An Online Chemical Information Resource. *Journal of Chemical Education* 87(11):1123-1124.
228. Kim S, *et al.* (2016) PubChem Substance and Compound databases. *Nucleic Acids Res* 44(D1):D1202-1213.
229. Watrous J, *et al.* (2012) Mass spectral molecular networking of living microbial colonies. *Proc Natl Acad Sci U S A* 109(26):E1743-1752.
230. Reymond JL & Awale M (2012) Exploring chemical space for drug discovery using the chemical universe database. *ACS Chem Neurosci* 3(9):649-657.
231. Olivon F, Roussi F, Litaudon M, & Touboul D (2017) Optimized experimental workflow for tandem mass spectrometry molecular networking in metabolomics. *Anal Bioanal Chem* 409(24):5767-5778.
232. Cao S, Sun LQ, & Wang M (2011) Antimicrobial activity and mechanism of action of Nu-3, a protonated modified nucleotide. *Ann Clin Microbiol Antimicrob* 10:1.
233. Fresco-Taboada A, *et al.* (2014) Nucleoside 2'-Deoxyribosyltransferase from Psychrophilic Bacterium *Bacillus psychrosaccharolyticus* - Preparation of an Immobilized Biocatalyst for the Enzymatic Synthesis of Therapeutic Nucleosides. *Molecules* 19(8):11231-11249.
234. Lewkowicz ES & Iribarren AM (2017) Whole cell biocatalysts for the preparation of nucleosides and their derivatives. *Curr Pharm Des.*
235. Fresco-Taboada A, *et al.* (2013) Genome of the Psychrophilic Bacterium *Bacillus psychrosaccharolyticus*, a Potential Source of 2'-Deoxyribosyltransferase for Industrial Nucleoside Synthesis. *Genome Announc* 1(3).
236. Clark AM, Hufford CD, Puri RK, & McChesney JD (1984) Production of a novel dimeric metabolite of primaquine by *Streptomyces rimosus*. *Appl Environ Microbiol* 47(3):540-543.
237. Hufford CD, Baker JK, McChesney JD, & Clark AM (1986) Novel sulfur-containing microbial metabolite of primaquine. *Antimicrob Agents Chemother* 30(2):234-237.

